

Causal Effect Estimation after Propensity Score Trimming with Continuous Treatments

Zach Branson, Edward H. Kennedy, Sivaraman Balakrishnan, Larry Wasserman

September 6, 2023

Abstract

Most works in causal inference focus on binary treatments where one estimates a single treatment-versus-control effect. When treatment is continuous, one must estimate a curve representing the causal relationship between treatment and outcome (the “dose-response curve”), which makes causal inference more challenging. This work proposes estimators using efficient influence functions (EIFs) for causal dose-response curves after propensity score trimming. Trimming involves estimating causal effects among subjects with propensity scores above a threshold, which addresses positivity violations that complicate estimation. Several challenges arise with continuous treatments. First, EIFs for trimmed dose-response curves do not exist, due to a lack of pathwise differentiability induced by trimming and a continuous treatment. Second, if the trimming threshold is not prespecified and is instead a parameter that must be estimated, then estimation uncertainty in the threshold must be accounted for. To address these challenges, we target a smoothed version of the trimmed dose-response curve for which an EIF exists. We allow the trimming threshold to be a user-specified quantile of the propensity score distribution, and we construct confidence intervals which reflect uncertainty involved in threshold estimation. Our resulting EIF-based estimators exhibit doubly-robust style guarantees, with error involving products or squares of errors for the outcome regression and propensity score. Thus, our estimators can exhibit parametric convergence rates even when the outcome regression and propensity score are estimated at slower nonparametric rates with flexible estimators. These findings are validated via simulation and an application, thereby showing how to efficiently-but-flexibly estimate a dose-response curve after trimming.

1 Introduction

We consider the problem of estimating average causal effects in an observational study with a continuous treatment. It’s well-known that, under standard identification assumptions, the average treatment effect (ATE) can be estimated with some combination of an outcome model that measures the relationship between the outcome, covariates, and treatment, and a propensity score model that measures the relationship between the treatment and covariates (e.g., Imbens and Rubin 2015, Chapter 12, Hernán and Robins 2020, Chapter 13). A ubiquitous assumption for identifying the ATE is positivity, which states that every subject has a non-zero probability of receiving any treatment, conditional on covariates (Rosenbaum and Rubin, 1983; Imbens, 2004; Hernán and Robins, 2006; D’Amour et al., 2021). Positivity is arguably less tenable when the treatment is continuous, because it can be unlikely that every subject has a non-zero conditional density at every treatment value. Furthermore, even if positivity holds, propensity scores close to zero adversely affect the bias and variance of most ATE estimators (Westreich and Cole, 2010; Khan and Tamer, 2010; Waernbaum, 2012; Petersen et al., 2012; Busso et al., 2014; Li et al., 2018). One common approach to address this issue is to discard subjects with extreme propensity scores when estimating causal effects; this is known as propensity score trimming (Heckman et al., 1997; Frölich, 2004; Smith and Todd, 2005; Crump et al., 2009; Lee et al., 2011; Yang and Ding, 2018).

Many empirical studies have demonstrated that propensity score trimming can improve the accuracy of causal effect estimators (Cole and Hernán, 2008; Stürmer et al., 2010; Lee et al., 2011; Austin and Stuart, 2015; Yang et al., 2016; Stürmer et al., 2021), such that it is common in practice. However, almost all works on trimming assume treatment is discrete, and there is little guidance for trimming with continuous treatments (Wu et al., 2018). In this paper we derive estimators based on efficient influence functions for trimmed average causal effects; in doing so, we address several challenges that uniquely arise for continuous treatments. First, we may want the amount of trimming (the trimming threshold) to depend on the treatment value, because the severity of positivity violations is likely to differ across treatment values. Second, if we allow the trimming threshold to be data-driven, uncertainty in this estimation also needs to be accounted for to conduct valid inference (Yang and Ding, 2018). Finally, although ATE estimators for discrete treatments can be constructed via efficient influence functions under some assumptions (Hines et al., 2022; Kennedy, 2022), an efficient influence function for a trimmed ATE with a continuous treatment does not exist, due to a lack of pathwise differentiability induced by the nonsmooth nature of trimming (Yang and Ding, 2018) and a continuous treatment (Kennedy et al., 2017). Relatedly, without parametric modeling assumptions, a $n^{-1/2}$ consistent estimator for the dose-response

curve does not exist (Díaz and van der Laan, 2013; Bonvini and Kennedy, 2022), let alone for a trimmed dose-response curve.

To address these challenges, we target a smoothed estimand that is close to the trimmed ATE but has an efficient influence function. We then derive efficient influence functions for this estimand when the trimming threshold is fixed and when it is defined as a quantile of the propensity score distribution, thereby allowing confidence intervals to reflect the uncertainty involved in estimating the threshold. The trimming threshold can depend on the treatment value, such that trimming can vary across the dose-response curve. Our resulting estimators have doubly-robust style guarantees, i.e. their error can be expressed as products or squares of errors for the outcome regression and propensity score. As a result, our estimators attain parametric $n^{-1/2}$ convergence rates even when the outcome regression and propensity score are estimated at slower rates with flexible estimators.

In Section 2, we outline notation to define the ATE, trimmed ATE, and the smoothed trimmed ATE (or STATE). In Section 3, we derive estimators based on efficient influence functions for the STATE, first when the trimming threshold is fixed, and then when it is estimated via a quantile of the propensity score distribution. In Section 4, we describe a data-driven way to select the smoothing parameters involved in defining the STATE. We then present simulations in Section 5 and a real application in Section 6 which validate that our estimators can flexibly and accurately estimate a trimmed dose-response curve; we find that when propensity scores are small, our estimators are more precise than dose-response estimators that do not incorporate trimming. We conclude with Section 7.

1.1 Related Work

Many works have considered causal effect estimators that combine outcome regression and inverse propensity score weights that are stabilized to alleviate issues with extreme propensity scores. This includes incorporating overlap weights (Li, 2020; Zhou et al., 2020), truncating inverse propensity score weights (Cole and Hernán, 2008; Petersen et al., 2012; Ju et al., 2019), and trimming. In particular, many have found empirical evidence that trimming can improve the performance of doubly robust estimators (Mao et al., 2019; Li, 2020; Zhang and Zhang, 2022; Huang et al., 2022); however, these works do not establish theoretical guarantees of these estimators after trimming. These studies usually consider a typical doubly robust estimator that is implemented on a trimmed sample; thus, the trimmed sample is conditioned on when conducting inference. However, the proportion of trimmed subjects can be viewed as an estimand whose uncertainty is driven by uncertainty in the propensity score. We derive efficient influence functions for the proportion of trimmed subjects, such

that inference naturally incorporates uncertainty in this proportion.

Our work adds to recent literature that tweaks inverse propensity score weighted estimators (Chaudhuri and Hill, 2014; Ma and Wang, 2020; Sasaki and Ura, 2022; Liu and Fan, 2023) and estimators that combine propensity score and outcome regression estimates (Cao et al., 2009; Rothe, 2017; Yang and Ding, 2018; Heiler and Kazak, 2021; Khan and Ugander, 2022; Ma et al., 2023) to be robust to extreme propensity scores. Our work is most similar to Yang and Ding (2018) and Khan and Ugander (2022), although they both focus on binary treatments. Yang and Ding (2018), like us, study a doubly robust estimator that incorporates smoothing on the trimming indicator and quantifies uncertainty in the proportion of trimmed subjects; however, they assume the propensity score follows a parametric generalized linear model. Thus, in order to conduct valid inference for the true trimmed effect, one must estimate the propensity score with a well-specified generalized linear model. Instead, we are agnostic to the form of the propensity score and outcome models, and we establish conditions for valid inference even when these models are estimated at slower-than-parametric rates. Meanwhile, Khan and Ugander (2022) also derive a trimmed doubly robust estimator that yields valid inference even when the propensity score and outcome regression are estimated nonparametrically; however, their estimand is the ATE for the estimated trimmed set, instead of for the true trimmed set. If we denote the estimated propensity score as $\hat{\pi}$ and the estimated trimming threshold as \hat{t} , then the estimated trimmed set is the subjects for whom $\hat{\pi} \geq \hat{t}$, instead of for whom $\pi \geq t$. Khan and Ugander (2022) acknowledge this change in estimand and note that deriving an efficient influence function of the ATE for the true trimmed set may be fruitful; that is the approach we take here.

Finally, all of the aforementioned works assume the treatment is binary, whereas we let treatment be continuous. Thus, our work contributes to the literature on causal dose-response estimation (Hirano and Imbens, 2004; Díaz and van der Laan, 2013; Kennedy et al., 2017; Fong et al., 2018; Wu et al., 2018; Bonvini and Kennedy, 2022; Huling et al., 2023) in the case where the positivity assumption is either violated or nearly violated. In the Appendix (Section H) we also illustrate how our results simplify when the treatment is discrete, thereby providing a way to nonparametrically estimate trimmed causal effects in the canonical discrete case.

2 Setup and Causal Estimands

2.1 Notation

For a possibly random function f , we denote sample averages with $\mathbb{P}_n\{f(Z)\} = n^{-1} \sum_{i=1}^n f(Z_i)$ and sample variances with $\text{Var}_n\{f(Z)\} = (n-1)^{-1} \sum_{i=1}^n [f(Z_i) - \mathbb{P}_n\{f(Z)\}]^2$. We denote the squared L_2 -norm of f with $\|f\|^2 = \int f(z)^2 dP(z)$. Finally, we use $\mathbb{I}(B)$ to denote the indicator function, equal to 1 if an event B occurs and 0 otherwise.

2.2 Review: Causal Dose-Response Estimation

Assume a vector of covariates X , a continuous treatment A , and a continuous outcome Y . Let $Y(a)$ denote the potential outcome for treatment value a , i.e., the outcome we observe if $A = a$. We denote the average treatment effect (ATE) at $A = a$ as $\psi(a) \equiv \mathbb{E}[Y(a)]$. Meanwhile, the causal dose-response curve corresponds to causal effects across treatment values, e.g., the set $\{\psi(a) : a \in \mathbb{R}\}$. For notational simplicity, we write causal effects in terms of a single treatment value $A = a$; in practice, one would estimate effects across many treatment values to obtain an estimated dose-response curve.

The following assumptions are sufficient for identifying $\psi(a)$ (Gill and Robins, 2001; Kennedy et al., 2017):

(A1) **No Unmeasured Confounding:** $Y(a) \perp\!\!\!\perp A|X$, for all a .

(A2) **Consistency:** If $A = a$, then $Y = Y(a)$, for all a .

(A3) **Positivity:** There is an $c > 0$ such that $c \leq \pi(a|x)$ for all a and x , where $\pi(a|x)$ is the conditional density of treatment a (the propensity score).

Under these three assumptions, we have the following identification result:

$$\psi(a) = \int \mu(x, a) dP(x), \tag{1}$$

where $\mu(x, a) = \mathbb{E}[Y|X = x, A = a]$. Equation (1) motivates estimating the outcome regression $\mu(x, a)$; for example, we could construct $\hat{\mu}(x, a)$, plug it into (1), and average across subjects. The accuracy of this plug-in estimator would generally depend on the accuracy of $\hat{\mu}(x, a)$. Thus, to ensure the outcome regression is well-specified, it's tempting to nonparametrically model $\mu(x, a)$ (Hill, 2011; Hill et al., 2020); however, the resulting estimator would typically inherit slow nonparametric convergence rates.

If we want to be robust to model misspecification for $\mu(x, a)$, we can instead develop estimators that utilize estimates of the propensity score $\pi(a|x)$ (Flores et al., 2012; Galvao and Wang, 2015; Zhang et al., 2016; Zhao et al., 2020). However, the aforementioned works assume some form of parametric model specification. To avoid parametric model specification, we can consider estimators based on the efficient influence function (EIF) of their corresponding estimand (Van der Vaart, 2000; Tsiatis, 2006; Kennedy, 2016, 2022). However, an EIF for $\psi(a)$ does not exist, due to a lack of pathwise differentiability at $A = a$ (Díaz and van der Laan, 2013). One option is to derive an EIF for an estimand that smooths across A while placing more weight on subjects with A near a . Given a smooth, symmetric kernel $K_h(\cdot)$ with bandwidth h , we can define and identify a kernel-smoothed version of $\psi(a)$:

$$\psi_h(a) = \int \int K_h(a_0 - a) \mu(x, a_0) da_0 dP(x). \quad (2)$$

We discuss an EIF-based estimator for $\psi_h(a)$ in Section 3.

The identification results for $\psi(a)$ in (1) and $\psi_h(a)$ in (2) rely on the positivity assumption (A3). Furthermore, even if positivity holds, estimation can be difficult if propensity scores are nonetheless close to zero, in the sense that standard doubly robust estimators can exhibit large bias (Bang and Robins, 2005; Kang and Schafer, 2007; Funk et al., 2011; Waernbaum, 2012) and variance (Robins et al., 2007; Cole and Hernán, 2008; Li et al., 2018, 2019). This complication is especially relevant for continuous treatments, because it is often likely that $\pi(a|x)$ will be small for some a . This motivates trimming.

2.3 Trimmed Causal Estimands

Propensity score trimming instead targets the ATE among subjects with non-extreme propensity scores. Given a trimming threshold t , the trimmed ATE is defined and identified as

$$\psi(a; t) = \mathbb{E}[Y(a) | \pi(a|X) > t] = \frac{\int \mathbb{I}(\pi(a|x) > t) \mu(x, a) dP(x)}{\int \mathbb{I}(\pi(a|x) > t) dP(x)}. \quad (3)$$

When A is binary, it is common to also trim subjects whose propensity scores are close to one (Crump et al., 2009), because then $P(A = 0|X)$ is close to zero. However, for continuous treatments, we only have to trim subjects whose propensity scores are close to zero at $A = a$.

The trimmed ATE $\psi(a; t)$ represents the ATE among subjects for whom $\pi(a|X) > t$ at $A = a$. Thus, the non-trimmed population can change across treatment values, because a subject's propensity score may be large for one treatment value but small for another value. Although it's well-known that trimming changes the implied population (Crump et al., 2009;

Stürmer et al., 2010; Yang and Ding, 2018), this can make interpreting trimmed effects with continuous treatments challenging. One option is to trim any subject whose propensity score is below t for any treatment value (Colangelo and Lee, 2020), but this may result in trimming many subjects. Alternatively, one can estimate how the non-trimmed population changes across treatment values, in addition to estimating causal effects. We focus on effect estimation in this section and the following section, and discuss how to interpret the non-trimmed population in Sections 5 and 6.

Equation (3) suggests the following plug-in estimator:

$$\widehat{\psi}(a; t) = \frac{\mathbb{P}_n\{\mathbb{I}(\widehat{\pi}(a|X) > t)\widehat{\mu}(X, a)\}}{\mathbb{P}_n\{\mathbb{I}(\widehat{\pi}(a|X) > t)\}}, \quad (4)$$

where $\widehat{\pi}(a|X)$ and $\widehat{\mu}(X, a)$ denote estimators for the propensity score and outcome regression, respectively. This estimator simply averages $\widehat{\mu}(X, a)$ among non-trimmed subjects. Intuitively, this estimator would require both $\mu(x, a)$ and $\pi(a|x)$ to be well-specified; correct specification for $\pi(a|x)$ ensures that the correct subpopulation is targeted, and correct specification for $\mu(x, a)$ ensures consistency of the estimator within that subpopulation. However, if we use flexible models for $\mu(x, a)$ and $\pi(a|x)$, the resulting estimator would typically inherit slow nonparametric convergence rates, which would also adversely affect inference.

Instead, we use efficiency theory to derive influence-function based estimators, such that parametric convergence rates can still be achieved even in nonparametric models. An EIF for the trimmed ATE $\psi(a; t)$ does not exist, due to a lack of differentiability at $A = a$ and from the trimming indicator $\mathbb{I}(\pi(a|x) > t)$. To overcome these limitations, we again use smoothing to target an estimand that admits an EIF. Specifically, we use kernel smoothing with $K_h(\cdot)$, and use a smoothed version of the indicator function $\mathbb{I}(\pi(a|x) > t)$, denoted $S(\pi(a|x), t)$. One example is $S(\pi(a|x), t) = \Phi_\epsilon\{\pi(a|x) - t\}$, where $\Phi_\epsilon(z)$ is the cumulative distribution function (CDF) of a Normal with mean zero and variance ϵ^2 (Yang and Ding, 2018). In this case, ϵ is a tuning parameter; however, in our notation, we suppress dependence on ϵ to remain agnostic to the type of smoothing indicator $S(\pi(a|x), t)$ one may use in practice.

Once $K_h(\cdot)$ and $S(\pi(a|x), t)$ are specified, the smoothed trimmed ATE (STATE) is defined and identified as:

$$\psi_h(a; t) = \frac{\int \int K_h(a_0 - a) S(\pi(a_0|x), t) \mu(x, a_0) da_0 dP(x)}{\int \int K_h(a_0 - a) S(\pi(a_0|x), t) da_0 dP(x)}. \quad (5)$$

The STATE $\psi_h(a; t)$ is a weighted average of $\psi_h(a)$ in (2), where subjects with propensity scores greater than t are given weight close to one, and subjects with propensity scores less than t are given weight close to zero. The amount that $\psi_h(a; t)$ differs from $\psi(a; t)$ depends

on h and ϵ ; standard results imply that $\psi_h(a; t) \rightarrow \psi(a; t)$ when $(h, \epsilon) \rightarrow (0, 0)$.

In the next section, we derive EIF-based estimators for the STATE, first when t is fixed, and then when it is estimated as a quantile of the propensity score; in both cases we assume h and ϵ are prespecified. We discuss data-driven ways to choose h and ϵ in Section 4.

3 Efficient Estimators for Trimmed Causal Effects

Here we derive estimators based on efficient influence functions (EIFs) for the smoothed trimmed ATE (STATE) $\psi_h(a; t)$ in (5). First, consider the smoothed ATE $\psi_h(a)$ in (2). Given a kernel $K_h(\cdot)$ and fixed bandwidth h , the uncentered EIF of $\psi_h(a)$ is

$$\varphi_h(a) = K_h(A - a) \frac{Y - \mu(X, A)}{\pi(A|X)} + \int K_h(a_0 - a) \mu(X, a_0) da_0 \quad (6)$$

(Bibaut and van der Laan, 2017). By “uncentered,” we mean that the EIF of $\psi_h(a)$ is $\varphi_h(a) - \psi_h(a)$, such that $\mathbb{E}[\varphi_h(a)] = \psi_h(a)$. Unless stated otherwise, the EIFs we derive will always be the uncentered EIF minus its respective estimand. The one-step estimator based on this EIF is:

$$\widehat{\psi}_h(a) = \mathbb{P}_n \{ \widehat{\varphi}_h(a) \} = \mathbb{P}_n \left\{ K_h(A - a) \frac{Y - \widehat{\mu}(X, A)}{\widehat{\pi}(A|X)} + \int K_h(a_0 - a) \widehat{\mu}(X, a_0) da_0 \right\}, \quad (7)$$

Because $\widehat{\psi}_h(a)$ is the one-step estimator based on the EIF of $\psi_h(a)$, if positivity holds, then, with additional assumptions on the convergence rates of $\widehat{\mu}(a, x)$ and $\widehat{\pi}(a|x)$, one can show that $\widehat{\psi}_h(a)$ is $n^{-1/2}$ consistent, asymptotically Normal, and semiparametrically efficient (van der Vaart 2002, Chapter 2; Kennedy 2022). Estimators similar to $\widehat{\psi}_h(a)$ in (7) have been proposed in Kallus and Zhou (2018), Su et al. (2019) and Colangelo and Lee (2020), who consider the estimator $\mathbb{P}_n \left\{ K_h(A - a) \frac{Y - \widehat{\mu}(X, a)}{\widehat{\pi}(a|X)} + \widehat{\mu}(X, a) \right\}$. Such an estimator is based on the EIF of the identification result $\psi(a) = \lim_{h \rightarrow 0} \mathbb{E} \left[\frac{K_h(A - a) Y}{\pi(a|X)} \right]$, which holds given additional assumptions on $\mu(x, a)$, $\pi(a|x)$, the kernel $K_h(\cdot)$, and bandwidth h . Instead, $\widehat{\psi}_h(a)$ is based on the identification result (2), which holds without these additional assumptions. Nonetheless, we would expect $\psi_h(a) \rightarrow \psi(a)$ as $h \rightarrow 0$, and thus anticipate that these estimators behave similarly. The estimator $\widehat{\psi}_h(a)$ is also similar to that of Kennedy et al. (2017), who use an outcome regression and inverse propensity score weighting to construct a pseudo-outcome that is regressed on A , e.g. using kernel smoothing.

The above estimator can be unstable when propensity scores are small, which motivates trimming; however, the estimand will be the STATE $\psi_h(a; t)$. To establish EIF-based esti-

mators for the STATE, it's helpful to write $\psi_h(a; t) = \psi_h^{\text{num}}(a; t)/\psi_h^{\text{den}}(a; t)$, where

$$\psi_h^{\text{num}}(a; t) = \int \int K_h(a_0 - a)S(\pi(a_0|x), t)\mu(x, a_0)da_0dP(x), \text{ and} \quad (8)$$

$$\psi_h^{\text{den}}(a; t) = \int \int K_h(a_0 - a)S(\pi(a_0|x), t)da_0dP(x). \quad (9)$$

This decomposition suggests two ways to derive EIF-based estimators for $\psi_h(a; t)$. First, we can derive EIFs for $\psi_h^{\text{num}}(a; t)$ and $\psi_h^{\text{den}}(a; t)$ and corresponding one-step estimators $\widehat{\psi}_h^{\text{num}}(a; t)$ and $\widehat{\psi}_h^{\text{den}}(a; t)$. Then, we can take their ratio. Alternatively, we can derive the EIF for $\psi_h(a; t)$ itself, and then derive a corresponding one-step estimator $\widehat{\psi}_h(a; t)$. We focus on the first approach, because the denominator estimate $\widehat{\psi}_h^{\text{den}}(a; t)$ represents the proportion of non-trimmed subjects, which is useful for estimating the trimming threshold t , as we discuss in Section 3.2. That said, both approaches are asymptotically equivalent, and for completeness we include results from the second approach in the Appendix (Section F).

3.1 When the Trimming Threshold is Fixed

In this subsection we establish the EIFs of $\psi_h^{\text{num}}(a; t)$ and $\psi_h^{\text{den}}(a; t)$ defined in (8) and (9) when the trimming threshold t is fixed. Because $S(\pi(a|x), t)$ is a function of the propensity score, the EIFs depend on the derivative of $S(\pi(a|x), t)$ with respect to the propensity score, which we denote as $\partial S(\pi(a|x), t)/\partial \pi$. For example, when $S(\pi(a|x), t) = \Phi_\epsilon\{\pi(a|x) - t\}$, $\partial S(\pi(a|x), t)/\partial \pi = \phi_\epsilon\{\pi(a|x) - t\}$, where $\Phi_\epsilon(z)$ and $\phi_\epsilon(z)$ are the CDF and PDF of the distribution $N(0, \epsilon^2)$, respectively.

In general, the EIF of an estimand ψ acts as its functional pathwise derivative (Newey, 1994; Tsiatis, 2006). Importantly, a (centered) EIF ξ satisfies the von Mises expansion (Mises, 1947), for two probability measures P and \bar{P} :

$$\psi(\bar{P}) - \psi(P) = \int \xi(\bar{P})d(\bar{P} - P)(x) + R_2(\bar{P}, P), \quad (10)$$

where $R_2(\bar{P}, P)$ is a second-order remainder of a functional Taylor expansion (Hines et al., 2022; Kennedy, 2022). Thus, one can derive a potential EIF ξ , and then verify that the von Mises expansion (10) holds by establishing that the remainder term $R_2(\bar{P}, P)$ is second-order in P and \bar{P} ; see the Appendix (Section A) for more details. We establish conditions when $R_2(\bar{P}, P) = o_P(n^{-1/2})$ and thus the estimator is characterized by the distribution of the first term, which is asymptotically Normal with mean zero for the estimator we derive.

The following theorem establishes the EIFs of $\psi_h^{\text{num}}(a; t)$ and $\psi_h^{\text{den}}(a; t)$. We then discuss their respective remainder terms $R_2(\bar{P}, P)$, as well as sufficient conditions for conducting

asymptotically unbiased and valid inference.

Theorem 1. *If the trimming threshold t is fixed, the uncentered EIFs for $\psi_h^{\text{num}}(a; t)$ and $\psi_h^{\text{den}}(a; t)$ defined in (8) and (9) are:*

$$\begin{aligned} \varphi_h^{\text{num}}(a; t) &= K_h(A - a) \frac{\{Y - \mu(X, A)\}S(\pi(A|X), t)}{\pi(A|X)} + \int K_h(a_0 - a)S(\pi(a_0|X), t)\mu(X, a_0)da_0 \\ &\quad + K_h(A - a)\mu(X, A)\frac{\partial S(\pi(A|X), t)}{\partial \pi} - \int K_h(a_0 - a)\mu(X, a_0)\frac{\partial S(\pi(a_0|X), t)}{\partial \pi}\pi(a_0|X)da_0, \end{aligned}$$

and

$$\begin{aligned} \varphi_h^{\text{den}}(a; t) &= \int K_h(a_0 - a)S(\pi(a_0|X), t)da_0 \\ &\quad + K_h(A - a)\frac{\partial S(\pi(A|X), t)}{\partial \pi} - \int K_h(a_0 - a)\frac{\partial S(\pi(a_0|X), t)}{\partial \pi}\pi(a_0|X)da_0. \end{aligned}$$

Remark 1. *We show in the Appendix (Section C) that the remainder terms of the von Mises expansions for the above parameters are:*

$$\begin{aligned} R_2^{\text{num}}(\bar{P}, P) &= \int \int K_h(a_0 - a) \left\{ \frac{S(\bar{\pi}(a_0|x), t)}{\bar{\pi}(a_0|x)} - \frac{\partial S(\bar{\pi}(a_0|x), t)}{\partial \bar{\pi}} \right\} \{\pi(a_0|x) - \bar{\pi}(a_0|x)\} \{\mu(x, a_0) - \bar{\mu}(x, a_0)\} da_0 dP(x) \\ &\quad - \int \int K_h(a_0 - a)\mu(x, a_0) \left[\frac{1}{2} \frac{\partial^2 S(\bar{\pi}(a_0|x), t)}{\partial \bar{\pi}^2} \{\pi(a_0|x) - \bar{\pi}(a_0|x)\}^2 + R_3(\pi - \bar{\pi}) \right] da_0 dP(x), \text{ and} \end{aligned}$$

$$R_2^{\text{den}}(\bar{P}, P) = - \int \int K_h(a_0 - a) \left[\frac{1}{2} \frac{\partial^2 S(\bar{\pi}(a_0|x), t)}{\partial \bar{\pi}^2} \{\pi(a_0|x) - \bar{\pi}(a_0|x)\}^2 + R_3(\pi - \bar{\pi}) \right] da_0 dP(x),$$

where $\bar{\pi}$ and $\bar{\mu}$ denote the propensity score and outcome regression under probability measure \bar{P} , and $R_3(\bar{\pi} - \pi)$ denotes the third-order remainder of the Taylor expansion of $S(\pi(a_0|x), t)$ around $\bar{\pi}(a_0|x)$. This demonstrates that sufficient conditions for the remainders of $\psi^{\text{num}}(a; t)$ and $\psi^{\text{den}}(a; t)$ to be $o_P(n^{-1/2})$ are that $\|\hat{\pi}(a|x) - \pi(a|x)\|^2 = o_P(n^{-1/2})$ and $\|\hat{\pi}(a|x) - \pi(a|x)\| \cdot \|\hat{\mu}(x, a) - \mu(x, a)\| = o_P(n^{-1/2})$.

The first two terms of $\varphi_h^{\text{num}}(a; t)$ are analogous to the terms that define the EIF $\varphi_h(a)$ in (6). Meanwhile, the two additional terms in $\varphi_h^{\text{num}}(a; t)$ reflect the fact that the smoothed trimming indicator $S(\pi(a|x), t)$ depends on the propensity score; this is why these terms also appear in $\varphi_h^{\text{den}}(a; t)$, which represents the EIF for the proportion of non-trimmed subjects. Thus, estimators based on the EIFs in Theorem 1 will reflect uncertainty in the estimated non-trimmed population, due to uncertainty in estimating the propensity score.

The one-step estimators based on the uncentered EIFs in Theorem 1 are again empirical averages of their estimated analogs. Let $\hat{\varphi}_h^{\text{num}}(a; t)$ be equal to $\varphi_h^{\text{num}}(a; t)$, but with $\mu(x, a)$ and $\pi(a|x)$ replaced by their estimators $\hat{\mu}(x, a)$ and $\hat{\pi}(a|x)$. Let $\hat{\varphi}_h^{\text{den}}(a; t)$ be analogously

defined. Then, the one-step estimators based on Theorem 1 are:

$$\widehat{\psi}_h^{\text{num}}(a; t) = \mathbb{P}_n \{ \widehat{\varphi}_h^{\text{num}}(a; t) \}, \quad \text{and} \quad \widehat{\psi}_h^{\text{den}}(a; t) = \mathbb{P}_n \{ \widehat{\varphi}_h^{\text{den}}(a; t) \}, \quad (11)$$

and an estimator for the estimand of interest, $\psi_h(a; t)$, is

$$\widehat{\psi}_h(a; t) = \widehat{\psi}_h^{\text{num}}(a; t) / \widehat{\psi}_h^{\text{den}}(a; t). \quad (12)$$

To establish the asymptotic distribution of $\widehat{\psi}_h(a; t)$ such that we can conduct inference, we must make further assumptions about the estimators $\widehat{\mu}(x, a)$ and $\widehat{\pi}(a|x)$. One option is to employ Donsker-type conditions on the EIFs in Theorem 1 and their corresponding estimators in (11), which assume that these functions are not overly complex; however, these conditions may require that $\mu(x, a)$ and $\pi(a|x)$ are not high-dimensional or that their estimators do not utilize adaptive methods like random forests (Zheng and Van Der Laan, 2010; Chernozhukov et al., 2018). Instead, we will assume that the sample used to estimate $\mu(x, a)$ and $\pi(a|x)$ is independent of the sample used to compute $\widehat{\psi}_h(a; t)$ in (12). For example, this can be achieved via sample-splitting, where the data is randomly divided into two halves. Given this assumption and standard arguments, we can use Theorem 1 to show that if (1) the estimation rate of $\pi(a|x)$ is at least $o_P(n^{-1/4})$, and (2) the product of estimation rates for $\mu(x, a)$ and $\pi(a|x)$ is at least $o_P(n^{-1/2})$, then $\widehat{\psi}_h(a; t)$ is asymptotically Normal. This allows for flexible estimation of $\mu(x, a)$ and $\pi(a|x)$ while still admitting valid inference. This is stated formally below.

Proposition 1. *If the trimming threshold t is fixed, $\mu(x, a)$ and $\pi(a|x)$ are estimated on an independent sample of size n ,*

$$\left(\|\widehat{\pi}(a|X) - \pi(a|X)\| + \|\widehat{\mu}(X, a) - \mu(X, a)\| \right) \|\widehat{\pi}(a|X) - \pi(a|X)\| = o_P(n^{-1/2}),$$

and the estimated EIFs are consistent such that $\|\widehat{\varphi}_h^{\text{num}}(a; t) - \varphi_h^{\text{num}}(a; t)\| = o_p(1)$ and $\|\widehat{\varphi}_h^{\text{den}}(a; t) - \varphi_h^{\text{den}}(a; t)\| = o_p(1)$, then

$$\sqrt{n} \left(\widehat{\psi}_h(a; t) - \psi_h(a; t) \right) \rightarrow N \left(0, \text{Var} \left\{ \frac{\varphi_h^{\text{num}}(a; t) - \psi_h(a; t) \varphi_h^{\text{den}}(a; t)}{\psi_h^{\text{den}}(a; t)} \right\} \right), \quad (13)$$

where $\varphi_h^{\text{num}}(a; t)$ and $\varphi_h^{\text{den}}(a; t)$ are the uncentered EIFs of $\psi_h^{\text{num}}(a; t)$ and $\psi_h^{\text{den}}(a; t)$, defined in Theorem 1.

To prove Proposition 1, we show that $\widehat{\psi}_h^{\text{num}}(a; t)$ and $\widehat{\psi}_h^{\text{den}}(a; t)$ are asymptotically Normal with means equal to their respective estimands and variances equal to $\text{Var}\{\varphi_h^{\text{num}}(a; t)\}/n$

and $\text{Var}\{\varphi_h^{\text{den}}(a; t)\}/n$. Then, Proposition 1 follows by the delta method. The independent-sample assumption, combined with the assumption that $\widehat{\varphi}_h^{\text{num}}(a; t)$ and $\widehat{\varphi}_h^{\text{den}}(a; t)$ are consistent at any rate, ensures that the empirical process term of the von Mises expansions for the EIFs in Theorem 1 are $o_P(n^{-1/2})$. Meanwhile, the rate conditions on $\widehat{\mu}(x, a)$ and $\widehat{\pi}(a|x)$ ensure that the corresponding remainder terms, defined in Remark 1, are also $o_P(n^{-1/2})$. This is weaker than assuming a well-specified parametric model for $\mu(x, a)$ and $\pi(a|x)$, and thus allows for flexible models that converge at a slower rate, such as lasso, random forests, and neural networks (Farrell, 2015; Chernozhukov et al., 2018; Farrell et al., 2021). This condition also suggests that the convergence rate for $\widehat{\pi}(a|x)$ is more crucial than that for $\widehat{\mu}(x, a)$: We require that $\|\widehat{\pi}(a|x) - \pi(a|x)\| = o_P(n^{-1/4})$, whereas $\widehat{\mu}(x, a)$ can converge more slowly if $\widehat{\pi}(a|x)$ converges faster than $o_P(n^{-1/4})$ (e.g., as in a well-specified parametric model). This is intuitive within the context of trimming: If the set of non-trimmed subjects cannot be well-estimated, then we cannot accurately estimate causal effects among those subjects.

The independent-sample assumption in Proposition 1 may seem to suggest that we need to use half our data to model $\mu(x, a)$ and $\pi(a|x)$, and half to compute $\widehat{\psi}_h(a; t)$, resulting in reduced efficiency. However, in practice, we recommend a sample-splitting and cross-fitting procedure to utilize the whole sample (Schick, 1986; Robins et al., 2008; Zheng and Van Der Laan, 2010). In this procedure, $\widehat{\mu}(x, a)$ and $\widehat{\pi}(a|x)$ are constructed on one half of the sample, $\widehat{\varphi}_h^{\text{num}}(a; t)$ and $\widehat{\varphi}_h^{\text{den}}(a; t)$ are constructed on the other half, and the process is repeated with the halves swapped to obtain estimates $\widehat{\varphi}_h^{\text{num}}(a; t)$ and $\widehat{\varphi}_h^{\text{den}}(a; t)$ for the whole sample. More than two folds are also possible. For a review of sample-splitting and cross-fitting for doubly robust estimators, see Chernozhukov et al. (2018) and Kennedy (2022).

Proposition 1 suggests a straightforward way to construct confidence intervals for $\psi_h(a; t)$. First, note that $\psi_h^{\text{den}}(a; t)$ and $\psi_h(a; t)$ can be consistently estimated by $\widehat{\psi}_h^{\text{den}}(a; t)$ in (11) and $\widehat{\psi}_h(a; t)$ in (12). Then, Proposition 1 suggests the following $(1 - \alpha)$ -level confidence interval:

$$\widehat{\psi}_h(a; t) \pm z_{\alpha/2} \sqrt{\frac{\text{Var}_n \left\{ \frac{\widehat{\varphi}_h^{\text{num}}(a; t) - \widehat{\psi}_h(a; t) \widehat{\varphi}_h^{\text{den}}(a; t)}{\widehat{\psi}_h^{\text{den}}(a; t)} \right\}}{n}}, \quad (14)$$

where $z_{\alpha/2}$ is the $\alpha/2$ quantile of a standard Normal distribution and $\text{Var}_n\{\cdot\}$ denotes a sample variance.

The above results assume that the trimming threshold t is fixed. In practice, we may want the trimming threshold to be data-driven, especially if positivity violations are more or less severe for certain treatment values. In the following subsection, we define t as a quantile of the propensity score $\pi(a|X)$, which must be estimated and will depend on the treatment value a . Estimating $\psi_h^{\text{num}}(a; t)$ and $\psi_h^{\text{den}}(a; t)$ separately provides a useful way to estimate t ,

as well as to estimate $\psi_h(a; t)$ in a way that incorporates uncertainty in estimating t .

3.2 When the Trimming Threshold is an Unknown Parameter

It can be difficult to specify a trimming threshold *a priori*, and thus it is common to frame t as a parameter that must be estimated. For example, one common choice is the γ -quantile of the propensity score (Cole and Hernán, 2008; Stürmer et al., 2010; Lee et al., 2011):

$$t_0 = F_a^{-1}(\gamma), \quad (15)$$

where $F_a^{-1}(\cdot)$ is the inverse of the CDF of $\pi(a|X)$. We use t_0 to denote the true trimming threshold, which in this case must be estimated. The estimand is then denoted as $\psi_h(a; t_0)$, i.e., the STATE when the trimming threshold is equal to t_0 .

One way to estimate t_0 is to take the empirical γ -quantile of the estimated propensity scores $\hat{\pi}(a|X)$. However, this demonstrates that estimation of t_0 also depends on estimation of $\pi(a|X)$. Thus, estimating t_0 will affect the EIFs for $\psi_h^{\text{num}}(a; t_0)$ and $\psi_h^{\text{den}}(a; t_0)$, which define the estimand $\psi_h(a; t_0)$. When t_0 is defined as (15), the EIF of t_0 does not exist, because (15) corresponds to the quantile of an unknown density. In order to admit an EIF, we instead define t_0 as a smoothed γ -quantile of $\pi(a|X)$:

$$t_0 = F_{a,h}^{-1}(\gamma), \quad (16)$$

where $F_{a,h}(t) = 1 - \int \int K_h(a_0 - a)S(\pi(a_0|x), t)da_0dP(x)$ is the smoothed CDF of $\pi(a|X)$. This is equivalent to defining t_0 as the threshold such that $\psi_h^{\text{den}}(a; t_0) = 1 - \gamma$.

In Section 3.1 we derived an efficient estimator for $\psi_h^{\text{den}}(a; t)$ for any fixed t . Thus, a natural way to estimate t_0 is to choose the t such that our estimator $\hat{\psi}_h^{\text{den}}(a; t) = 1 - \gamma$:

$$\hat{t} = \inf\{t : \hat{\psi}_h^{\text{den}}(a; t) \leq 1 - \gamma\}, \quad (17)$$

where $\hat{\psi}_h^{\text{den}}(a; t)$ is defined in (11). In practice, \hat{t} can be computed via a line search after $\hat{\psi}_h^{\text{den}}(a; t)$ is constructed for any fixed t . Then, a natural estimator for $\psi_h(a; t_0)$ is:

$$\hat{\psi}_h(a; \hat{t}) = \hat{\psi}_h^{\text{num}}(a; \hat{t}) / (1 - \gamma), \quad (18)$$

where $\hat{\psi}_h^{\text{num}}(a; t)$ is the estimator $\hat{\psi}_h^{\text{num}}(a; t)$ in (11) with t set equal to \hat{t} in (17).

To study the behavior of $\hat{\psi}_h(a; \hat{t})$, we can decompose its error by writing

$$\hat{\psi}_h(a; \hat{t}) - \psi_h(a; t_0) = (1 - \gamma)^{-1} \left(\hat{\psi}_h^{\text{num}}(a; \hat{t}) - \psi_h^{\text{num}}(a; \hat{t}) + \psi_h^{\text{num}}(a; \hat{t}) - \psi_h^{\text{num}}(a; t_0) \right).$$

The first term represents our error in estimating $\psi_h^{\text{num}}(a; t)$ for a fixed t . As established by Theorem 1, this will behave like a sample average as long as the estimation rate of $\pi(a|x)$ is at least $o_P(n^{-1/4})$ and the product of estimation rates for $\mu(x, a)$ and $\pi(a|x)$ is at least $o_P(n^{-1/2})$. Meanwhile, the second term represents our error in estimating t_0 , which depends on our error in estimating $\psi_h^{\text{den}}(a; t)$ for any fixed t ; this will also behave like a sample average as long as the estimation rate of $\pi(a|x)$ is at least $o_P(n^{-1/4})$. Thus, the error of our estimator can be decomposed into the error in estimating $\psi_h^{\text{num}}(a; t)$ and the error in estimating $\psi_h^{\text{den}}(a; t)$ for any fixed t . This is stated formally in Theorem 2. For the following theorem, we write the uncentered EIF $\varphi_h^{\text{num}}(a; t)$ as $\varphi_h^{\text{num}}(a; t, \eta)$ for $\eta = (\pi, \mu)$ to emphasize its dependency on the propensity score $\pi(a|x)$ and outcome regression $\mu(x, a)$. For example, we can write our estimator for $\psi_h^{\text{num}}(a; t)$ as $\widehat{\psi}_h^{\text{num}}(a; t) = \mathbb{P}_n\{\varphi_h^{\text{num}}(a; t, \widehat{\eta})\}$.

Theorem 2. *Let t_0 denote the true trimming threshold for a given $\gamma \in (0, 1)$. Furthermore, let $\eta_0 = (\pi_0, \mu_0)$ denote the true propensity score and true outcome regression. Finally, let $\varphi_h^{\text{num}}(a; t, \eta)$ and $\varphi_h^{\text{den}}(a; t, \eta)$ denote the uncentered EIFs of $\psi_h^{\text{num}}(a; t)$ and $\psi_h^{\text{den}}(a; t)$, defined in Theorem 1. Assume that*

1. *The propensity score and outcome regression estimators $\widehat{\eta} = (\widehat{\pi}, \widehat{\mu})$ are estimated on an independent sample of size n (e.g. via sample-splitting).*
2. *The function classes $\{\varphi_h^{\text{num}}(a; t, \eta) : t \in \mathbb{R}^+\}$ and $\{\varphi_h^{\text{den}}(a; t, \eta) : t \in \mathbb{R}^+\}$ are Donsker in t for any fixed η .*
3. *The trimming threshold estimator, propensity score estimator, and outcome regression estimator are consistent, i.e., $|\widehat{t} - t_0| = o_P(1)$ and $\|\widehat{\eta} - \eta_0\| = o_P(1)$. Furthermore, the estimated EIFs are consistent, i.e., $\|\widehat{\varphi}_h^{\text{num}}(a; t) - \varphi_h^{\text{num}}(a; t)\| = o_p(1)$ and $\|\widehat{\varphi}_h^{\text{den}}(a; t) - \varphi_h^{\text{den}}(a; t)\| = o_p(1)$ for any fixed t .*
4. *The maps $t \mapsto \psi_h^{\text{num}}(a; t, \eta)$ and $t \mapsto \psi_h^{\text{den}}(a; t, \eta)$ are differentiable at t_0 uniformly in η , where $\frac{\partial}{\partial t}\psi_h^{\text{num}}(a; t_0, \widehat{\eta}) \xrightarrow{p} \frac{\partial}{\partial t}\psi_h^{\text{num}}(a; t_0, \eta_0)$ and $\frac{\partial}{\partial t}\psi_h^{\text{den}}(a; t_0, \widehat{\eta}) \xrightarrow{p} \frac{\partial}{\partial t}\psi_h^{\text{den}}(a; t_0, \eta_0)$. Furthermore, $|\frac{\partial}{\partial t}\psi_h^{\text{num}}(a; t_0, \eta_0)|$ and $|1/\frac{\partial}{\partial t}\psi_h^{\text{den}}(a; t_0, \eta_0)|$ are bounded.*

Then,

$$(1 - \gamma)\{\widehat{\psi}_h(a; \widehat{t}) - \psi_h(a; t_0)\} = (\mathbb{P}_n - \mathbb{P})\{\varphi_h^{\text{num}}(a; t_0, \eta_0)\} - \frac{\partial\psi_h^{\text{num}}(a; t_0, \eta_0)/\partial t}{\partial\psi_h^{\text{den}}(a; t_0, \eta_0)/\partial t}(\mathbb{P}_n - \mathbb{P})\{\varphi_h^{\text{den}}(a; t_0, \eta_0)\} \\ + O_P(R_2^{\text{num}}) + O_P(R_2^{\text{den}}) + o_P(n^{-1/2}),$$

where $R_2^{\text{num}} = \mathbb{P}\{\varphi_h^{\text{num}}(a; t_0, \widehat{\eta}) - \varphi_h^{\text{num}}(a; t_0, \eta_0)\}$ and $R_2^{\text{den}} = \mathbb{P}\{\varphi_h^{\text{den}}(a; t_0, \widehat{\eta}) - \varphi_h^{\text{den}}(a; t_0, \eta_0)\}$.

Before discussing the consequences of Theorem 2, we first discuss its assumptions. Similar to Proposition 1, the first assumption ensures the nuisance functions are estimated on an independent sample, so that the numerator and denominator estimators behave like sample averages. The second assumption requires that the EIFs in Theorem 1 are not overly complex functions of t , although they can be arbitrarily complex functions of the outcome regression and propensity score. The third assumption only requires that the trimming threshold, nuisance functions, and EIFs are consistently estimated at any rate. Finally, the last assumption requires that the numerator and denominator estimands are somewhat smooth in t , such that we can use a Taylor expansion to characterize the behavior of the threshold estimator's bias, $\hat{t} - t_0$.

Theorem 2 establishes that $\hat{\psi}_h(a; \hat{t})$ in (18) is $n^{-1/2}$ consistent and asymptotically Normal if $\psi_h^{\text{num}}(a; t)$ and $\psi_h^{\text{den}}(a; t)$ are estimated at $n^{-1/2}$ rates; this is the case when $\|\hat{\pi}(a|x) - \pi(a|x)\|^2 = o_P(n^{-1/2})$ and $\|\hat{\pi}(a|x) - \pi(a|x)\| \cdot \|\hat{\mu}(x, a) - \mu(x, a)\| = o_P(n^{-1/2})$. Thus, we can still conduct valid inference even when the propensity score and outcome regression are flexibly estimated at nonparametric rates. This is stated formally below.

Corollary 1. *Assume that Assumptions 1-4 in Theorem 2 hold. Then, if \hat{t} is estimated as in (17), and $\mu(x, a)$ and $\pi(a|x)$ are estimated on an independent sample of size n such that*

$$\left(\|\hat{\pi}(a|X) - \pi(a|X)\| + \|\hat{\mu}(X, a) - \mu(X, a)\| \right) \|\hat{\pi}(a|X) - \pi(a|X)\| = o_P(n^{-1/2}),$$

then,

$$\sqrt{n}(1 - \gamma) \left(\hat{\psi}_h(a; \hat{t}) - \psi_h(a; t_0) \right) \rightarrow N \left(0, \text{Var} \left\{ \varphi_h^{\text{num}}(a; t_0) - \frac{\partial \psi_h^{\text{num}}(a; t_0) / \partial t}{\partial \psi_h^{\text{den}}(a; t_0) / \partial t} \varphi_h^{\text{den}}(a; t_0) \right\} \right), \quad (19)$$

where $\varphi_h^{\text{num}}(a; t_0)$ and $\varphi_h^{\text{den}}(a; t_0)$ are the uncentered EIFs of $\psi_h^{\text{num}}(a; t)$ and $\psi_h^{\text{den}}(a; t)$, defined in Theorem 1.

It's worth noting that, when t is fixed as in Section 3.1, Theorem 1 implies that when $\left(\|\hat{\pi}(a|X) - \pi(a|X)\| + \|\hat{\mu}(X, a) - \mu(X, a)\| \right) \|\hat{\pi}(a|X) - \pi(a|X)\| = o_P(n^{-1/2})$, then

$$\sqrt{n} \left(\hat{\psi}_h^{\text{num}}(a; t) - \psi_h^{\text{num}}(a; t) \right) \rightarrow N \left(0, \text{Var} \left\{ \varphi_h^{\text{num}}(a; t) \right\} \right).$$

Thus, Corollary 1 demonstrates that allowing t to be estimated induces additional uncertainty, as reflected by the presence of $\varphi_h^{\text{den}}(a; t_0)$, which is used to estimate the threshold.

Corollary 1 suggests that, in order to conduct inference, we must estimate the derivatives $\partial \psi_h^{\text{num}}(a; t_0) / \partial t$ and $\partial \psi_h^{\text{den}}(a; t_0) / \partial t$. First, define $\varphi_h^{\text{num}}(a; t)$ as the derivative of $\varphi_h^{\text{num}}(a; t)$

with respect to t ; this is equal to $\varphi_h^{\text{num}}(a; t)$ in Theorem 1, but with the smoothed indicator $S(\pi(a|x), t)$ replaced by its derivative $\partial S(\pi(a|x), t)/\partial t$ and the derivative $\partial S(\pi(a|x), t)/\partial \pi$ replaced with its second-order partial derivative $\partial^2 S(\pi(a|x), t)/\partial \pi \partial t$. Define $\varphi_h^{\text{den}}(a; t)$ analogously. Then, assuming suitable regularity conditions such that we can exchange derivatives and expectations, natural estimators for these derivatives are

$$\widehat{\psi}_h^{\text{num}}(a; \widehat{t}) = \mathbb{P}_n \{ \widehat{\varphi}_h^{\text{num}}(a; \widehat{t}) \}, \quad \text{and} \quad \widehat{\psi}_h^{\text{den}}(a; \widehat{t}) = \mathbb{P}_n \{ \widehat{\varphi}_h^{\text{den}}(a; \widehat{t}) \},$$

where $\widehat{\varphi}_h^{\text{num}}(a; \widehat{t})$ and $\widehat{\varphi}_h^{\text{den}}(a; \widehat{t})$ are equal to $\varphi_h^{\text{num}}(a; t)$ and $\varphi_h^{\text{den}}(a; t)$, but with $\mu(x, a)$ and $\pi(a|x)$ replaced by $\widehat{\mu}(x, a)$ and $\widehat{\pi}(a|x)$, and with t replaced by \widehat{t} in (17). Then, Corollary 1 suggests the following $(1 - \alpha)$ -level confidence interval for $\psi_h(a; t)$:

$$\widehat{\psi}_h(a; \widehat{t}) \pm z_{\alpha/2} \sqrt{\frac{\text{Var}_n \left\{ \widehat{\varphi}_h^{\text{num}}(a; \widehat{t}) - \frac{\widehat{\psi}_h^{\text{num}}(a; \widehat{t})}{\widehat{\psi}_h^{\text{den}}(a; \widehat{t})} \widehat{\varphi}_h^{\text{den}}(a; \widehat{t}) \right\}}{n(1 - \gamma)^2}}. \quad (20)$$

Similar to Corollary 1, here we assumed that $\mu(x, a)$ and $\pi(a|x)$ are estimated on an independent sample. In practice, we recommend employing a sample-splitting and cross-fitting procedure when computing $\widehat{\psi}_h(a; \widehat{t})$ and the above confidence interval, as discussed in Section 3.1. Compared to Section 3.1, the only additional nuance is that we need to compute the estimated trimming threshold \widehat{t} in (17). In practice, one can follow the cross-fitting procedure in Section 3.1 to construct the estimators $\widehat{\psi}_h^{\text{num}}(a; t)$ and $\widehat{\psi}_h^{\text{den}}(a; t)$ for any fixed t . Then, one can repeat this procedure across a line search of t values to select \widehat{t} such that $\widehat{\psi}_h^{\text{den}}(a; \widehat{t}) = 1 - \gamma$ for a prespecified $\gamma \in (0, 1)$. Note that the estimates for $\mu(x, a)$ and $\pi(a|x)$ only need to be fit twice (once for one half of the data, and once for the other half of the data), and then these same estimates can be used across different choices of t .

4 Choosing Bandwidth h and Smoothing Parameter ϵ

In Section 3, we derived estimators for the STATE $\psi_h(a; t)$ in (5) based on the efficient influence functions for $\psi_h^{\text{num}}(a; t)$ and $\psi_h^{\text{den}}(a; t)$ in (8) and (9). Throughout, we assumed that the bandwidth h for the kernel $K_h(\cdot)$ and the smoothing parameter ϵ for the smoothed indicator $S(\pi(a|x), t) = \Phi_\epsilon\{\pi(a|x) - t\}$ were also prespecified. Here we outline how to specify these tuning parameters in practice. We provide a data-driven procedure for selecting the bandwidth h by minimizing the expected squared difference between our smoothed trimmed ATE (STATE) estimator $\widehat{\psi}_h(a; t)$ and a non-smoothed analog. Meanwhile, we provide a rule-of-thumb to select the smoothing parameter ϵ based on entropy. For notational simplicity

we consider the trimming threshold t fixed in this section; however, our procedures would remain the same if t were estimated, e.g. using Equation (17).

4.1 Risk Minimization Procedure to Select Bandwidth h

Recall that, when incorporating kernel smoothing, our estimand is the STATE $\psi_h(a; t)$, defined in (5). The non-smoothed analog of this estimand is

$$\tilde{\psi}(a; t) = \frac{\int S(\pi(a|x), t)\mu(x, a)dP(x)}{\int S(\pi(a|x), t)dP(x)},$$

where we still incorporate smoothing in the trimming indicator $\mathbb{I}(\pi(a|x) > t)$ via $S(\pi(a|x), t)$, and we still view its smoothing parameter ϵ as fixed. Intuitively, we would like to choose a bandwidth such that $\psi_h(a; t)$ is close to $\tilde{\psi}(a; t)$, and we can consistently estimate $\psi_h(a; t)$ with our estimator $\hat{\psi}_h(a; t)$. A ubiquitous way to estimate bandwidths in nonparametric regression and density estimation problems is to minimize an estimate of mean squared error (Silverman, 1986; Fan and Gijbels, 1996; Wasserman, 2006), and we take the same approach to choose h . Specifically, we consider minimizing the expected squared difference (or “risk”) between $\hat{\psi}_h(a; t)$ and $\tilde{\psi}(a; t)$ among a set of candidate bandwidths \mathcal{H} :

$$\arg \min_{h \in \mathcal{H}} \int \left\{ \hat{\psi}_h(a; t) - \tilde{\psi}(a; t) \right\}^2 w(a) da = \arg \min_{h \in \mathcal{H}} \int \left\{ \hat{\psi}_h^2(a; t) - 2\hat{\psi}_h(a; t)\tilde{\psi}(a; t) \right\} w(a) da,$$

where $w(a)$ is a weight function. The above equality holds because $\tilde{\psi}(a; t)$ does not depend on h . Define the above objective function as

$$R\left(\hat{\psi}_h\right) = \int \left\{ \hat{\psi}_h^2(a; t) - 2\hat{\psi}_h(a; t)\tilde{\psi}(a; t) \right\} w(a) da. \quad (21)$$

Note that (21) is not a function of a ; it is the squared error averaged across treatment values. Thus, we choose a single bandwidth h that is used for $\hat{\psi}_h(a; t)$ across all treatment values, and do not let h vary across a . Our procedure involves constructing a risk estimator $\hat{R}\left(\hat{\psi}_h\right)$ and, among candidate bandwidths \mathcal{H} , selecting the bandwidth as

$$\hat{h} = \arg \min_{h \in \mathcal{H}} \hat{R}\left(\hat{\psi}_h\right). \quad (22)$$

Equation (21) depends on the weight function $w(a)$. A natural choice is

$$w(a) = \int S(\pi(a|x), t)dP(x). \quad (23)$$

This weight represents the smoothed proportion of non-trimmed subjects; it will be small for treatment values with many propensity scores below the trimming threshold t . Given weight $w(a)$ in (23), the objective function becomes

$$R(\widehat{\psi}_h) = \int \int \widehat{\psi}_h^2(a; t) S(\pi(a|x), t) da dP(x) - 2 \int \int \widehat{\psi}_h(a; t) S(\pi(a|x), t) \mu(x, a) da dP(x). \quad (24)$$

Thus, once $\widehat{\psi}_h(a; t)$ is computed for a given bandwidth, a natural estimator for the risk is

$$\widehat{R}(\widehat{\psi}_h) = \mathbb{P}_n \left\{ \int \widehat{\psi}_h^2(a; t) S(\widehat{\pi}(a|x), t) da \right\} - 2 \mathbb{P}_n \left\{ \int \widehat{\psi}_h(a; t) S(\widehat{\pi}(a|x), t) \widehat{\mu}(x, a) da \right\}. \quad (25)$$

As discussed in Section 3.1, the sample used to estimate $\pi(a|x)$ and $\mu(x, a)$ must be independent of the sample used to compute $\widehat{\psi}_h(a; t)$. Thus, in practice, the data is split into halves, where the first half is used to estimate $\pi(a|x)$ and $\mu(x, a)$, and the second half is used to compute $\widehat{\psi}_h(a; t)$ and $\widehat{R}(\widehat{\psi}_h)$. As discussed in Section 3.1, cross-fitting can also be used to utilize the full sample size. This process can be computed for all candidate bandwidths $h \in \mathcal{H}$, and finally the bandwidth can be selected using \widehat{h} in (22).

Remark 2. *The first term in the risk (24) is the same as $\psi_h^{den}(a; t)$ in (9), but with the kernel $K_h(\cdot)$ is replaced with $\widehat{\psi}_h^2(a; t)$. Meanwhile, the second term is the same as $\psi_h^{num}(a; t)$ in (8), but with $K_h(\cdot)$ replaced with $\widehat{\psi}_h(a; t)$. Thus, an alternative risk estimator can be derived based on the EIF of (24), which will involve the EIFs in Theorem 1 with the kernel terms replaced with $\widehat{\psi}_h^2(a; t)$ or $\widehat{\psi}_h(a; t)$. This requires computing $\widehat{\psi}_h(A; t)$, i.e., the estimated treatment effect at every observed treatment value, which may be far from the treatment values where causal effects were estimated. Thus, we recommend the risk estimator (25) in practice.*

4.2 Entropy-based Procedure to Select Smoothing Parameter ϵ

Unlike kernel smoothing with bandwidth h , smoothing the trimming indicator $\mathbb{I}(\pi(a|x) > t)$ via $S(\pi(a|x), t)$ with parameter ϵ does not naturally suggest a data-driven selection procedure. Indeed, Yang and Ding (2018) recommend simply conducting several analyses for different choices of ϵ , and assess if the analysis is sensitive to this choice. While we also recommend this sensitivity analysis in practice, researchers may nonetheless want some guidance for how to choose ϵ . Here we consider a way to interpret ϵ that suggests a rule-of-thumb for selecting this parameter. Although our parameter ϵ refers to our example $S(\pi(a|x), t) = \Phi_\epsilon\{\pi(a|x) - t\}$, where $\Phi_\epsilon(\cdot)$ is the CDF of $N(0, \epsilon^2)$, the following interpretation would apply for any smoothed indicator function with its own smoothing parameter.

In general, a trimmed estimand is a weighted average with weights proportional to $S(\pi(a|x), t)$. For example, when $\epsilon \rightarrow \infty$, $S(\pi(a|x), t) = 0.5$, and thus every subject contributes equally to this average. Meanwhile, when $\epsilon \rightarrow 0$, $S(\pi(a|x), t) = \mathbb{I}(\pi(a|x) > t)$, and thus only subjects with propensity scores above t contribute to this average. Thus, we can interpret a trimmed estimand as an average among subjects who are randomly selected via a selection variable $S|X \sim \text{Bern}\{s(a|X)\}$, where we write $s(a|x) = S(\pi(a|x), t)$ for notational simplicity. To aid in interpreting ϵ , we consider the entropy of this selection rule, defined as:

$$H(S|X) = -\mathbb{E}[s(a|X) \log_2\{s(a|X)\} + \{1 - s(a|X)\} \log_2\{1 - s(a|X)\}]. \quad (26)$$

Again consider the two extremes of ϵ . When $\epsilon \rightarrow \infty$, $s(a|X) = 0.5$ and $H(S|X) = -\mathbb{E}[\log_2(0.5)] = 1$. When $\epsilon \rightarrow 0$, $s(a|X) = \mathbb{I}(\pi(a|X) > t)$ and

$$H(S|X) = -\mathbb{E}[\mathbb{I}(\pi(a|X) > t) \log_2\{\mathbb{I}(\pi(a|X) > t)\} + \mathbb{I}(\pi(a|X) \leq t) \log_2\{\mathbb{I}(\pi(a|X) \leq t)\}] = 0.$$

In practice, intermediate values of ϵ that lead to small, non-zero entropy will be most useful. For example, one could choose ϵ such that $H(S|X) \approx 0.05$; this would have the same entropy as a coin flip whose probability of heads is 0.9944.

This introduces the following procedure for selecting ϵ . First, estimate the propensity score $\pi(a|x)$. Then, consider a set of candidate parameters $\epsilon \in \mathcal{E}$ (e.g., $10^{-1}, 10^{-2}, \dots$). For each ϵ , compute the estimated entropy:

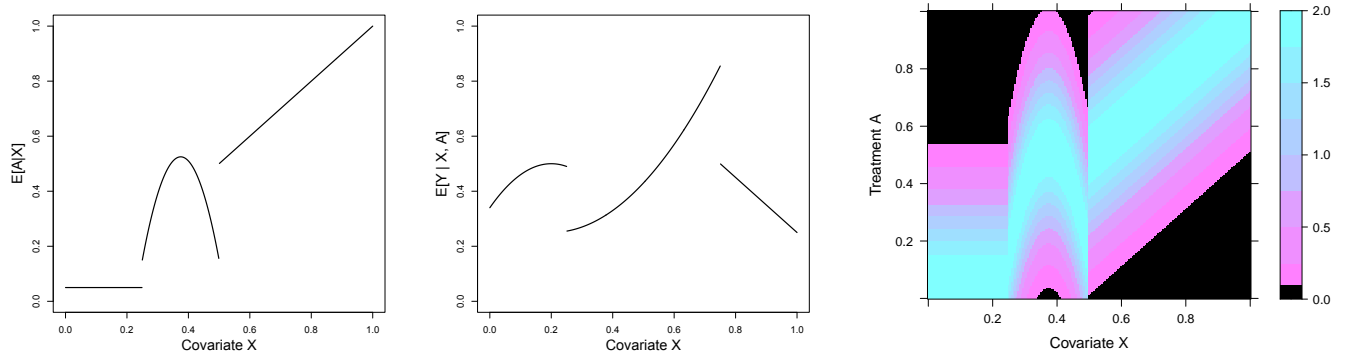
$$\widehat{H}_\epsilon(S|X) = -\mathbb{P}_n[\widehat{s}(a|X) \log_2\{\widehat{s}(a|X)\} + \{1 - \widehat{s}(a|X)\} \log_2\{1 - \widehat{s}(a|X)\}] \quad (27)$$

where $\widehat{s}(a|X) = S(\widehat{\pi}(a|X), t)$. Finally, choose the ϵ such that $\widehat{H}_\epsilon(S|X)$ is close to an intermediate value, e.g. 0.05. While such a choice does not optimize a measure of error (e.g., risk, as in the previous subsection), it nonetheless provides a way to interpret ϵ in practice.

In the following section, we present simulation results when, for simplicity, h and ϵ are fixed. Then, in Section 6, we present an application where we illustrate how to choose h and ϵ in practice using the above selection procedures.

5 Simulations

We consider an illustrative example with a covariate X that ranges from 0 to 1, a continuous outcome Y , and a continuous treatment A . As we describe below, we simulated data with positivity violations for some treatment values, motivating trimming, and where the propensity score and outcome regression were complex functions of X , motivating nonparametric



(a) $m(X) = \mathbb{E}[A|X]$, which defines the propensity score. (b) $\mu(X) = \mathbb{E}[Y|X, A]$, which doesn't depend on A . (c) $\pi(a|x)$ for $(a, x) \in [0, 1]^2$. Black denotes $\pi(a|x) < 0.1$.

Figure 1: Nuisance functions used in the data-generating process.

models. We generated 1000 datasets, each with $n = 1000$ subjects, as follows:

1. The covariate is generated as $X \sim \text{Unif}(0, 1)$.
2. The treatment A is generated as $A|X \sim N(m(X), 0.2^2)$, where $m(X)$ is visualized in Figure 1a.
3. The outcome Y is generated as $Y|X, A \sim N(\mu(X), 0.5^2)$, where $\mu(X)$ is visualized in Figure 1b. Thus, the conditional mean of Y does not depend on A .

The exact specification of $m(X)$ and $\mu(X)$ are in the Appendix (Section G). Here, $\mathbb{E}[A|X]$ ranges from 0 to 1. Thus, we consider estimating $\psi(a) = \mathbb{E}[Y(a)]$ for $a \in [0, 1]$. When consistency, unconfoundedness, and positivity hold, $\psi(a) = \mathbb{E}[\mu(X, a)]$, where $\mu(X, a) = \mathbb{E}[Y|X, A = a]$. For this example, $\mu(X, a) = \mu(X)$ for all a . Thus, the dose-response curve is flat, as is its smoothed counterpart $\psi_h(a) = \mathbb{E}[\int K_h(a_0 - a)\mu(x, a_0)da_0]$. A complication is that propensity scores are very small for some a . Figure 1c displays the true propensity scores $\pi(a|x)$ for $(x, a) \in [0, 1]^2$; areas where $\pi(a|x) < 0.1$ are in black. The propensity scores become smaller for a near 0 or 1, such that the edges of the dose-response curve are difficult to estimate.

We consider three estimands, shown in Table 1: The smoothed ATE (SATE); trimmed ATE (TATE), and smoothed trimmed ATE (STATE). The SATE $\psi_h(a)$ is a kernel-smoothed average of $\mu(X, a)$, the TATE $\psi(a; t)$ is an average of $\mu(X, a)$ among subjects with $\pi(a|X) > t$, and the STATE $\psi_h(a; t)$ averages $\mu(X, a)$ via kernel smoothing and a smoothed trimming indicator. Table 1 also displays the estimators we consider for each estimand. The SATE estimator averages the estimated efficient influence function (EIF) values $\hat{\varphi}_h(a)$, defined in

Estimand	Definition	Estimators
SATE	$\psi_h(a) = \int \int K_h(a_0 - a) \mu(x, a_0) da_0 dP(x)$	$\widehat{\psi}_h(a) = \mathbb{P}_n \{ \widehat{\varphi}_h(a) \}$
TATE	$\psi(a; t) = \frac{\int \mathbb{I}(\pi(a x) > t) \mu(x, a) dP(x)}{\int \mathbb{I}(\pi(a x) > t) dP(x)}$	$\widehat{\psi}(a; t) = \frac{\mathbb{P}_n \{ \mathbb{I}(\widehat{\pi}(a X) > t) \widehat{\mu}(X, a) \}}{\mathbb{P}_n \{ \mathbb{I}(\widehat{\pi}(a X) > t) \}}$ $\widehat{\psi}^{\text{alt}}(a; t) = \frac{\mathbb{P}_n \{ \mathbb{I}(\widehat{\pi}(a X) > t) \widehat{\varphi}_h(a) \}}{\mathbb{P}_n \{ \mathbb{I}(\widehat{\pi}(a X) > t) \}}$
STATE	$\psi_h(a; t) = \frac{\int \int K_h(a_0 - a) S(\pi(a_0 x), t) \mu(x, a_0) da_0 dP(x)}{\int \int K_h(a_0 - a) S(\pi(a_0 x), t) da_0 dP(x)}$	$\widehat{\psi}_h(a; t) = \frac{\widehat{\psi}_h^{\text{num}}(a; t)}{\widehat{\psi}_h^{\text{den}}(a; t)} = \frac{\mathbb{P}_n \{ \widehat{\varphi}_h^{\text{num}}(a; t) \}}{\mathbb{P}_n \{ \widehat{\varphi}_h^{\text{den}}(a; t) \}}$

Table 1: The three estimands SATE, TATE, and STATE, their definitions, and their respective estimators that we consider. The definitions of these estimands were originally defined in (2), (3), and (5), respectively.

(7). This is a doubly robust estimator based on the EIF for the SATE, but may perform poorly when propensity scores are small. Meanwhile, for the TATE, we consider two plug-in estimators. The first estimator averages $\widehat{\mu}(X, a)$ among subjects whose $\widehat{\pi}(a|X) > t$; we call this the “trimmed plug-in,” because it plugs $\widehat{\mu}(X, a)$ and $\widehat{\pi}(a|X)$ into the identification result for $\psi(a; t)$ in (3). The second estimator is similar, but replaces $\widehat{\mu}(X, a)$ with $\widehat{\varphi}_h(a)$; thus, it computes the typical doubly robust estimator on the trimmed sample, which is common in practice for binary treatments (Mao et al., 2019; Li, 2020; Zhang and Zhang, 2022; Huang et al., 2022). We call this the “EIF-based trimmed plug-in,” because it uses the estimated EIF values $\widehat{\varphi}_h(a)$ within a plug-in estimator. Finally, the STATE estimator is the estimator we derived in Section 3.

All these estimators depend on propensity score estimates $\widehat{\pi}(a|x)$ and outcome regression estimates $\widehat{\mu}(x, a)$. To remain agnostic to the type of estimators one may use for these nuisance functions, for each dataset we simulated estimators as, for any value a ,¹

$$\widehat{\pi}(a|X) \sim \pi(a|X) + 2 \cdot \text{expit}[\text{logit}\{\pi(a|X)/2\} + N(n^{-\alpha}, n^{-2\alpha})]$$

$$\widehat{\mu}(X, a) \sim \mu(X, a) + N(n^{-\alpha}, n^{-2\alpha}),$$

such that the root mean squared error (RMSE) of $\widehat{\pi}(a|X)$ and $\widehat{\mu}(X, a)$ are $O_P(n^{-\alpha})$, and thus we can control the estimators’ convergence rate via the rate parameter α . We used the transformation $\text{logit}\{\pi(a|X)/2\}$ to place propensity scores on the real line, such that simulating Normal errors is sensible (in this case, $\max_{a,x} \pi(a|x) \leq 2$, such that $\pi(a|x)/2 \in [0, 1]$ for all a and x). This follows previous simulation studies that evaluate causal effect estimators when nuisance functions are estimated at different rates (Kennedy, 2020; McClean et al., 2022; Zeng et al., 2023). We considered convergence rates $\alpha \in \{0.1, 0.2, 0.3, 0.4, 0.5\}$.

¹To compute the causal effect estimators for any given a , we simulated $\widehat{\pi}(A|X)$, $\widehat{\pi}(a|X)$, and $\widehat{\pi}(a_0|X)$ for $a_0 \in \{-0.5, -0.45, \dots, 1.45, 1.50\}$, and analogously for the outcome regression. The last quantity is needed to evaluate integrals over treatment values a_0 .

For the estimands and their estimators, we focus on a Gaussian kernel for $K_h(\cdot)$ with fixed bandwidth $h = 0.1$ and smoothed indicator $S(\pi(a|x), t) = \Phi_\epsilon\{\pi(a|x) - t\}$, where $\Phi_\epsilon(z)$ is the CDF of $N(0, \epsilon^2)$, with fixed $\epsilon = 0.01$. We first consider a fixed trimming threshold $t = 0.1$, and then consider estimating this threshold as a quantile of the propensity score. In the Appendix (Section H) we present results when instead the treatment is binary; the results are very similar.

5.1 Results When the Threshold is Fixed to $t = 0.1$

We implemented the four estimators for each of the 1000 simulated datasets to estimate causal effects for treatment values $a \in \{0, 0.05, \dots, 0.95, 1\}$. Following previous simulation studies for dose-response estimation (Kennedy et al., 2017; Wu et al., 2018), for a given estimand $\theta(a)$ and estimator $\hat{\theta}_s(a)$ on simulated dataset s , we computed its root mean squared error (RMSE), averaged across the distribution of A :

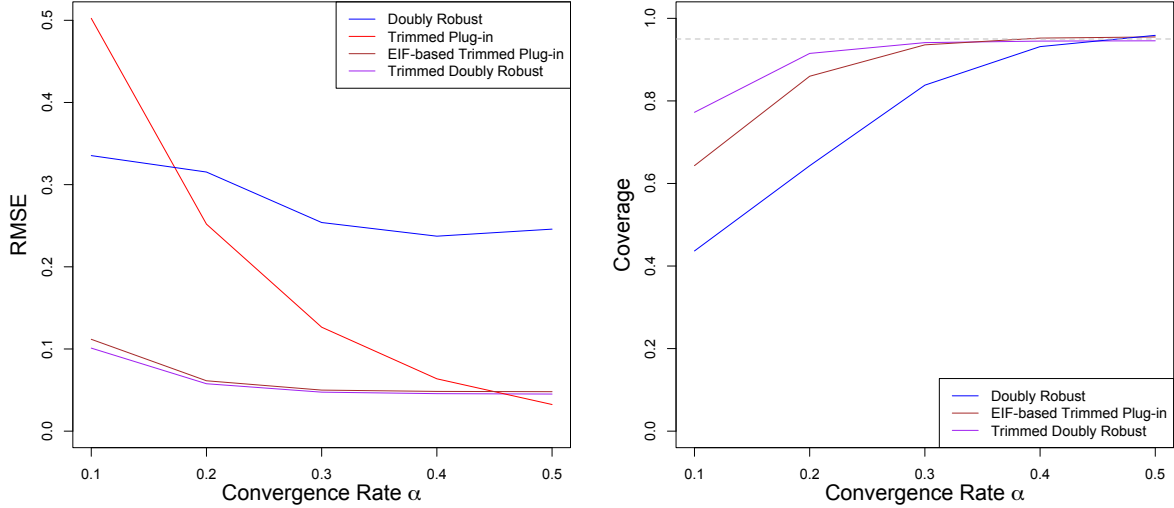
$$\text{RMSE} = \int \left(\frac{1}{1000} \sum_{s=1}^{1000} \{\hat{\theta}_s(a) - \theta(a)\}^2 \right)^{1/2} dP(a).$$

Figure 2a displays the RMSE for each estimator for different convergence rates for the nuisance functions, $\alpha \in \{0.1, 0.2, 0.3, 0.4, 0.5\}$. Our trimmed doubly robust estimator $\hat{\psi}_h(a; t)$, as well as the EIF-based trimmed plug-in estimator $\hat{\psi}^{\text{alt}}(a; t)$, both exhibit low RMSE across convergence rates. Meanwhile, the RMSE is high for the doubly robust estimator $\hat{\psi}_h(a)$, even for fast convergence rates, due to small propensity scores inflating its variance. Finally, the plug-in estimator $\hat{\psi}(a; t)$ inherits the convergence rate of nuisance function estimation, and thus also exhibits high RMSE unless the nuisance functions are estimated at an $\alpha = 0.5$ parametric rate.

We also considered the coverage of 95% confidence intervals. The 95% confidence interval for the typical doubly robust estimator is $\hat{\psi}_h(a) \pm z_{0.025} \sqrt{\text{Var}_n\{\hat{\varphi}_h(a)\}/n}$. Meanwhile, for the EIF-based trimmed plug-in estimator, we computed an analogous interval within the trimmed sample. Finally, for our trimmed doubly robust estimator, we computed the interval (14). Then, for a given estimand $\theta(a)$ with confidence interval $[\hat{\theta}_{\ell,s}(a), \hat{\theta}_{u,s}(a)]$ for simulated dataset s , we computed its average coverage:

$$\text{coverage} = \int \left(\frac{1}{1000} \sum_{s=1}^{1000} \mathbb{I} \left\{ \theta(a) \in [\hat{\theta}_{\ell,s}(a), \hat{\theta}_{u,s}(a)] \right\} \right) dP(a).$$

We did not compute confidence intervals for the trimmed plug-in estimator $\hat{\psi}(a; t)$ —which



(a) Estimators’ average RMSE across convergence rates. (b) Average coverage of 95% confidence intervals’ average coverage across convergence rates.

Figure 2: Performance of the four estimators in terms of average RMSE (left) and average coverage (right) across convergence rates $\alpha \in \{0.1, 0.2, 0.3, 0.4, 0.5\}$. These averages were computed across treatment values $a \in \{0, 0.05, \dots, 0.95, 1\}$.

would require implementing a bootstrap procedure—but we expect coverage of such intervals to be low, given its poor RMSE performance. Figure 2b displays the coverage results. Coverage is worst for the doubly robust estimator, as expected, due to its poor performance in the presence of small propensity scores. Meanwhile, our estimator has coverage close to the nominal level once $\alpha \geq 0.3$, confirming that we can conduct valid inference even when the nuisance functions are estimated at slower nonparametric rates, as established by Proposition 1. Coverage for the EIF-based trimmed plug-in estimator is slightly lower than that of our estimator, but still preferable to the doubly robust estimator.

The fact that the alternative plug-in estimator $\hat{\psi}^{\text{alt}}(a; t)$ performs similarly to our estimator may at first seem surprising, because it uses a plug-in estimator for the trimming indicator $\mathbb{I}\{\pi(a|X) > t\}$. Thus, we may expect this estimator to inherit the convergence rate of $\hat{\pi}(a|X)$. However, even when $\pi(a|X)$ is estimated poorly, $\mathbb{I}\{\pi(a|X) > t\}$ may nonetheless be estimated well. This is the case for this simulation setup, but it may not be the case in general; we discuss this nuance in the Appendix (Section H). We find that these estimators perform differently when t is estimated, as we discuss next.

5.2 Results When the Threshold is Estimated

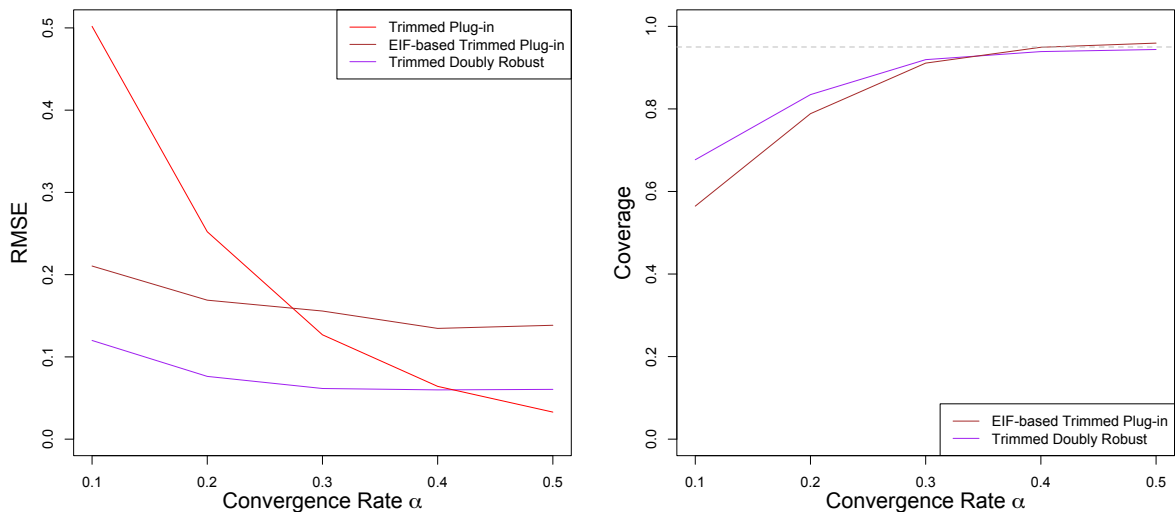
Although the threshold was fixed at $t = 0.1$ in the previous subsection, the proportion of trimmed subjects varied across treatment values: Figure 1c suggests that approximately 50% of subjects were trimmed on the edges of the dose-response curve, whereas almost no subjects were trimmed in the center. Instead, researchers may set t such that a fixed proportion of subjects are trimmed. A common choice is the γ -quantile of the estimated propensity scores:

$$\hat{t}_{\text{pi}} = \hat{F}_a^{-1}(\gamma), \quad (28)$$

where $\hat{F}_a^{-1}(\gamma)$ is the inverse empirical CDF of $\hat{\pi}(a|X)$. This is a plug-in estimator, because it plugs $\hat{\pi}(a|X)$ into the estimating equation $\mathbb{E}[\mathbb{I}(\pi(a|X) > t)] = 1 - \gamma$. Thus, \hat{t}_{pi} ensures the denominator of the plug-in estimators are equal to $1 - \gamma$. Similarly, in Section 3.2 we proposed an estimator \hat{t} that ensures the denominator of our estimator $\hat{\psi}_h(a; \hat{t})$ is equal to $1 - \gamma$. We consider these choices for t and the properties of the resulting causal effect estimators.

We consider $\gamma = 0.2$, such that 20% of subjects are trimmed. We simulated $\hat{\pi}(a|X)$ and $\hat{\mu}(X, a)$ as in the previous subsection; once these are defined, \hat{t}_{pi} is straightforward to compute. Meanwhile, to compute our estimator \hat{t} in (17), we computed $\hat{\psi}_h^{\text{den}}(a; t)$ for $t \in [0, 0.5]$ in increments of 0.005, and selected the smallest t such that $\hat{\psi}_h^{\text{den}}(a; t) \leq 1 - \gamma$. Importantly, these threshold estimators target true thresholds t_0^{pi} and t_0 , respectively, where t_0^{pi} is the t such that $\mathbb{E}[\mathbb{I}(\pi(a|X) > t)] = 1 - \gamma$, and t_0 is the t such that $\psi_h^{\text{den}}(a; t) = 1 - \gamma$. Thus, the TATE in this case corresponds to $\psi(a; t_0^{\text{pi}})$, and the STATE corresponds to $\psi_h(a; t_0)$; the following results are with respect to these estimands. We do not further consider the SATE, which is unaffected by the choice of threshold.

Figure 3a displays the RMSE across convergence rates for the plug-in estimators $\hat{\psi}(a; \hat{t}_{\text{pi}})$ and $\hat{\psi}^{\text{alt}}(a; \hat{t}_{\text{pi}})$ as well as our trimmed doubly robust estimator $\hat{\psi}_h(a; \hat{t})$. Again our estimator performs well across convergence rates, whereas the plug-in estimator $\hat{\psi}(a; \hat{t}_{\text{pi}})$ performs poorly for slow rates. Meanwhile, in this case, the EIF-based plug-in estimator $\hat{\psi}^{\text{alt}}(a; \hat{t}_{\text{pi}})$ performs worse than the trimmed doubly robust estimator, whereas it performed similarly in the previous subsection. There are two reasons for this. First, this estimator utilizes a plug-in estimator for the trimming threshold, and thus it can inherit the slow convergence rate of the nuisance functions. Second, as discussed earlier, in this case we are performing a more moderate amount of trimming on the edges of the dose-response curve, compared to the previous subsection when $t = 0.1$. As a result, small propensity scores still remain when estimating causal effects, which can adversely affect the typical doubly robust estimator involved in $\hat{\psi}^{\text{alt}}(a; \hat{t}_{\text{pi}})$.



(a) Estimators' average RMSE across convergence rates.

(b) Average coverage of 95% confidence intervals' average coverage across convergence rates.

Figure 3: Performance of the TATE and STATE estimators in terms of average RMSE (left) and average coverage (right) across convergence rates $\alpha \in \{0.1, 0.2, 0.3, 0.4, 0.5\}$. For the TATE estimators, the trimming threshold was estimated with \hat{t}_{pi} in (28), and for the STATE estimator, it was estimated with \hat{t} in (17). These averages were computed across treatment values $a \in \{0, 0.05, \dots, 0.95, 1\}$.

Finally, Figure 3b displays the coverage results. For the trimmed doubly robust estimator, we used our interval (20) from Section 3.2; and for the EIF-based trimmed plug-in estimator, we again computed the confidence interval for the typical doubly robust estimator, but within the trimmed sample. Similar to the previous subsection, the EIF-based trimmed plug-in estimator exhibits less coverage, but coverage for both estimators approaches the nominal level as the convergence rate increases.

5.3 Summary of Results, and Interpreting Trimmed Effects

Our trimmed doubly robust estimators from Section 3 performed well in terms of RMSE and coverage, whether the trimming threshold was fixed or estimated. Meanwhile, the typical doubly robust estimator performed poorly in the presence of small propensity scores, and the typical plug-in estimator performed poorly when nuisance functions' convergence rate was slow. Finally, the typical doubly robust estimator on a trimmed sample tended to perform well, but could still be susceptible to small propensity scores if trimming was not extensive. Thus, researchers should be cautious when selecting trimming thresholds via quantiles for

continuous treatments, because many subjects can have small propensity scores for some areas of the dose-response curve.

These results reflect the estimators' ability to estimate causal effects at any given treatment value a . In practice, researchers will likely estimate causal effects across treatment values (as we have done here), and then interpret the resulting estimated dose-response curve. However, a challenge arises when interpreting a trimmed dose-response curve. In general, the trimmed estimands $\psi(a; t)$ and $\psi_h(a; t)$ will differ from $\psi_h(a)$, to the extent that the non-trimmed population differs from the whole population. This discrepancy between populations and thus estimands is well-known when trimming (Crump et al., 2006; Stürmer et al., 2010; Yang and Ding, 2018). For example, for this simulation setup, when $t = 0.1$ and $a = 0$, the non-trimmed population corresponds to subjects with $X \leq 0.5$, as shown in Figure 1c. However, the non-trimmed population can change with a . For example, Figure 1c suggests that, when $a = 1$, the non-trimmed population is (roughly) subjects with $X \geq 0.5$, which differs from the non-trimmed population when $a = 0$. As a result, even though the dose-response curve is flat (i.e., $\psi(a) = \psi$ for some constant ψ for all a), the trimmed dose-response curve $\psi(a; t)$ is not flat, due to the change in non-trimmed populations across a . Thus, even though there is not a treatment effect for anyone in the population, the trimmed dose-response curve may nonetheless change across a . Illustrations of the dose-response curves for this simulation setup are in the Appendix (Section G).

To our knowledge, this complication has not been previously acknowledged in the literature, in part because trimming has focused on binary treatments. One option is to trim subjects whose propensity score is small for any treatment value (Lee, 2018; Colangelo and Lee, 2020); however, this would likely result in trimming most if not all subjects, as would be the case for this simulation setup and our application below. Instead, we recommend that researchers examine how the non-trimmed population differs from the whole population across treatment values. We illustrate how to do this in the application below, where understanding the non-trimmed population will be important for interpreting results.

6 Application: Estimating the Effect of Smoking on Medical Expenditure

As a real-world example, we consider data from the 1987 National Medical Expenditure Survey (NMES), which has been used in previous works to measure the causal impact of smoking on medical expenses among people who smoke (Johnson et al., 2003; Imai and Van Dyk, 2004; Zhao et al., 2020). In these works, the outcome variable is annual medical

expenditure (in United States dollars), log-transformed to account for its strong right-skew.² Meanwhile, the treatment variable is a continuous measure of smoking use, defined as

$$A = \log(0.05 \times \text{number of cigarettes per day} \times \text{number of years smoked}), \quad (29)$$

where again a log-transformation is used to account for strong right-skew, and 0.05 is used to measure packs of cigarettes. Thus, previous works have called (29) “log pack-years.” Finally, the covariates X include: categorical measures of gender, race, marriage status, education, geographic region, income, and seatbelt use; and quantitative measures of age at the time of the survey, age when the subject started smoking, and their quadratic transformations. Following these previous works, we focus on the subset of observations without missing data.³ Furthermore, following Zhao et al. (2020), we focus on the subset of subjects whose medical expenditure $Y > 0$. As discussed in Zhao et al. (2020), to account for subjects with $Y = 0$, it would be appropriate to model the probability $P(Y > 0|A, X)$ and the distribution of Y conditional on A, X , and $Y > 0$. We only consider this second model to focus on the challenges of dose-response estimation. This results in a final set of 8263 subjects. Following previous works, in our analyses we also incorporate subjects’ survey-sampling weights provided within the NMES dataset.

The goal of these studies was to determine whether a change in log pack-years leads to a change in annual medical expenditure. Imai and Van Dyk (2004) focused on estimating a marginal version of the dose-response curve, whereas Zhao et al. (2020) extended their methodology to flexibly estimate the full dose-response curve. Specifically, Zhao et al. (2020) noted that if consistency, no unmeasured confounding, and positivity hold, then $\mathbb{E}[Y(a)] = \mathbb{E}[\mathbb{E}\{Y|\pi(A|X), A = a\}]$. This motivates constructing a propensity score estimator $\hat{\pi}(A|X)$ and then regressing Y on $\hat{\pi}(A|X)$ and A . Zhao et al. (2020) assumed that the propensity score was parameterized by θ and thus proposed regressing Y on $\hat{\theta}$ and A . They used linear regression to estimate the propensity score and splines for the second-stage regression. We’ll instead consider flexible models for both the propensity score and outcome regression.

A challenge for this application is that there are severe positivity violations for some treatment values. We used the **SuperLearner** R package (Van der Laan et al., 2007) to estimate propensity scores via an ensemble of adaptive regression splines, generalized linear models, generalized additive models, regression trees, and random forests.⁴ Specifically,

²Medical expenditure was self-reported in the 1987 NMES, but was also verified with interviews and data from clinicians and hospitals. See Johnson et al. (2003) for details.

³Johnson et al. (2003) found that accounting for the missing data via multiple imputation did not notably change results. Thus, Imai and Van Dyk (2004) and Zhao et al. (2020) conducted complete-case causal analyses, as we do here.

⁴We focus on this ensemble-based approach because it has shown to be a useful way to flexibly estimate

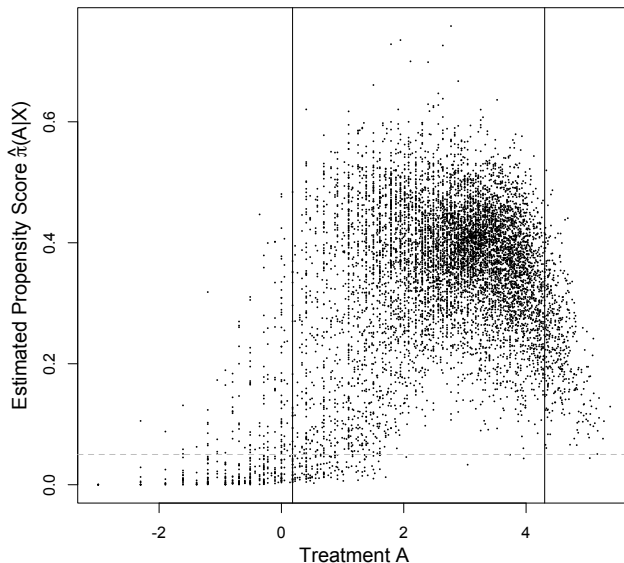
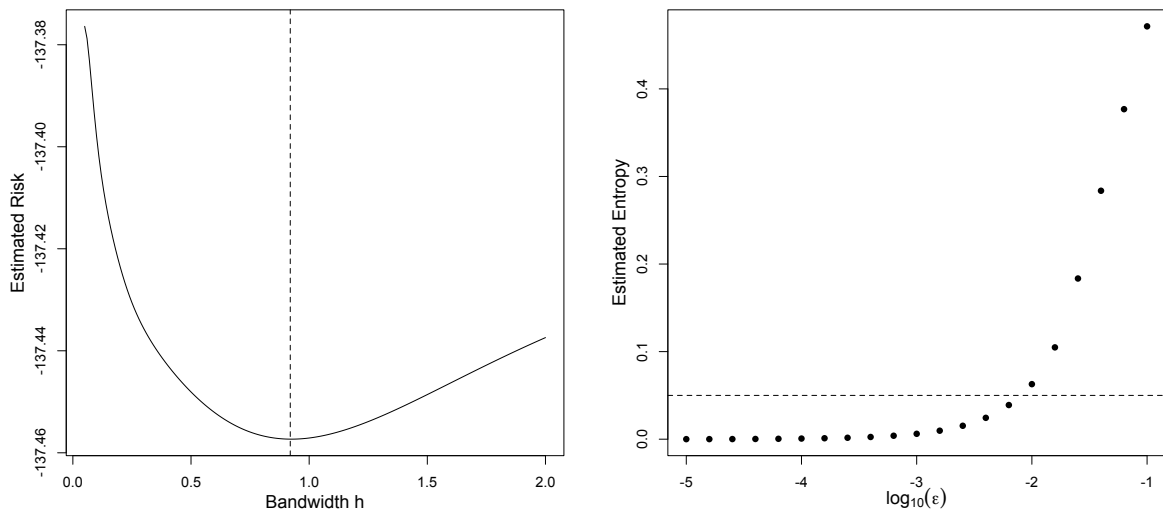


Figure 4: Scatterplot of A and estimated propensity scores $\hat{\pi}(A|X)$. Horizontal dashed line denotes $t = 0.05$; vertical lines denote the 5% and 95% quantiles of A .

we estimated the treatment’s conditional mean and variance, denoted as $m(X) = \mathbb{E}[A|X]$ and $s(X) = \text{Var}(A|X)$; then, we computed $\hat{\pi}(a|X)$ as the density at a for the distribution $N(\hat{m}(X), \hat{s}(X))$. A similar procedure was done in Zhao et al. (2020), but with a linear regression model for $m(X)$ and a homoskedasticity assumption for $s(X)$. Figure 4 displays the estimated propensity scores across treatment values. There are many estimated propensity scores close to 0 for low treatment values, suggesting that low amounts of smoking are not prevalent in this dataset. At worst, the average causal effect is not identified for these treatment values, and at best, this area of the dose-response curve is difficult to estimate precisely. Although Zhao et al. (2020) did not focus on positivity violations in this application, this validates their emphasis to “advise caution in that all available methods [for causal dose-response estimation] can be biased by model misspecification and extrapolation.”

Similar to Zhao et al. (2020), we estimate the causal effect at 10 equally-spaced points between the 5% and 95% quantiles of A , denoted in Figure 4. Even within these quantiles, positivity is nearly violated, which motivates trimming. We consider the doubly robust estimator without trimming, $\hat{\psi}_h(a)$, and with trimming, $\hat{\psi}_h(a; t)$. For both estimators, we again used the ensemble approach described above to estimate $\mu(x, a) = \mathbb{E}[Y|X = x, A = a]$; furthermore, we used the cross-fitting procedure described in Section 3.1 with two splits

nuisance functions within causal inference; e.g., see Van der Laan et al. (2011); Schuler and Rose (2017); Kreif and DiazOrdaz (2019) for discussion.



(a) The estimated risk (25) for bandwidths $h \in \{0.05, 0.06, \dots, 1.99, 2\}$. Dashed vertical line denotes $\hat{h} = 0.92$.

(b) The estimated entropy (27) for $\epsilon = 10^{-c}$ where $c \in \{0.1, 0.12, \dots, 4.98, 5\}$. Dashed horizontal line denotes 0.05.

Figure 5: Selecting the bandwidth h via risk minimization (left) and selecting the smoothing parameter ϵ via entropy (right).

of equal size. Figure 4 suggests a fixed trimming threshold $t = 0.05$, which will result in some trimming for the left-hand side of the dose-response curve but almost no trimming elsewhere. Meanwhile, to choose h , we implemented the procedure outlined in Section 4.1, where we computed the estimated risk (25) for $h \in \{0.05, 0.06, \dots, 1.99, 2\}$. This resulted in a bandwidth $\hat{h} = 0.92$ for $\hat{\psi}_h(a; t)$, as visualized in Figure 5a. We followed an analogous process for $\hat{\psi}_h(a)$, which resulted in a bandwidth $\hat{h} = 0.21$.⁵ We present results for both bandwidth choices below, and discuss why these estimators chose different bandwidths. Finally, to choose the smoothing parameter ϵ , we implemented the procedure outlined in Section 4.2, where we computed the estimated entropy (27) for $\epsilon = 10^{-c}$ where $c \in \{1, 1.2, \dots, 4.8, 5\}$. This process is visualized in Figure 5b; we set $\epsilon = 10^{-2}$ because it results in an entropy close to 0.05, as discussed in Section 4.2. Following recommendations from Yang and Ding (2018), we also implemented our analyses for several choices ϵ , and found that results were quite similar to those presented here.

Figure 6a displays point estimates and 95% confidence intervals for $\hat{\psi}_h(a)$ and $\hat{\psi}_h(a; t)$ when $h = 0.21$, i.e., the optimal bandwidth for the non-trimmed estimator. The non-trimmed estimator is very unstable in areas where propensity scores are close to 0, with

⁵In other words, we again minimized an estimated risk, but where the risk was defined with respect to $\psi_h(a)$, which does not incorporate the smoothed trimming indicator.

very wide confidence intervals, whereas the trimmed estimator exhibits notably narrower confidence intervals across the dose-response curve. Meanwhile, Figure 6b displays results when $h = 0.92$, i.e., the optimal bandwidth for the trimmed estimator. In this case the non-trimmed estimator is completely unstable, because the larger bandwidth makes small propensity scores influence larger areas of the dose-response curve. Meanwhile, results for the trimmed estimator are quite similar for both bandwidths, although $h = 0.92$ leads to slightly tighter confidence intervals.

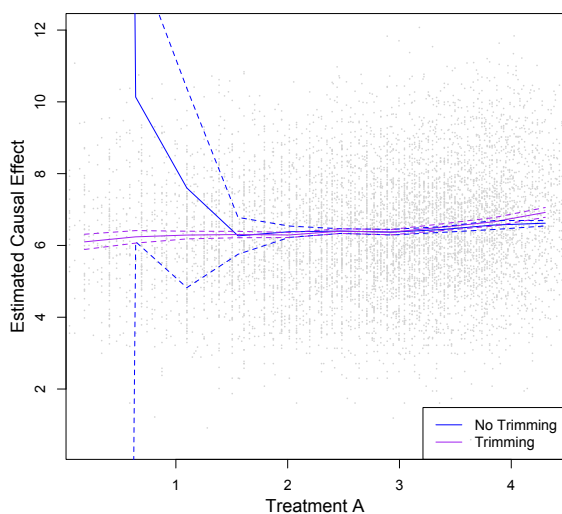
Reading each plot in Figure 6 from right to left, the trimmed estimator suggests that the estimated average medical expenditure decreases very slightly as smoking decreases, but plateaus around $A = 1$. This suggests that a high-level smoker may decrease medical expenditures by smoking less, but this isn't necessarily the case for a moderate-level smoker. For example, two treatment values considered were $a = 4.30$ and $a = 2.01$; this corresponds to smoking $\exp(4.30) \approx 73.70$ pack-years versus $\exp(2.01) \approx 7.46$ pack-years. For the trimmed estimator with $h = 0.92$, the intervals for $\exp\{\widehat{\psi}_h(4.30; t)\}$ and $\exp\{\widehat{\psi}_h(2.01; t)\}$ were $(\$748.59, \$855.64)$ and $(\$549.40, \$596.59)$, respectively, suggesting a statistically significant decrease in annual medical expenditure, with a point estimate of $\exp\{\widehat{\psi}_h(4.30; t)\} - \exp\{\widehat{\psi}_h(2.01; t)\} = \227.82 . That said, this point estimate (in 1987 US dollars, which is approximately \$613.05 in 2023 US dollars) may be considered a modest decrease. Meanwhile, confidence intervals for $\exp\{\widehat{\psi}_h(a; t)\}$ overlap substantially for $a < 2$.

Results from the approach of Zhao et al. (2020) are similar to those for our trimmed estimator; indeed, our estimated propensity scores in Figure 4 are similar to propensity scores estimated just with linear regression, as in Zhao et al. (2020). However, unlike the non-trimmed doubly robust estimator $\widehat{\psi}_h(a)$, their estimator was not sensitive to positivity violations. The reason is that their estimator is a plug-in estimator based on the identification result $\mathbb{E}[Y(a)] = \mathbb{E}[\mathbb{E}\{Y|\pi(A|X), A = a\}]$. As we saw in Section 5, plug-in estimators' variance can be insensitive to positivity violations, but bias can be severe when nuisance functions are estimated at slow rates. The fact that our results are similar gives some reassurance that propensity scores could be adequately modeled with parametric models for this dataset.

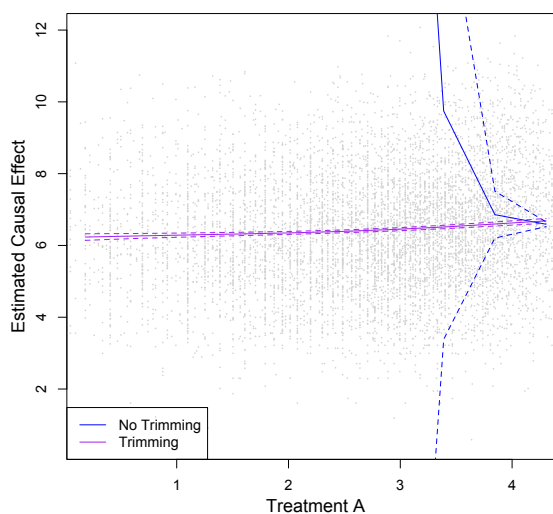
Finally, it's important to recognize that the trimmed sample may differ from the full sample. To understand this, we computed kernel-smoothed covariate means before and after trimming, respectively defined as

$$\bar{X}_h(a) = \frac{\sum_{i=1}^n K_h(A_i - a)X_i}{\sum_{i=1}^n K_h(A_i - a)}, \quad \text{and} \quad \bar{X}_h(a; t) = \frac{\sum_{i=1}^n K_h(A_i - a)S(\widehat{\pi}(a|X_i), t)X_i}{\sum_{i=1}^n K_h(A_i - a)S(\widehat{\pi}(a|X_i), t)},$$

where $S(\widehat{\pi}(a|X_i), t)$ is the smoothed version of $\mathbb{I}(\widehat{\pi}(a|X_i) > t)$. Again we consider bandwidths

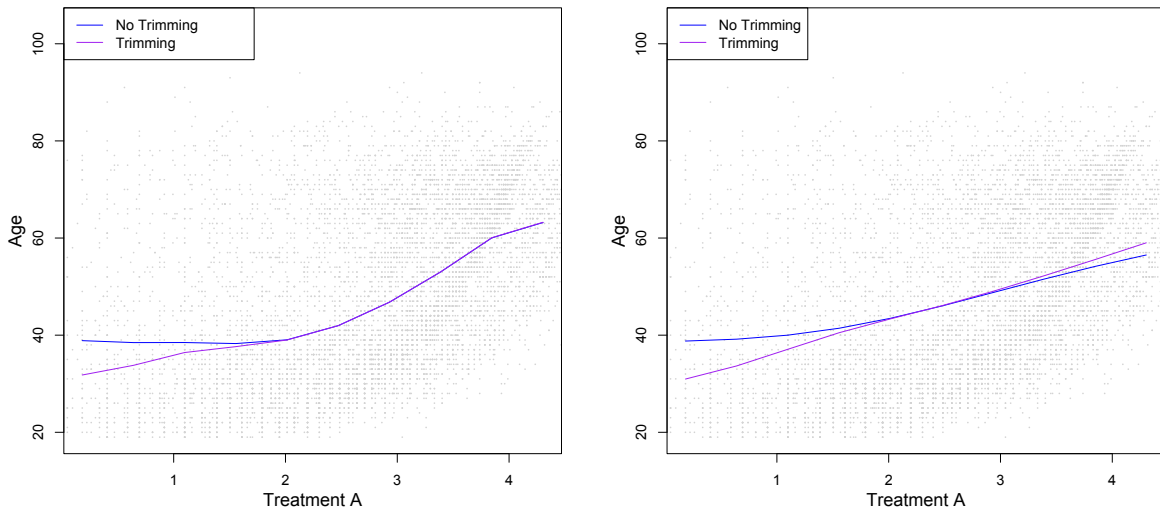


(a) Results when $h = 0.21$.



(b) Results when $h = 0.92$.

Figure 6: Estimated causal effects when $h = 0.21$ (left) and $h = 0.92$ (right). The former is the chosen bandwidth for the non-trimmed estimator; the latter is the chosen bandwidth for the trimmed estimator. In both plots, blue denotes the doubly robust estimator without trimming, and purple denotes the estimator with trimming. Point estimates are solid lines, and 95% confidence intervals are dashed lines. Gray dots denote individual (A, Y) observations.



(a) Smoothed age when $h = 0.21$.

(b) Smoothed age when $h = 0.92$.

Figure 7: The smoothed age without trimming, $\bar{X}_h(a)$ in blue, and the smoothed age with trimming, $\bar{X}_h(a; t)$ in purple, when $h = 0.21$ (left) and $h = 0.92$ (right). Individual (A, X) observations are in light gray.

$h = 0.21$ and $h = 0.92$. Figure 7 displays $\bar{X}_h(a)$ in blue and $\bar{X}_h(a; t)$ in purple for subjects' age at the time of the survey, which previous works found is the covariate most associated with the outcome. The trimmed sample is much younger for low treatment values, compared to the full sample; nonetheless, it's useful that we can precisely estimate the dose-response curve for low treatment values, albeit for a younger sample.

In summary, we were able to use trimming to precisely estimate a dose-response curve, even in areas where there are many small propensity scores. The trimmed analysis suggests that decreasing smoking can decrease annual medical expenditure, but only to a modest degree and only for high-level smokers. Furthermore, when estimating the causal effect for low-level smokers, the trimmed sample was younger than the full sample.

7 Discussion and Conclusion

Although the positivity assumption—i.e., that propensity scores are bounded away from zero—is commonly invoked to identify and estimate causal effects, positivity violations are also common, thereby destabilizing many causal effect estimators. There are many well-known approaches for addressing positivity violations, including overlap weights (Li et al., 2018), matching (Stuart, 2010), truncating propensity score weights (Cole and Hernán, 2008),

and propensity score trimming (Crump et al., 2009). Although studies have found empirical evidence that trimming can stabilize doubly robust estimators (Mao et al., 2019; Li, 2020; Zhang and Zhang, 2022; Huang et al., 2022), their theoretical guarantees are unclear, and almost all works assume the treatment is discrete.

When the treatment is continuous, positivity violations are likely a greater concern, because it is often the case that some subjects’ propensity scores are zero for some treatment values. In this work we derived estimators for trimmed causal effects in the continuous treatment case. Our estimators incorporate kernel smoothing and a smoothed trimming indicator, such that efficient influence functions for the resulting trimmed estimand exists. As a consequence, our estimators exhibit doubly robust style guarantees, such that we can conduct valid inference even when the propensity score and outcome regression are estimated at slower-than-parameteric rates. We allowed the trimming threshold to be fixed or estimated as a quantile of the propensity score, and we provided data-driven ways to select the parameters involved in kernel smoothing and the smoothed trimming indicator. Through a simulation study and an application, we found that our estimators could precisely estimate a trimmed dose-response curve even when some propensity scores are small and nonparametric models are used for the propensity score and outcome regression.

That said, there are several limitations to this work. First, a common theme among methods that address positivity violations is that the estimand changes; for example, using overlap weights targets effects for the “overlap population,” and matching targets effects for the matched population. Similarly, our estimand is the trimmed dose-response curve, which differs from the dose-response curve to the extent that the non-trimmed population differs from the full population. As we illustrated in our application, we recommend measuring how the non-trimmed population differs from the full population, which follows other recommendations in the trimming literature (Crump et al., 2006; Stürmer et al., 2010). Alternatively, this discrepancy in estimands can be framed as “trimming bias,” and some recent works have employed bias-correction approaches to target the full-population estimand (Chaudhuri and Hill, 2014; Ma and Wang, 2020). One promising approach is that of Sasaki and Ura (2022), who use sieve estimators to model the trimmed causal effect as a function of the proportion of trimmed subjects, and then conduct a bias correction when this proportion is zero. Although this approach requires additional modeling assumptions, one could potentially use it in conjunction with our estimators to target the original dose-response curve.

Second, it can be challenging to understand how the non-trimmed population differs from the full population in the case of a continuous treatment, because it can change across treatment values. For example, in our application estimating the effect of smoking on medical expenditure, we found that the non-trimmed population was increasingly younger than the

full population for smaller treatment values. Because this discrepancy was monotonic in age—and because previous works validated that age was an important predictor variable—the trimmed dose-response curve was still relatively easy to interpret. However, in general, the population may change in complex ways across treatment values, especially when covariates are high-dimensional. Instead, one could create a single non-trimmed population by trimming any subject whose propensity score is small for any treatment value (Lee, 2018; Colangelo and Lee, 2020). However, this would likely trim most if not all subjects, as would have been the case in our application. Alternatively, one could only conduct dose-response estimation for treatment values where positivity is not severely violated; in short, one could trim treatment values instead of subjects. However, this is unsatisfactory if one is interested in the full dose-response curve. In future work, it would be useful to develop tools that diagnose how a non-trimmed sample differs from a full population. More broadly, this would be useful for assessing the representativeness of subsets within observational studies, e.g. matched sets (Bennett et al., 2020; Degtiar and Rose, 2023).

Finally, our trimmed estimand depends on three parameters: the trimming threshold t , the bandwidth h for kernel smoothing, and the parameter ϵ for the smoothed trimming indicator. We allowed t to be estimated, such that confidence intervals reflected uncertainty in estimating the threshold. Meanwhile, we provided a risk-minimization approach to select h and an entropy-based approach to select ϵ ; however, our confidence intervals do not reflect uncertainty in estimating these parameters. On the one hand, practitioners likely want h and ϵ to be small, such that the smoothed dose-response curve is close to the true dose-response curve; on the other hand, making h and ϵ very small can adversely affect the variance of our estimators. In future work, it would be useful to derive an optimal way to choose these parameters, while also having inference reflect the uncertainty involved in this choice.

References

- Austin, P. C. and Stuart, E. A. (2015). Moving towards best practice when using inverse probability of treatment weighting (iptw) using the propensity score to estimate causal treatment effects in observational studies. *Statistics in Medicine*, 34(28):3661–3679.
- Bang, H. and Robins, J. M. (2005). Doubly robust estimation in missing data and causal inference models. *Biometrics*, 61(4):962–973.
- Bennett, M., Vielma, J. P., and Zubizarreta, J. R. (2020). Building representative matched samples with multi-valued treatments in large observational studies. *Journal of Computational and Graphical Statistics*, 29(4):744–757.

- Bibaut, A. F. and van der Laan, M. J. (2017). Data-adaptive smoothing for optimal-rate estimation of possibly non-regular parameters. *arXiv preprint arXiv:1706.07408*.
- Bonvini, M. and Kennedy, E. H. (2022). Fast convergence rates for dose-response estimation. *arXiv preprint arXiv:2207.11825*.
- Busso, M., DiNardo, J., and McCrary, J. (2014). New evidence on the finite sample properties of propensity score reweighting and matching estimators. *Review of Economics and Statistics*, 96(5):885–897.
- Cao, W., Tsiatis, A. A., and Davidian, M. (2009). Improving efficiency and robustness of the doubly robust estimator for a population mean with incomplete data. *Biometrika*, 96(3):723–734.
- Chaudhuri, S. and Hill, J. B. (2014). Heavy tail robust estimation and inference for average treatment effects. Technical report, Working paper.
- Chernozhukov, V., Chetverikov, D., Demirer, M., Duflo, E., Hansen, C., Newey, W., and Robins, J. (2018). Double/debiased machine learning for treatment and structural parameters. *The Econometrics Journal*, 21.
- Colangelo, K. and Lee, Y.-Y. (2020). Double debiased machine learning nonparametric inference with continuous treatments. *arXiv preprint arXiv:2004.03036*.
- Cole, S. R. and Hernán, M. A. (2008). Constructing inverse probability weights for marginal structural models. *American Journal of Epidemiology*, 168(6):656–664.
- Crump, R. K., Hotz, V. J., Imbens, G., and Mitnik, O. (2006). Moving the goalposts: Addressing limited overlap in the estimation of average treatment effects by changing the estimand.
- Crump, R. K., Hotz, V. J., Imbens, G. W., and Mitnik, O. A. (2009). Dealing with limited overlap in estimation of average treatment effects. *Biometrika*, 96(1):187–199.
- D’Amour, A., Ding, P., Feller, A., Lei, L., and Sekhon, J. (2021). Overlap in observational studies with high-dimensional covariates. *Journal of Econometrics*, 221(2):644–654.
- Degtiar, I. and Rose, S. (2023). A review of generalizability and transportability. *Annual Review of Statistics and Its Application*, 10:501–524.
- Díaz, I. and van der Laan, M. J. (2013). Targeted data adaptive estimation of the causal dose–response curve. *Journal of Causal Inference*, 1(2):171–192.

- Fan, J. and Gijbels, I. (1996). *Local polynomial modelling and its applications: monographs on statistics and applied probability 66*, volume 66. CRC Press.
- Farrell, M. H. (2015). Robust inference on average treatment effects with possibly more covariates than observations. *Journal of Econometrics*, 189(1):1–23.
- Farrell, M. H., Liang, T., and Misra, S. (2021). Deep neural networks for estimation and inference. *Econometrica*, 89(1):181–213.
- Flores, C. A., Flores-Lagunes, A., Gonzalez, A., and Neumann, T. C. (2012). Estimating the effects of length of exposure to instruction in a training program: The case of job corps. *Review of Economics and Statistics*, 94(1):153–171.
- Fong, C., Hazlett, C., and Imai, K. (2018). Covariate balancing propensity score for a continuous treatment: Application to the efficacy of political advertisements. *The Annals of Applied Statistics*, 12(1):156–177.
- Frölich, M. (2004). Finite-sample properties of propensity-score matching and weighting estimators. *Review of Economics and Statistics*, 86(1):77–90.
- Funk, M. J., Westreich, D., Wiesen, C., Stürmer, T., Brookhart, M. A., and Davidian, M. (2011). Doubly robust estimation of causal effects. *American Journal of Epidemiology*, 173(7):761–767.
- Galvao, A. F. and Wang, L. (2015). Uniformly semiparametric efficient estimation of treatment effects with a continuous treatment. *Journal of the American Statistical Association*, 110(512):1528–1542.
- Gill, R. D. and Robins, J. M. (2001). Causal inference for complex longitudinal data: the continuous case. *Annals of Statistics*, pages 1785–1811.
- Heckman, J. J., Ichimura, H., and Todd, P. E. (1997). Matching as an econometric evaluation estimator: Evidence from evaluating a job training programme. *The Review of Economic Studies*, 64(4):605–654.
- Heiler, P. and Kazak, E. (2021). Valid inference for treatment effect parameters under irregular identification and many extreme propensity scores. *Journal of Econometrics*, 222(2):1083–1108.
- Hernán, M. A. and Robins, J. M. (2006). Estimating causal effects from epidemiological data. *Journal of Epidemiology & Community Health*, 60(7):578–586.

- Hernán, M. A. and Robins, J. M. (2020). *Causal Inference: What If*. Boca Raton: Chapman & Hall/CRC.
- Hill, J., Linero, A., and Murray, J. (2020). Bayesian additive regression trees: A review and look forward. *Annual Review of Statistics and Its Application*, 7(1).
- Hill, J. L. (2011). Bayesian nonparametric modeling for causal inference. *Journal of Computational and Graphical Statistics*, 20(1):217–240.
- Hines, O., Dukes, O., Diaz-Ordaz, K., and Vansteelandt, S. (2022). Demystifying statistical learning based on efficient influence functions. *The American Statistician*, 76(3):292–304.
- Hirano, K. and Imbens, G. W. (2004). The propensity score with continuous treatments. *Applied Bayesian modeling and causal inference from incomplete-data perspectives*, 226164:73–84.
- Huang, Y., Leung, C. H., Wu, Q., Yan, X., Ma, S., Yuan, Z., Wang, D., and Huang, Z. (2022). Robust causal learning for the estimation of average treatment effects. In *2022 International Joint Conference on Neural Networks (IJCNN)*, pages 1–9. IEEE.
- Huling, J. D., Greifer, N., and Chen, G. (2023). Independence weights for causal inference with continuous treatments. *Journal of the American Statistical Association*, (just-accepted):1–25.
- Ichimura, H. and Newey, W. K. (2022). The influence function of semiparametric estimators. *Quantitative Economics*, 13(1):29–61.
- Imai, K. and Van Dyk, D. A. (2004). Causal inference with general treatment regimes: Generalizing the propensity score. *Journal of the American Statistical Association*, 99(467):854–866.
- Imbens, G. W. (2004). Nonparametric estimation of average treatment effects under exogeneity: A review. *Review of Economics and Statistics*, 86(1):4–29.
- Imbens, G. W. and Rubin, D. B. (2015). *Causal inference in statistics, social, and biomedical sciences*. Cambridge University Press.
- Johnson, E., Dominici, F., Griswold, M., and Zeger, S. L. (2003). Disease cases and their medical costs attributable to smoking: an analysis of the national medical expenditure survey. *Journal of Econometrics*, 112(1):135–151.

- Ju, C., Schwab, J., and van der Laan, M. J. (2019). On adaptive propensity score truncation in causal inference. *Statistical Methods in Medical Research*, 28(6):1741–1760.
- Kallus, N. and Zhou, A. (2018). Policy evaluation and optimization with continuous treatments. In *International conference on artificial intelligence and statistics*, pages 1243–1251. PMLR.
- Kang, J. D. and Schafer, J. L. (2007). Demystifying double robustness: A comparison of alternative strategies for estimating a population mean from incomplete data. *Statistical Science*, 22(4):523–539.
- Kennedy, E. H. (2016). Semiparametric theory and empirical processes in causal inference. In *Statistical causal inferences and their applications in public health research*, pages 141–167. Springer.
- Kennedy, E. H. (2020). Towards optimal doubly robust estimation of heterogeneous causal effects. *arXiv preprint arXiv:2004.14497*.
- Kennedy, E. H. (2022). Semiparametric doubly robust targeted double machine learning: a review. *arXiv preprint arXiv:2203.06469*.
- Kennedy, E. H., Balakrishnan, S., and G’Sell, M. (2020). Sharp instruments for classifying compliers and generalizing causal effects. *Annals of Statistics*, 48.
- Kennedy, E. H., Balakrishnan, S., and Wasserman, L. (2023). Semiparametric counterfactual density estimation. *Biometrika*.
- Kennedy, E. H., Ma, Z., McHugh, M. D., and Small, D. S. (2017). Non-parametric methods for doubly robust estimation of continuous treatment effects. *Journal of the Royal Statistical Society: Series B (Statistical Methodology)*, 79(4):1229–1245.
- Khan, S. and Tamer, E. (2010). Irregular identification, support conditions, and inverse weight estimation. *Econometrica*, 78(6):2021–2042.
- Khan, S. and Ugander, J. (2022). Heteroscedasticity-aware sample trimming for causal inference. *arXiv preprint arXiv:2210.10171*.
- Kreif, N. and DiazOrdaz, K. (2019). Machine learning in policy evaluation: new tools for causal inference. *arXiv preprint arXiv:1903.00402*.
- Lee, B. K., Lessler, J., and Stuart, E. A. (2011). Weight trimming and propensity score weighting. *PloS One*, 6(3):e18174.

- Lee, Y.-Y. (2018). Partial mean processes with generated regressors: Continuous treatment effects and nonseparable models. *arXiv preprint arXiv:1811.00157*.
- Li, F. (2020). Comment: Stabilizing the doubly-robust estimators of the average treatment effect under positivity violations. *Statistical Science*.
- Li, F., Morgan, K. L., and Zaslavsky, A. M. (2018). Balancing covariates via propensity score weighting. *Journal of the American Statistical Association*, 113(521):390–400.
- Li, F., Thomas, L. E., and Li, F. (2019). Addressing extreme propensity scores via the overlap weights. *American Journal of Epidemiology*, 188(1):250–257.
- Liu, Y. and Fan, Y. (2023). Biased-sample empirical likelihood weighting for missing data problems: an alternative to inverse probability weighting. *Journal of the Royal Statistical Society Series B: Statistical Methodology*, 85(1):67–83.
- Ma, X. and Wang, J. (2020). Robust inference using inverse probability weighting. *Journal of the American Statistical Association*, 115(532):1851–1860.
- Ma, Y., Sant’Anna, P. H., Sasaki, Y., and Ura, T. (2023). Doubly robust estimators with weak overlap. *arXiv preprint arXiv:2304.08974*.
- Mao, H., Li, L., and Greene, T. (2019). Propensity score weighting analysis and treatment effect discovery. *Statistical Methods in Medical Research*, 28(8):2439–2454.
- McClellan, A., Branson, Z., and Kennedy, E. H. (2022). Nonparametric estimation of conditional incremental effects. *arXiv preprint arXiv:2212.03578*.
- Mises, R. v. (1947). On the asymptotic distribution of differentiable statistical functions. *The Annals of Mathematical Statistics*, 18(3):309–348.
- Newey, W. K. (1994). The asymptotic variance of semiparametric estimators. *Econometrica: Journal of the Econometric Society*, pages 1349–1382.
- Petersen, M. L., Porter, K. E., Gruber, S., Wang, Y., and Van Der Laan, M. J. (2012). Diagnosing and responding to violations in the positivity assumption. *Statistical Methods in Medical Research*, 21(1):31–54.
- Robins, J., Li, L., Tchetgen, E., van der Vaart, A., et al. (2008). Higher order influence functions and minimax estimation of nonlinear functionals. In *Probability and statistics: essays in honor of David A. Freedman*, volume 2, pages 335–422. Institute of Mathematical Statistics.

- Robins, J., Sued, M., Lei-Gomez, Q., and Rotnitzky, A. (2007). Comment: Performance of double-robust estimators when “inverse probability” weights are highly variable. *Statistical Science*, 22(4):544–559.
- Rosenbaum, P. R. and Rubin, D. B. (1983). The central role of the propensity score in observational studies for causal effects. *Biometrika*, 70(1):41–55.
- Rothe, C. (2017). Robust confidence intervals for average treatment effects under limited overlap. *Econometrica*, 85(2):645–660.
- Sasaki, Y. and Ura, T. (2022). Estimation and inference for moments of ratios with robustness against large trimming bias. *Econometric Theory*, 38(1):66–112.
- Schick, A. (1986). On asymptotically efficient estimation in semiparametric models. *The Annals of Statistics*, pages 1139–1151.
- Schuler, M. S. and Rose, S. (2017). Targeted maximum likelihood estimation for causal inference in observational studies. *American Journal of Epidemiology*, 185(1):65–73.
- Silverman, B. W. (1986). *Density estimation for statistics and data analysis*, volume 26. CRC press.
- Smith, J. A. and Todd, P. E. (2005). Does matching overcome lalonde’s critique of nonexperimental estimators? *Journal of Econometrics*, 125(1-2):305–353.
- Stuart, E. A. (2010). Matching methods for causal inference: A review and a look forward. *Statistical Science*, 25(1):1.
- Stürmer, T., Rothman, K. J., Avorn, J., and Glynn, R. J. (2010). Treatment effects in the presence of unmeasured confounding: dealing with observations in the tails of the propensity score distribution—a simulation study. *American Journal of Epidemiology*, 172(7):843–854.
- Stürmer, T., Webster-Clark, M., Lund, J. L., Wyss, R., Ellis, A. R., Lunt, M., Rothman, K. J., and Glynn, R. J. (2021). Propensity score weighting and trimming strategies for reducing variance and bias of treatment effect estimates: a simulation study. *American Journal of Epidemiology*, 190(8):1659–1670.
- Su, L., Ura, T., and Zhang, Y. (2019). Non-separable models with high-dimensional data. *Journal of Econometrics*, 212(2):646–677.
- Tsiatis, A. A. (2006). Semiparametric theory and missing data.

- Van der Laan, M. J., Polley, E. C., and Hubbard, A. E. (2007). Super learner. *Statistical Applications in Genetics and Molecular Biology*, 6(1).
- Van der Laan, M. J., Rose, S., et al. (2011). *Targeted learning: causal inference for observational and experimental data*, volume 4. Springer.
- Van der Vaart, A. W. (2000). *Asymptotic Statistics*, volume 3. Cambridge university press.
- van der Vaart, A. W. (2002). Semiparametric statistics. *Lecture Notes in Math.*, (1781).
- Waernbaum, I. (2012). Model misspecification and robustness in causal inference: comparing matching with doubly robust estimation. *Statistics in medicine*, 31(15):1572–1581.
- Wasserman, L. (2006). *All of nonparametric statistics*. Springer Science & Business Media.
- Westreich, D. and Cole, S. R. (2010). Invited commentary: positivity in practice. *American Journal of Epidemiology*, 171(6):674–677.
- Wu, X., Mealli, F., Kioumourtzoglou, M.-A., Dominici, F., and Braun, D. (2018). Matching on generalized propensity scores with continuous exposures. *arXiv preprint arXiv:1812.06575*.
- Yang, S. and Ding, P. (2018). Asymptotic inference of causal effects with observational studies trimmed by the estimated propensity scores. *Biometrika*, 105(2):487–493.
- Yang, S., Imbens, G. W., Cui, Z., Faries, D. E., and Kadziola, Z. (2016). Propensity score matching and subclassification in observational studies with multi-level treatments. *Biometrics*, 72(4):1055–1065.
- Zeng, Z., Kennedy, E. H., Bodnar, L. M., and Naimi, A. I. (2023). Efficient generalization and transportation. *arXiv preprint arXiv:2302.00092*.
- Zhang, M. and Zhang, B. (2022). A stable and more efficient doubly robust estimator. *Statistica Sinica*, 32:1143–1163.
- Zhang, Z., Zhou, J., Cao, W., and Zhang, J. (2016). Causal inference with a quantitative exposure. *Statistical Methods in Medical Research*, 25(1):315–335.
- Zhao, S., van Dyk, D. A., and Imai, K. (2020). Propensity score-based methods for causal inference in observational studies with non-binary treatments. *Statistical Methods in Medical Research*, 29(3):709–727.

Zheng, W. and Van Der Laan, M. J. (2010). Asymptotic theory for cross-validated targeted maximum likelihood estimation.

Zhou, Y., Matsouaka, R. A., and Thomas, L. (2020). Propensity score weighting under limited overlap and model misspecification. *Statistical Methods in Medical Research*, 29(12):3721–3756.

A How Efficient Influence Functions are Derived

In this Appendix we will derive several efficient influence functions (EIFs). In general, the EIF of a parameter or estimand ψ (e.g., the STATE $\psi_h(a; t)$ in (5)) acts as the pathwise derivative of the functional ψ (Newey, 1994; Tsiatis, 2006). Importantly, a (centered) EIF ξ satisfies the von Mises expansion (Mises, 1947), for two probability measures P and \bar{P} :

$$\psi(\bar{P}) - \psi(P) = \int \xi(\bar{P})d(\bar{P} - P)(x) + R_2(\bar{P}, P) \quad (30)$$

where $R_2(\bar{P}, P)$ is a second-order remainder of a functional Taylor expansion (Hines et al., 2022; Kennedy, 2022). Thus, one can first derive a potential EIF ξ , and then verify that the von Mises expansion (30) holds by establishing that the remainder term $R_2(\bar{P}, P)$ is indeed second-order in the probability measures \bar{P} and P . One common way to derive potential EIFs is via Gateaux derivatives (Ichimura and Newey, 2022; Hines et al., 2022). Instead, we will follow “tricks” for deriving influence functions, proposed in Kennedy (2022), which recognize that influence functions—as a pathwise derivative—obey differentiation rules (e.g. product and chain rules). Specifically, the “tricks” we use are:

1. *Discretization trick*: Momentarily treat the data as discrete when deriving influence functions.
2. *Product rule*: For two estimands ψ_1 and ψ_2 , the EIF of their product is $\mathbb{IF}(\psi_1\psi_2) = \mathbb{IF}(\psi_1)\psi_2 + \psi_1\mathbb{IF}(\psi_2)$.
3. *Chain rule*: For an estimand ψ and function $f(\psi)$, its EIF is $\mathbb{IF}(f(\psi)) = f'(\psi)\mathbb{IF}(\psi)$, where $f'(\psi)$ is the derivative of f with respect to ψ .

See Kennedy (2022) for details why these “tricks” are justified for deriving EIFs. After deriving a proposed EIF ξ , we confirm that the von Mises expansion (30) holds, thereby verifying that our proposed ξ is indeed the EIF for the estimand ψ of interest. Thus, the “tricks” are simply useful tools for finding potential EIFs, which are then verified rigorously. Throughout, we will use the notation $\mathbb{IF}(\psi)$ to denote the EIF of ψ .

B Proof of Theorem 1

First, let

$$\begin{aligned}\psi_h^{\text{num}}(a; t) &= \int \int K_h(a_0 - a) S(\pi(a_0|x), t) \mu(x, a_0) da_0 dP(x) \\ \psi_h^{\text{den}}(a; t) &= \int \int K_h(a_0 - a) S(\pi(a_0|x), t) da_0 dP(x)\end{aligned}$$

Our goal is to derive the EIFs for these two quantities. First, note that when A and X are discrete, we have the following influence functions:

$$\begin{aligned}\mathbb{IF}\{\mu(x, a)\} &= \frac{\mathbb{I}(X = x, A = a)}{\pi(a|x)p(x)} (Y - \mu(x, a)) \\ \mathbb{IF}\{S(\pi(a|x), t)\} &= \frac{\partial S(\pi(a|x), t)}{\partial \pi} \mathbb{IF}\{\pi(a|x)\} \\ &= \frac{\partial S(\pi(a|x), t)}{\partial \pi} \frac{\mathbb{I}(X = x)}{P(X = x)} (\mathbb{I}(A = a) - \pi(a|x)) \\ \mathbb{IF}\{p(x)\} &= \mathbb{I}(X = x) - p(x)\end{aligned}$$

First we'll derive the EIF for $\psi_h^{\text{den}}(a; t)$. We have the following:

$$\begin{aligned}\mathbb{IF}\{\psi_h^{\text{den}}(a; t)\} &= \mathbb{IF}\left\{\sum_x \sum_{a_0} K_h(a_0 - a) S(\pi(a_0|x), t) p(x)\right\} && \text{(by discretization trick)} \\ &= \sum_x \sum_{a_0} K_h(a_0 - a) \mathbb{IF}\{S(\pi(a_0|x), t) p(x)\} && (K_h(\cdot) \text{ is constant}) \\ &= \sum_x \sum_{a_0} K_h(a_0 - a) [\mathbb{IF}\{S(\pi(a_0|x), t)\} p(x) + S(\pi(a_0|x)) \mathbb{IF}\{p(x)\}] \\ &&& \text{(product rule)} \\ &= \sum_x \sum_{a_0} K_h(a_0 - a) \frac{\partial S(\pi(a_0|x), t)}{\partial \pi} \mathbb{I}(X = x) (\mathbb{I}(A = a_0) - \pi(a_0|x)) \\ &+ \sum_x \sum_{a_0} K_h(a_0 - a) S(\pi(a_0|x)) (\mathbb{I}(X = x) - p(x)) && \text{(plugging in IFs)} \\ &= K_h(A - a) \frac{\partial S(\pi(A|X), t)}{\partial \pi} - \sum_{a_0} K_h(a_0 - a) \frac{\partial S(\pi(a_0|X), t)}{\partial \pi} \pi(a_0|X) \\ &+ \sum_{a_0} K_h(a_0 - a) S(\pi(a_0|X), t) - \psi_h^{\text{den}}(a; t) && \text{(simplifying)} \\ &= K_h(A - a) \frac{\partial S(\pi(A|X), t)}{\partial \pi} - \int K_h(a_0 - a) \frac{\partial S(\pi(a_0|X), t)}{\partial \pi} \pi(a_0|X) da_0 \\ &+ \int K_h(a_0 - a) S(\pi(a_0|X), t) da_0 - \psi_h^{\text{den}}(a; t) && \text{(sums to integrals)}\end{aligned}$$

The above quantity is the EIF of $\psi_h^{\text{den}}(a; t)$, which we'll verify in the next subsection. Note that, in Theorem 1, $\varphi_h^{\text{den}}(a; t) = \mathbb{IF}\{\psi_h^{\text{den}}(a; t)\} + \psi_h^{\text{den}}(a; t)$ is the uncentered EIF.

Now we'll derive the EIF for $\psi_h^{\text{num}}(a; t)$. First, note that we have the following, by the discretization trick and product rule:

$$\begin{aligned} \mathbb{IF}\{\psi_h^{\text{num}}(a; t)\} &= \mathbb{IF}\left\{\sum_x \sum_{a_0} K_h(a_0 - a) S(\pi(a_0|x), t) \mu(x, a_0) p(x)\right\} \\ &= \sum_x \sum_{a_0} K_h(a_0 - a) \mathbb{IF}\{\mu(x, a_0)\} S(\pi(a_0|x), t) p(x) \end{aligned} \quad (1)$$

$$+ \sum_x \sum_{a_0} K_h(a_0 - a) \mu(x, a_0) \mathbb{IF}\{S(\pi(a_0|x), t)\} p(x) \quad (2)$$

$$+ \sum_x \sum_{a_0} K_h(a_0 - a) \mu(x, a_0) S(\pi(a_0|x), t) \mathbb{IF}\{p(x)\} \quad (3)$$

Now we will compute terms (1), (2), and (3). First, for (1), we have:

$$\begin{aligned} (1) &= \sum_x \sum_{a_0} K_h(a_0 - a) \frac{\mathbb{I}(X = x, A = a_0)}{\pi(a_0|x)} \{Y - \mu(x, a_0)\} S(\pi(a_0|x), t) \\ &= K_h(A - a) \frac{\{Y - \mu(X, A)\} S(\pi(A|X), t)}{\pi(A|X)} \end{aligned}$$

Meanwhile, for (2) and (3), note that the same terms appeared in our work for the EIF of $\psi_h^{\text{den}}(a; t)$ (where now we multiply these two terms by $\mu(x, a_0)$). Thus, for (2), we have:

$$(2) = K_h(A - a) \mu(X, A) \frac{\partial S(\pi(A|X), t)}{\partial \pi} - \int K_h(a_0 - a) \mu(X, a_0) \frac{\partial S(\pi(a_0|x), t)}{\partial \pi} \pi(a_0|X) da_0$$

and for (3), we have:

$$(3) = \int K_h(a_0 - a) S(\pi(a_0|X), t) \mu(X, a_0) da_0 - \psi_h^{\text{num}}(a; t)$$

Plugging these all back into our original derivation of $\mathbb{IF}\{\psi_h^{\text{num}}(a; t)\}$, we have:

$$\begin{aligned} \mathbb{IF}\{\psi_h^{\text{num}}(a; t)\} &= K_h(A - a) \frac{\{Y - \mu(X, A)\} S(\pi(A|X), t)}{\pi(A|X)} \\ &+ K_h(A - a) \mu(X, A) \frac{\partial S(\pi(A|X), t)}{\partial \pi} - \int K_h(a_0 - a) \mu(X, a_0) \frac{\partial S(\pi(a_0|X), t)}{\partial \pi} \pi(a_0|X) da_0 \\ &+ \int K_h(a_0 - a) S(\pi(a_0|X), t) \mu(X, a_0) da_0 - \psi_h^{\text{num}}(a; t) \end{aligned}$$

The above quantity is the EIF of $\psi_h^{\text{num}}(a; t)$. Again, note that, in Theorem 1, $\varphi_h^{\text{num}}(a; t) =$

$\mathbb{E}\{\psi_h^{\text{num}}(a; t)\} + \psi_h^{\text{num}}(a; t)$ is the uncentered EIF.

This completes the proof. To formally verify that the above quantities are indeed EIFs, we must establish their second-order bias, which we do in the following section.

C Analyzing the Remainder Terms of Theorem 1

First we must extend our notation such it can incorporate probability distributions P and \bar{P} . Our estimands, for a particular probability distribution P , are defined as:

$$\begin{aligned}\psi_h^{\text{num}}(a; t; P) &= \int \int K_h(a_0 - a) S(\pi(a_0|x), t) \mu(x, a_0) da_0 dP(x) \\ \psi_h^{\text{den}}(a; t; P) &= \int \int K_h(a_0 - a) S(\pi(a_0|x), t) da_0 dP(x)\end{aligned}$$

Note that, implicitly, μ and π are also indexed by P . In the previous section (and in Theorem 1), we posit that the corresponding (centered) EIFs, indexed by P , are:

$$\begin{aligned}\xi_h^{\text{num}}(a; t; P) &= K_h(A - a) \frac{\{Y - \mu(X, A)\} S(\pi(A|X), t)}{\pi(A|X)} \\ &+ K_h(A - a) \mu(X, A) \frac{\partial S(\pi(A|X), t)}{\partial \pi} - \int K_h(a_0 - a) \mu(X, a_0) \frac{\partial S(\pi(a_0|X), t)}{\partial \pi} \pi(a_0|X) da_0 \\ &+ \int K_h(a_0 - a) S(\pi(a_0|X), t) \mu(X, a_0) da_0 - \psi_h^{\text{num}}(a; t; P)\end{aligned}$$

$$\begin{aligned}\xi_h^{\text{den}}(a; t; P) &= K_h(A - a) \frac{\partial S(\pi(A|X), t)}{\partial \pi} - \int K_h(a_0 - a) \frac{\partial S(\pi(a_0|X), t)}{\partial \pi} \pi(a_0|X) da_0 \\ &+ \int K_h(a_0 - a) S(\pi(a_0|X), t) da_0 - \psi_h^{\text{den}}(a; t; P)\end{aligned}$$

Note that in order for the von Mises expansion (30) to be valid for these quantities, it must be the case that $\mathbb{E}_P[\xi_h^{\text{num}}(a; t; P)] = 0$ and $\mathbb{E}_P[\xi_h^{\text{den}}(a; t; P)] = 0$. For completeness, we'll first confirm this, and then we will study the remainder terms for these quantities based on the von Mises expansion.

First let's start with $\xi_h^{\text{den}}(a; t; P)$. Note that

$$\mathbb{E}_P \left[K_h(A - a) \frac{\partial S(\pi(A|X), t)}{\partial \pi} \right] = \int \int K_h(a_0 - a) \frac{\partial S(\pi(a_0|x), t)}{\partial \pi} \pi(a_0|x) da_0 dP(x)$$

Thus, we can readily see that $\mathbb{E}_P[\xi_h^{\text{den}}(a; t; P)] = 0$. Meanwhile, by iterated expectations and

the definition of $\mu(X, A) = \mathbb{E}[Y|X, A]$, we have

$$\begin{aligned} \mathbb{E}_P \left[K_h(A - a) \frac{\{Y - \mu(X, A)\} S(\pi(A|X), t)}{\pi(A|X)} \right] &= \mathbb{E}_P \left[\mathbb{E}_P \left[K_h(A - a) \frac{\{Y - \mu(X, A)\} S(\pi(A|X), t)}{\pi(A|X)} \middle| X, A \right] \right] \\ &= \mathbb{E}_P \left[K_h(A - a) \frac{\{\mu(X, A) - \mu(X, A)\} S(\pi(A|X), t)}{\pi(A|X)} \right] \\ &= 0 \end{aligned}$$

Thus, we can also readily see that $\mathbb{E}_P[\xi_h^{\text{num}}(a; t; P)] = 0$.

C.1 Second-Order Remainder for the Denominator Estimand

We have the following lemma, which establishes that the remainder term for the EIF of $\psi_h^{\text{den}}(a; t)$ based on the von Mises expansion (30) is second-order.

Lemma 1. *Consider the estimand $\psi_h^{\text{den}}(a; t)$ and two probability measures P and \bar{P} . Let $\pi(a|x)$ and $\bar{\pi}(a|x)$ denote the propensity score under P and \bar{P} , respectively. The remainder term is:*

$$\begin{aligned} R_2^{\text{den}}(\bar{P}, P) &= \psi_h^{\text{den}}(a; t; \bar{P}) - \psi_h^{\text{den}}(a; t; P) + \mathbb{E}_P [\xi_h^{\text{den}}(a; t; \bar{P})] \\ &= - \int \int K_h(a_0 - a) \left[\frac{1}{2} \frac{\partial^2 S(\bar{\pi}(a_0|x), t)}{\partial \bar{\pi}^2} \{\pi(a_0|x) - \bar{\pi}(a_0|x)\}^2 + R_3(\pi - \bar{\pi}) \right] da_0 dP(x) \end{aligned}$$

where $R_3(\pi - \bar{\pi})$ denotes the higher-order remainder (third-order and above) of the Taylor expansion of $S(\pi(a_0|x), t)$ around $\bar{\pi}(a_0|x)$.

Proof. First, note that the expectation of $\xi_h^{\text{den}}(a; t; \bar{P})$ is

$$\begin{aligned} \mathbb{E}_P [\xi_h^{\text{den}}(a; t; \bar{P})] &= \mathbb{E}_P \left[K_h(A - a) \frac{\partial S(\bar{\pi}(A|X), t)}{\partial \bar{\pi}} \right] - \mathbb{E}_P \left[\int K_h(a_0 - a) \frac{\partial S(\bar{\pi}(a_0|X), t)}{\partial \bar{\pi}} \bar{\pi}(a_0|X) da_0 \right] \\ &\quad + \mathbb{E}_P \left[\int K_h(a_0 - a) S(\bar{\pi}(a_0|X), t) da_0 \right] - \mathbb{E}_P [\psi_h^{\text{den}}(a; t; \bar{P})] \\ &= \int \int K_h(a_0 - a) \frac{\partial S(\bar{\pi}(a_0|x), t)}{\partial \bar{\pi}} \pi(a_0|x) da_0 dP(x) \\ &\quad - \int \int K_h(a_0 - a) \frac{\partial S(\bar{\pi}(a_0|x), t)}{\partial \bar{\pi}} \bar{\pi}(a_0|x) da_0 dP(x) \\ &\quad + \int \int K_h(a_0 - a) S(\bar{\pi}(a_0|x), t) da_0 dP(x) - \psi_h^{\text{den}}(a; t; \bar{P}) \\ &= \int \int K_h(a_0 - a) \frac{\partial S(\bar{\pi}(a_0|x), t)}{\partial \bar{\pi}} \{\pi(a_0|x) - \bar{\pi}(a_0|x)\} da_0 dP(x) \\ &\quad + \int \int K_h(a_0 - a) S(\bar{\pi}(a_0|x), t) da_0 dP(x) - \psi_h^{\text{den}}(a; t; \bar{P}) \end{aligned}$$

Plugging this back into the decomposition of $R_2^{\text{den}}(\bar{P}, P)$ above, we have

$$\begin{aligned}
R_2^{\text{den}}(\bar{P}, P) &= -\psi_h^{\text{den}}(a; t; P) + \int \int K_h(a_0 - a) \frac{\partial S(\bar{\pi}(a_0|x), t)}{\partial \bar{\pi}} \{\pi(a_0|x) - \bar{\pi}(a_0|x)\} da_0 dP(x) \\
&+ \int \int K_h(a_0 - a) S(\bar{\pi}(a_0|x), t) da_0 dP(x) \\
&= \int \int K_h(a_0 - a) \frac{\partial S(\bar{\pi}(a_0|x), t)}{\partial \bar{\pi}} \{\pi(a_0|x) - \bar{\pi}(a_0|x)\} da_0 dP(x) \\
&+ \int \int K_h(a_0 - a) S(\bar{\pi}(a_0|x), t) da_0 dP(x) \\
&- \int \int K_h(a_0 - a) S(\pi(a_0|x), t) da_0 dP(x) \\
&= \int \int K_h(a_0 - a) \frac{\partial S(\bar{\pi}(a_0|x), t)}{\partial \bar{\pi}} \{\pi(a_0|x) - \bar{\pi}(a_0|x)\} da_0 dP(x) \\
&+ \int \int K_h(a_0 - a) \{S(\bar{\pi}(a_0|x), t) - S(\pi(a_0|x), t)\} da_0 dP(x)
\end{aligned}$$

Now note that we can do a Taylor's expansion of $S(\pi(a_0|x), t)$ around $\bar{\pi}(a_0|x)$ to obtain:

$$\begin{aligned}
S(\pi(a_0|x), t) &= S(\bar{\pi}(a_0|x), t) + \frac{\partial S(\bar{\pi}(a_0|x), t)}{\partial \bar{\pi}} \{\pi(a_0|x) - \bar{\pi}(a_0|x)\} \\
&+ \frac{1}{2} \frac{\partial^2 S(\bar{\pi}(a_0|x), t)}{\partial \bar{\pi}^2} \{\pi(a_0|x) - \bar{\pi}(a_0|x)\}^2 + R_3(\pi - \bar{\pi})
\end{aligned}$$

where $R_3(\pi - \bar{\pi})$ denotes the higher-order remainder of the Taylor expansion of $S(\pi(a_0|x), t)$ around $\bar{\pi}(a_0|x)$. Thus:

$$\begin{aligned}
\frac{\partial S(\bar{\pi}(a_0|x), t)}{\partial \bar{\pi}} \{\pi(a_0|x) - \bar{\pi}(a_0|x)\} &= S(\pi(a_0|x), t) - S(\bar{\pi}(a_0|x), t) \\
&- \frac{1}{2} \frac{\partial^2 S(\bar{\pi}(a_0|x), t)}{\partial \bar{\pi}^2} \{\pi(a_0|x) - \bar{\pi}(a_0|x)\}^2 - R_3(\pi - \bar{\pi})
\end{aligned}$$

Then, plugging this into the above for $R_2^{\text{den}}(\bar{P}, P)$, we have:

$$R_2^{\text{den}}(\bar{P}, P) = - \int \int K_h(a_0 - a) \left[\frac{1}{2} \frac{\partial^2 S(\bar{\pi}(a_0|x), t)}{\partial \bar{\pi}^2} \{\pi(a_0|x) - \bar{\pi}(a_0|x)\}^2 + R_3(\pi - \bar{\pi}) \right] da_0 dP(x)$$

which completes the proof. \square

C.2 Second-Order Remainder for the Numerator Estimand

We have the following lemma, which establishes that the remainder term for the EIF of $\psi_h^{\text{num}}(a; t)$ based on the von Mises expansion (30) is second-order.

Lemma 2. Consider the estimand $\varphi_h^{num}(a; t)$ and two probability measures P and \bar{P} . Let $\pi(a|x)$ and $\bar{\pi}(a|x)$ denote the propensity score under P and \bar{P} , respectively, and let $\mu(x, a)$ and $\bar{\mu}(x, a)$ denote the outcome regression function under P and \bar{P} , respectively. The remainder term is:

$$\begin{aligned} R_2^{num}(\bar{P}, P) &= \psi_h^{num}(a; t; \bar{P}) - \psi_h^{num}(a; t; P) + \mathbb{E}_P [\xi_h^{num}(a; t; \bar{P})] \\ &= \int \int K_h(a_0 - a) \left\{ \frac{S(\bar{\pi}(a_0|x), t)}{\bar{\pi}(a_0|x)} - \frac{\partial S(\bar{\pi}(a_0|x), t)}{\partial \bar{\pi}} \right\} \{\pi(a_0|x) - \bar{\pi}(a_0|x)\} \{\mu(x, a_0) - \bar{\mu}(x, a_0)\} da_0 dP(x) \\ &\quad - \int \int K_h(a_0 - a) \mu(x, a_0) \left[\frac{1}{2} \frac{\partial^2 S(\bar{\pi}(a_0|x), t)}{\partial \bar{\pi}^2} \{\pi(a_0|x) - \bar{\pi}(a_0|x)\}^2 + R_3(\pi - \bar{\pi}) \right] da_0 dP(x) \end{aligned}$$

where $R_3(\pi - \bar{\pi})$ denotes the higher-order remainder (third-order and above) of the Taylor expansion of $S(\pi(a_0|x), t)$ around $\bar{\pi}(a_0|x)$.

Proof. First, it's useful to note that the $\psi_h^{num}(a; t; \bar{P})$ will cancel with the same term contained in $\xi_h^{num}(a; t; \bar{P})$, in the same way as the previous remainder term. Thus,

$$\begin{aligned} \mathbb{E}_P [\xi_h^{num}(a; t; \bar{P})] + \psi_h^{num}(a; t; \bar{P}) &= \mathbb{E}_P \left[K_h(A - a) \frac{(Y - \bar{\mu}(X, A))S(\bar{\pi}(A|X), t)}{\bar{\pi}(A|X)} \right] \\ &\quad + \mathbb{E}_P \left[K_h(A - a) \bar{\mu}(X, A) \frac{\partial S(\bar{\pi}(A|X), t)}{\partial \bar{\pi}} \right] \\ &\quad - \mathbb{E}_P \left[\int K_h(a_0 - a) \bar{\mu}(X, a_0) \frac{\partial S(\bar{\pi}(a_0|X), t)}{\partial \bar{\pi}} \bar{\pi}(a_0|X) da_0 \right] \\ &\quad + \mathbb{E}_P \left[\int K_h(a_0 - a) S(\bar{\pi}(a_0, X), t) \bar{\mu}(X, a_0) da_0 \right] \\ &= \mathbb{E}_P \left[K_h(A - a) \frac{(Y - \bar{\mu}(X, A))S(\bar{\pi}(A|X), t)}{\bar{\pi}(A|X)} \right] \\ &\quad + \int \int K_h(a_0 - a) \bar{\mu}(x, a_0) \frac{\partial S(\bar{\pi}(a_0, x), t)}{\partial \bar{\pi}} \{\pi(a_0|x) - \bar{\pi}(a_0|x)\} da_0 dP(x) \\ &\quad + \mathbb{E}_P \left[\int K_h(a_0 - a) S(\bar{\pi}(a_0, X), t) \bar{\mu}(X, a_0) da_0 \right] \end{aligned}$$

Now let's look at the first expectation in the above decomposition. Note that, by iterated expectations:

$$\begin{aligned} \mathbb{E}_P \left[K_h(A - a) \frac{(Y - \bar{\mu}(X, A))S(\bar{\pi}(A|X), t)}{\bar{\pi}(A|X)} \right] &= \mathbb{E}_P \left[\mathbb{E}_P \left[K_h(A - a) \frac{(Y - \bar{\mu}(X, A))S(\bar{\pi}(A|X), t)}{\bar{\pi}(A|X)} \middle| X, A \right] \right] \\ &= \mathbb{E}_P \left[K_h(A - a) \frac{(\mu(X, A) - \bar{\mu}(X, A))S(\bar{\pi}(A|X), t)}{\bar{\pi}(A|X)} \right] \end{aligned}$$

Thus, given this decomposition, we have:

$$\begin{aligned}
R_2^{\text{num}}(\bar{P}, P) &= -\psi_h^{\text{num}}(a; t; P) + \mathbb{E}_P [\xi_h^{\text{num}}(a; t; \bar{P})] + \psi_h^{\text{num}}(a; t; \bar{P}) \\
&= - \int \int K_h(a_0 - a) S(\pi(a_0|x), t) \mu(x, a_0) da_0 dP(x) \\
&\quad + \mathbb{E}_P \left[K_h(A - a) \frac{(\mu(X, A) - \bar{\mu}(X, A)) S(\bar{\pi}(A|X), t)}{\bar{\pi}(A|X)} \right] \\
&\quad + \int \int K_h(a_0 - a) \bar{\mu}(x, a_0) \frac{\partial S(\bar{\pi}(a_0, x), t)}{\partial \bar{\pi}} \{\pi(a_0|x) - \bar{\pi}(a_0|x)\} da_0 dP(x) \\
&\quad + \mathbb{E}_P \left[\int K_h(a_0 - a) S(\bar{\pi}(a_0, X), t) \bar{\mu}(X, a_0) da_0 \right] \\
&= - \int \int K_h(a_0 - a) S(\pi(a_0|x), t) \mu(x, a_0) da_0 dP(x) \\
&\quad + \int \int K_h(a_0 - a) \frac{(\mu(x, a_0) - \bar{\mu}(x, a_0)) S(\bar{\pi}(a_0|x), t)}{\bar{\pi}(a_0|x)} \pi(a_0|x) da_0 dP(x) \\
&\quad + \int \int K_h(a_0 - a) \bar{\mu}(x, a_0) \frac{\partial S(\bar{\pi}(a_0, x), t)}{\partial \bar{\pi}} \{\pi(a_0|x) - \bar{\pi}(a_0|x)\} da_0 dP(x) \\
&\quad + \int \int K_h(a_0 - a) S(\bar{\pi}(a_0, x), t) \bar{\mu}(x, a_0) da_0 dP(x)
\end{aligned}$$

Now let's look specifically at the first and fourth terms. We have:

$$\begin{aligned}
&\int \int K_h(a_0 - a) S(\bar{\pi}(a_0, x), t) \bar{\mu}(x, a_0) da_0 dP(x) - \int \int K_h(a_0 - a) S(\pi(a_0|x), t) \mu(x, a_0) da_0 dP(x) \\
&= \int \int K_h(a_0 - a) S(\pi(a_0|x), t) \{\bar{\mu}(x, a_0) - \mu(x, a_0)\} da_0 dP(x) \\
&\quad + \int \int K_h(a_0 - a) \bar{\mu}(x, a_0) \{S(\bar{\pi}(a_0, x), t) - S(\pi(a_0, x), t)\} da_0 dP(x)
\end{aligned}$$

Plugging this into the above decomposition, we have:

$$\begin{aligned}
R_2^{\text{num}}(\bar{P}, P) &= \int \int K_h(a_0 - a) \frac{(\mu(x, a_0) - \bar{\mu}(x, a_0)) S(\bar{\pi}(a_0|x), t)}{\bar{\pi}(a_0|x)} \pi(a_0|x) da_0 dP(x) \\
&\quad + \int \int K_h(a_0 - a) \bar{\mu}(x, a_0) \frac{\partial S(\bar{\pi}(a_0, x), t)}{\partial \bar{\pi}} \{\pi(a_0|x) - \bar{\pi}(a_0|x)\} da_0 dP(x) \\
&\quad + \int \int K_h(a_0 - a) S(\pi(a_0|x), t) \{\bar{\mu}(x, a_0) - \mu(x, a_0)\} da_0 dP(x) \\
&\quad + \int \int K_h(a_0 - a) \bar{\mu}(x, a_0) \{S(\bar{\pi}(a_0, x), t) - S(\pi(a_0, x), t)\} da_0 dP(x)
\end{aligned}$$

Now let's look at the first and third terms. For simplicity, let's ignore the integrals and $K_h(a_0 - a)$ term; furthermore, let's write $\mu, \bar{\mu}$ and $\pi, \bar{\pi}$ for notational simplicity. We have

that these first and third terms equal:

$$\begin{aligned}
\frac{(\mu - \bar{\mu})S(\bar{\pi}, t)}{\bar{\pi}}\pi - S(\pi, t)(\mu - \bar{\mu}) &= \left(\frac{1}{\bar{\pi}} - \frac{1}{\pi}\right) (\mu - \bar{\mu})S(\bar{\pi}, t)\pi + (\mu - \bar{\mu})S(\bar{\pi}, t) - S(\pi, t)(\mu - \bar{\mu}) \\
&= \left(\frac{1}{\bar{\pi}} - \frac{1}{\pi}\right) (\mu - \bar{\mu})S(\bar{\pi}, t)\pi + (\mu - \bar{\mu})\{S(\bar{\pi}, t) - S(\pi, t)\} \\
&= (\pi - \bar{\pi})(\mu - \bar{\mu})\frac{S(\bar{\pi}, t)}{\bar{\pi}} + (\mu - \bar{\mu})\{S(\bar{\pi}, t) - S(\pi, t)\}
\end{aligned}$$

Plugging this back into the first and third terms of $R_2^{\text{num}}(\bar{P}, P)$ above, we have:

$$\begin{aligned}
R_2^{\text{num}}(\bar{P}, P) &= \int \int K_h(a_0 - a) \frac{S(\bar{\pi}(a_0|x), t)}{\bar{\pi}(a_0|x)} \{\pi(a_0|x) - \bar{\pi}(a_0|x)\} \{\mu(x, a_0) - \bar{\mu}(x, a_0)\} da_0 dP(x) \\
&\quad + \int \int K_h(a_0 - a) \{\mu(x, a_0) - \bar{\mu}(x, a_0)\} \{S(\bar{\pi}(a_0|x), t) - S(\pi(a_0|x), t)\} da_0 dP(x) \\
&\quad + \int \int K_h(a_0 - a) \bar{\mu}(x, a_0) \frac{\partial S(\bar{\pi}(a_0|x), t)}{\partial \bar{\pi}} \{\pi(a_0|x) - \bar{\pi}(a_0|x)\} da_0 dP(x) \\
&\quad + \int \int K_h(a_0 - a) \bar{\mu}(x, a_0) \{S(\bar{\pi}(a_0|x), t) - S(\pi(a_0|x), t)\} da_0 dP(x)
\end{aligned}$$

Now let's inspect the third and fourth terms—these are identical to the terms involved in $R_2^{\text{den}}(\bar{P}, P)$, except there is a $\bar{\mu}(x, a_0)$ involved in the integral. Thus, following the same procedure as the proof of Lemma 1, we have:

$$\begin{aligned}
R_2^{\text{num}}(\bar{P}, P) &= \int \int K_h(a_0 - a) \frac{S(\bar{\pi}(a_0|x), t)}{\bar{\pi}(a_0|x)} \{\pi(a_0|x) - \bar{\pi}(a_0|x)\} \{\mu(x, a_0) - \bar{\mu}(x, a_0)\} da_0 dP(x) \\
&\quad + \int \int K_h(a_0 - a) \{\mu(x, a_0) - \bar{\mu}(x, a_0)\} \{S(\bar{\pi}(a_0|x), t) - S(\pi(a_0|x), t)\} da_0 dP(x) \\
&\quad - \int \int K_h(a_0 - a) \bar{\mu}(x, a_0) \left[\frac{1}{2} \frac{\partial^2 S(\bar{\pi}(a_0|x), t)}{\partial \bar{\pi}^2} \{\pi(a_0|x) - \bar{\pi}(a_0|x)\}^2 + R_3(\pi - \bar{\pi}) \right] da_0 dP(x)
\end{aligned}$$

where $R_3(\pi - \bar{\pi})$ denotes the higher-order remainder of the Taylor expansion of $S(\pi(a_0|x), t)$ around $\bar{\pi}(a_0|x)$. Again, note that this Taylor expansion is:

$$\begin{aligned}
S(\pi(a_0|x), t) &= S(\bar{\pi}(a_0|x), t) + \frac{\partial S(\bar{\pi}(a_0|x), t)}{\partial \bar{\pi}} \{\pi(a_0|x) - \bar{\pi}(a_0|x)\} \\
&\quad + \frac{1}{2} \frac{\partial^2 S(\bar{\pi}(a_0|x), t)}{\partial \bar{\pi}^2} \{\pi(a_0|x) - \bar{\pi}(a_0|x)\}^2 + R_3(\pi - \bar{\pi})
\end{aligned}$$

Thus:

$$S(\bar{\pi}(a_0|x), t) - S(\pi(a_0|x), t) = \frac{\partial S(\bar{\pi}(a_0|x), t)}{\partial \bar{\pi}} \{\bar{\pi}(a_0|x) - \pi(a_0|x)\} \\ - \frac{1}{2} \frac{\partial^2 S(\bar{\pi}(a_0|x), t)}{\partial \bar{\pi}^2} \{\pi(a_0|x) - \bar{\pi}(a_0|x)\}^2 - R_3(\pi - \bar{\pi})$$

Therefore, plugging this back into $R_2^{\text{num}}(\bar{P}, P)$, we have:

$$R_2^{\text{num}}(\bar{P}, P) = \int \int K_h(a_0 - a) \frac{S(\bar{\pi}(a_0|x), t)}{\bar{\pi}(a_0|x)} \{\pi(a_0|x) - \bar{\pi}(a_0|x)\} \{\mu(x, a_0) - \bar{\mu}(x, a_0)\} da_0 dP(x) \\ + \int \int K_h(a_0 - a) \frac{\partial S(\bar{\pi}(a_0|x), t)}{\partial \bar{\pi}} \{\mu(x, a_0) - \bar{\mu}(x, a_0)\} \{\bar{\pi}(a_0|x) - \pi(a_0|x)\} da_0 dP(x) \\ - \int \int K_h(a_0 - a) \mu(x, a_0) \left[\frac{1}{2} \frac{\partial^2 S(\bar{\pi}(a_0|x), t)}{\partial \bar{\pi}^2} \{\pi(a_0|x) - \bar{\pi}(a_0|x)\}^2 + R_3(\pi - \bar{\pi}) \right] da_0 dP(x)$$

Now by collapsing the first two terms, we have:

$$R_2^{\text{num}}(\bar{P}, P) = \int \int K_h(a_0 - a) \left\{ \frac{S(\bar{\pi}(a_0|x), t)}{\bar{\pi}(a_0|x)} - \frac{\partial S(\bar{\pi}(a_0|x), t)}{\partial \bar{\pi}} \right\} \{\pi(a_0|x) - \bar{\pi}(a_0|x)\} \{\mu(x, a_0) - \bar{\mu}(x, a_0)\} da_0 dP(x) \\ - \int \int K_h(a_0 - a) \mu(x, a_0) \left[\frac{1}{2} \frac{\partial^2 S(\bar{\pi}(a_0|x), t)}{\partial \bar{\pi}^2} \{\pi(a_0|x) - \bar{\pi}(a_0|x)\}^2 + R_3(\pi - \bar{\pi}) \right] da_0 dP(x)$$

This completes the proof. \square

D Proof of Proposition 1

To prove Proposition 1, it is sufficient to prove that

$$\sqrt{n}(\widehat{\psi}_h^{\text{num}}(a; t) - \psi_h^{\text{num}}(a; t)) \rightarrow N(0, \text{Var}\{\varphi_h^{\text{num}}(a; t)\}), \text{ and} \quad (31)$$

$$\sqrt{n}(\widehat{\psi}_h^{\text{den}}(a; t) - \psi_h^{\text{den}}(a; t)) \rightarrow N(0, \text{Var}\{\varphi_h^{\text{den}}(a; t)\}) \quad (32)$$

because, given (31) and (32), Proposition 1 immediately follows by the delta method.

First, note that $\widehat{\psi}_h^{\text{num}}(a; t) = \mathbb{P}_n\{\widehat{\varphi}_h^{\text{num}}(a; t)\}$ and $\psi_h^{\text{num}}(a; t) = \mathbb{P}\{\varphi_h^{\text{num}}(a; t)\}$. Thus, we have the following decomposition by adding and subtracting terms:

$$\widehat{\psi}_h^{\text{num}}(a; t) - \psi_h^{\text{num}}(a; t) = (\mathbb{P}_n - \mathbb{P})\{\varphi_h^{\text{num}}(a; t)\} + (\mathbb{P}_n - \mathbb{P})\{\widehat{\varphi}_h^{\text{num}}(a; t) - \varphi_h^{\text{num}}(a; t)\} + R_2^{\text{num}}(\mathbb{P}_n, \mathbb{P}), \quad (33)$$

where $R_2^{\text{num}}(\mathbb{P}_n, \mathbb{P}) = \mathbb{P}\{\widehat{\varphi}_h^{\text{num}}(a; t) - \varphi_h^{\text{num}}(a; t)\}$ is the remainder term defined in Remark 1. The first term in (33) is the difference between a sample average and the expectation of a fixed function, and thus by the central limit theorem will be asymptotically Normal with

mean zero and variance $\text{Var}(\varphi_h^{\text{num}})/n$ up to error $o_P(n^{-1/2})$; this is the same distribution in (31). Thus, in order to prove (31), we need to establish that the second and third terms in (33) are $o_P(n^{-1/2})$.

By assumption, the sample used to compute $\widehat{\varphi}_h^{\text{num}}(a; t)$ is independent of the sample that defines the above empirical measure $\mathbb{P}_n\{\cdot\}$. Thus, for the second term in (33), we can write:

$$(\mathbb{P}_n - \mathbb{P})\{\widehat{\varphi}_h^{\text{num}}(a; t) - \varphi_h^{\text{num}}(a; t)\} = O_P(n^{-1/2}\|\widehat{\varphi}_h^{\text{num}}(a; t) - \varphi_h^{\text{num}}(a; t)\|) = o_P(n^{-1/2}),$$

where the first equality follows by Lemma 2 in Kennedy et al. (2020), and the second equality follows by our assumption that $\|\widehat{\varphi}_h^{\text{num}}(a; t) - \varphi_h^{\text{num}}(a; t)\| = o_P(1)$.

Lastly, by assumption, $\|\widehat{\pi}(a|X) - \pi(a|X)\|^2 = o_P(n^{-1/2})$ and $\|\widehat{\mu}(X, a) - \mu(X, a)\| \cdot \|\widehat{\pi}(a|X) - \pi(a|X)\| = o_P(n^{-1/2})$ and thus, as discussed in Remark 1, $R_2^{\text{num}}(\mathbb{P}_n, \mathbb{P}) = o_P(n^{-1/2})$.

This proves (31). The proof for (32) is exactly the same, with the only difference being that $\varphi_h^{\text{num}}(a; t)$ and $\widehat{\varphi}_h^{\text{num}}(a; t)$ are replaced with $\varphi_h^{\text{den}}(a; t)$ and $\widehat{\varphi}_h^{\text{den}}(a; t)$.

E Proof of Theorem 2

First, note that $\widehat{\psi}_h^{\text{num}}(a; t) = \mathbb{P}_n\{\varphi_h^{\text{num}}(a; t, \widehat{\eta})\}$ and $\psi_h^{\text{num}}(a; t_0) = \mathbb{P}\{\varphi_h^{\text{num}}(a; t_0, \eta_0)\}$. Thus,

$$\begin{aligned} \widehat{\psi}_h^{\text{num}}(a; \widehat{t}) - \psi_h^{\text{num}}(a; t_0) &= \mathbb{P}_n\{\varphi_h^{\text{num}}(a; \widehat{t}, \widehat{\eta})\} - \mathbb{P}\{\varphi_h^{\text{num}}(a; t_0, \eta_0)\} \\ &= (\mathbb{P}_n - \mathbb{P})\{\varphi_h^{\text{num}}(a; t_0, \eta_0)\} + (\mathbb{P}_n - \mathbb{P})\{\varphi_h^{\text{num}}(a; \widehat{t}, \widehat{\eta}) - \varphi_h^{\text{num}}(a; t_0, \widehat{\eta})\} \end{aligned} \quad (34)$$

$$+ (\mathbb{P}_n - \mathbb{P})\{\varphi_h^{\text{num}}(a; t_0, \widehat{\eta}) - \varphi_h^{\text{num}}(a; t_0, \eta_0)\} \quad (35)$$

$$+ \mathbb{P}\{\varphi_h^{\text{num}}(a; \widehat{t}, \widehat{\eta}) - \varphi_h^{\text{num}}(a; t_0, \widehat{\eta})\} + \mathbb{P}\{\varphi_h^{\text{num}}(a; t_0, \widehat{\eta}) - \varphi_h^{\text{num}}(a; t_0, \eta_0)\} \quad (36)$$

which follows by adding and subtracting terms. We will analyze each of the three terms above, (34), (35), and (36), in turn.

The first term in (34) is the difference between a sample average and the expectation of a fixed function, and thus by the central limit theorem will be asymptotically Normal. Meanwhile, because $\varphi_h^{\text{num}}(a; t, \widehat{\eta})$ is Donsker in t by assumption and \widehat{t} is consistent by assumption, the second term in (34) is $o_P(n^{-1/2})$ according to Lemma 19.24 of Van der Vaart (2000).

Meanwhile, because $\widehat{\eta}$ is consistent and is estimated on an independent sample by assumption, (35) is $o_P(n^{-1/2})$ by Lemma 2 of Kennedy et al. (2020).

Finally, because the map $t \mapsto \psi_h^{\text{num}}(a; t, \eta)$ is differentiable at t_0 uniformly in η , and noting that $\mathbb{P}\{\varphi_h^{\text{num}}(a; t_0, \widehat{\eta})\} = \psi_h^{\text{num}}(a; t_0, \widehat{\eta})$, we can use a Taylor expansion to write the

first term of (36) as

$$\begin{aligned}\mathbb{P}\{\varphi_h^{\text{num}}(a; \hat{t}, \hat{\eta}) - \varphi_h^{\text{num}}(a; t_0, \hat{\eta})\} &= \left\{ \frac{\partial}{\partial t} \psi_h^{\text{num}}(a; t_0, \hat{\eta}) \right\} (\hat{t} - t_0) + o_P(\|\hat{t} - t_0\|) \\ &= \left\{ \frac{\partial}{\partial t} \psi_h^{\text{num}}(a; t_0, \eta_0) \right\} (\hat{t} - t_0) + o_P(\|\hat{t} - t_0\|)\end{aligned}$$

where the second equality follows by the assumption that $\frac{\partial}{\partial t} \psi_h^{\text{num}}(a; t_0, \hat{\eta}) \xrightarrow{p} \frac{\partial}{\partial t} \psi_h^{\text{num}}(a; t_0, \eta_0)$.

Putting these results together, we have

$$\begin{aligned}\hat{\psi}_h^{\text{num}}(a; \hat{t}) - \psi_h^{\text{num}}(a; t_0) &= (\mathbb{P}_n - \mathbb{P})\{\varphi_h^{\text{num}}(a; t_0, \eta_0)\} + \left\{ \frac{\partial}{\partial t} \psi_h^{\text{num}}(a; t_0, \eta_0) \right\} (\hat{t} - t_0) \\ &\quad + O_P(R_2^{\text{num}}) + o_P(\|\hat{t} - t_0\|) + o_P(n^{-1/2})\end{aligned}\tag{37}$$

where $R_2^{\text{num}} = \mathbb{P}\{\varphi_h^{\text{num}}(a; t_0, \hat{\eta}) - \varphi_h^{\text{num}}(a; t_0, \eta_0)\}$ is the last term in (36).

Now recall that \hat{t} is estimated as

$$\hat{t} = \inf\{t : \hat{\psi}_h^{\text{den}}(a; t) \leq 1 - \gamma\}$$

In other words, t is estimated via the estimating equation

$$1 - \gamma - \varphi_h^{\text{den}}(a; t, \eta) = 0$$

First, note that for the true t_0 and η_0 , $\mathbb{P}\{1 - \gamma - \varphi_h^{\text{den}}(a; t_0, \eta_0)\} = 0$, because $\varphi_h^{\text{den}}(a; t, \eta)$ is the uncentered EIF for $\psi_h^{\text{den}}(a; \eta, t)$, and the true t_0 is defined such that $\psi_h^{\text{den}}(a; t_0, \eta_0) = 1 - \gamma$. Meanwhile, \hat{t} is chosen such that $\mathbb{P}_n\{1 - \gamma - \varphi_h^{\text{den}}(a; \hat{t}, \hat{\eta})\} = 0$, because $\mathbb{P}_n\{\varphi_h^{\text{den}}(a; t, \hat{\eta})\} = \hat{\psi}_h^{\text{den}}(a; t)$. Given this and Assumptions 1-4, we have by Lemma 3 of Kennedy et al. (2023) that

$$\begin{aligned}\hat{t} - t_0 &= \left\{ \frac{\partial}{\partial t} \psi_h^{\text{den}}(a; t_0, \eta_0) \right\}^{-1} (\mathbb{P}_n - \mathbb{P})\{1 - \gamma - \varphi_h^{\text{den}}(a; t_0, \eta_0)\} + O_P(R_2^{\text{den}}) + o_P(n^{-1/2}) \\ &= - \left\{ \frac{\partial}{\partial t} \psi_h^{\text{den}}(a; t_0, \eta_0) \right\}^{-1} (\mathbb{P}_n - \mathbb{P})\{\varphi_h^{\text{den}}(a; t_0, \eta_0)\} + O_P(R_2^{\text{den}}) + o_P(n^{-1/2})\end{aligned}\tag{38}$$

where $R_2^{\text{den}} = \mathbb{P}\{\varphi_h^{\text{den}}(a; t_0, \hat{\eta}) - \varphi_h^{\text{den}}(a; t_0, \eta_0)\}$, and furthermore that

$$o_P(\|\hat{t} - t_0\|) = o_P(n^{-1/2}) + o_P(R_2^{\text{den}})\tag{39}$$

Plugging this into (37), we have

$$\begin{aligned}
\widehat{\psi}_h^{\text{num}}(a; \widehat{t}) - \psi_h^{\text{num}}(a; t_0, \eta_0) &= (\mathbb{P}_n - \mathbb{P})\{\varphi_h^{\text{num}}(a; t_0, \eta_0)\} - \frac{\partial \psi_h^{\text{num}}(a; t_0, \eta_0)/\partial t}{\partial \psi_h^{\text{den}}(a; t_0, \eta_0)/\partial t} (\mathbb{P}_n - \mathbb{P})\{\varphi_h^{\text{den}}(a; t_0, \eta_0)\} \\
&\quad + \left\{ \frac{\partial}{\partial t} \psi_h^{\text{num}}(a; t_0, \eta_0) \right\} \{O_P(R_2^{\text{den}}) + o_P(n^{-1/2})\} \\
&\quad + O_P(R_2^{\text{num}}) + o_P(\|\widehat{t} - t_0\|) + o_P(n^{-1/2}) \\
&= (\mathbb{P}_n - \mathbb{P})\{\varphi_h^{\text{num}}(a; t_0, \eta_0)\} - \frac{\partial \psi_h^{\text{num}}(a; t_0, \eta_0)/\partial t}{\partial \psi_h^{\text{den}}(a; t_0, \eta_0)/\partial t} (\mathbb{P}_n - \mathbb{P})\{\varphi_h^{\text{den}}(a; t_0, \eta_0)\} \\
&\quad + \left\{ \frac{\partial}{\partial t} \psi_h^{\text{num}}(a; t_0, \eta_0) \right\} \{O_P(R_2^{\text{den}}) + o_P(n^{-1/2})\} \\
&\quad + O_P(R_2^{\text{num}}) + o_P(R_2^{\text{den}}) + o_P(n^{-1/2}) \\
&= (\mathbb{P}_n - \mathbb{P})\{\varphi_h^{\text{num}}(a; t_0, \eta_0)\} - \frac{\partial \psi_h^{\text{num}}(a; t_0, \eta_0)/\partial t}{\partial \psi_h^{\text{den}}(a; t_0, \eta_0)/\partial t} (\mathbb{P}_n - \mathbb{P})\{\varphi_h^{\text{den}}(a; t_0, \eta_0)\} \\
&\quad + O_P(R_2^{\text{num}}) + O_P(R_2^{\text{den}}) + o_P(n^{-1/2})
\end{aligned}$$

where the first equality follows by plugging (38) into (37), the second equality follows by plugging in (39), and the third equality follows by assuming $|\frac{\partial}{\partial t} \psi_h^{\text{num}}(a; t_0, \eta_0)|$ is bounded and recognizing that $O_p(R_2^{\text{den}}) + o_p(R_2^{\text{den}}) = O_p(R_2^{\text{den}})$. This completes the proof.

F Efficient Influence Function for the Ratio $\psi_h(a; t)$

The main text derives estimators for STATE $\psi_h(a; t)$ defined in (5). Specifically, we wrote $\psi_h(a; t) \equiv \frac{\psi_h^{\text{num}}(a; t)}{\psi_h^{\text{den}}(a; t)}$, and then derived efficient influence functions (EIFs) for $\psi_h^{\text{num}}(a; t)$ and $\psi_h^{\text{den}}(a; t)$. An alternative, asymptotically equivalent approach is to instead derive the EIF of $\psi_h(a; t)$ itself. The following corollary communicates the EIF $\psi_h(a; t)$ when the trimming threshold t is fixed.

Corollary 2. *Let $\psi_h(a; t) = \psi_h^{\text{num}}(a; t)/\psi_h^{\text{den}}(a; t)$, where $\psi_h^{\text{num}}(a; t)$ and $\psi_h^{\text{den}}(a; t)$ are defined in (8) and (9). Then, if the trimming threshold t is fixed and $\psi_h^{\text{den}}(a; t) \geq b > 0$ for some*

constant b , the EIF of $\psi_h(a; t)$ is

$$\begin{aligned} \varphi_h(a; t) = & \frac{1}{\psi_h^{\text{den}}(a; t)} \left[K_h(A - a) \frac{\{Y - \mu(X, A)\} S(\pi(A|X), t)}{\pi(A|X)} \right. \\ & + K_h(A - a) \frac{\partial S(\pi(A|X), t)}{\partial \pi} \{\mu(X, A) - \psi_h(a; t)\} \\ & \left. + \int K_h(a_0 - a) \left\{ S(\pi(a_0|X), t) - \frac{\partial S(\pi(a_0|X), t)}{\partial \pi} \pi(a_0|X) \right\} \{\mu(X, a_0) - \psi_h(a; t)\} da_0 \right]. \end{aligned}$$

Proof. First, let $\psi_h(a; t) \equiv \frac{\psi_h^{\text{num}}(a; t)}{\psi_h^{\text{den}}(a; t)}$, where

$$\begin{aligned} \psi_h^{\text{num}}(a; t) &= \int \int \mu(x, a_0) S(\pi(a_0|x), t) K_h(a_0 - a) da_0 dP(x) \\ \psi_h^{\text{den}}(a; t) &= \int \int S(\pi(a_0|x), t) K_h(a_0 - a) da_0 dP(x) \end{aligned}$$

Our goal here is to derive the efficient influence function for $\psi_h(a; t)$. First, by the influence function “product rule,” we have:

$$\mathbb{IF}(\psi_h(a; t)) = \frac{\mathbb{IF}(\psi_h^{\text{num}}(a; t))}{\psi_h^{\text{den}}(a; t)} - \left(\frac{\psi_h^{\text{num}}(a; t)}{\psi_h^{\text{den}}(a; t)} \right) \frac{\mathbb{IF}(\psi_h^{\text{den}}(a; t))}{\psi_h^{\text{den}}(a; t)} \quad (40)$$

$$= \frac{1}{\psi_h^{\text{den}}(a; t)} \left[\mathbb{IF}(\psi_h^{\text{num}}(a; t)) - \psi_h(a; t) \mathbb{IF}(\psi_h^{\text{den}}(a; t)) \right] \quad (41)$$

In Theorem 1 we found $\mathbb{IF}(\psi_h^{\text{num}}(a; t))$ and $\mathbb{IF}(\psi_h^{\text{den}}(a; t))$, which can be plugged into (41) to get the following:

$$\begin{aligned} \mathbb{IF}(\psi_h(a; t)) &= \frac{1}{\psi_h^{\text{den}}(a; t)} \left[\mathbb{IF}(\psi_h^{\text{num}}(a; t)) - \psi_h(a; t) \mathbb{IF}(\psi_h^{\text{den}}(a; t)) \right] \\ &= \frac{1}{\psi_h^{\text{den}}(a; t)} \left[K_h(A - a) \frac{(Y - \mu(X, A)) S(\pi(A|X), t)}{\pi(A|X)} + K_h(A - a) \mu(X, A) \frac{\partial S(\pi(A|X), t)}{\partial \pi} \right. \\ &+ \int K_h(a_0 - a) \mu(X, a_0) \left\{ S(\pi(a_0|X), t) - \frac{\partial S(\pi(a_0|X), t)}{\partial \pi} \pi(a_0|X) \right\} da_0 \\ &- \psi_h(a; t) \left\{ K_h(A - a) \frac{\partial S(\pi(A|X), t)}{\partial \pi} \right. \\ &\left. \left. + \int K_h(a_0 - a) \left\{ S(\pi(a_0|X), t) - \frac{\partial S(\pi(a_0|X), t)}{\partial \pi} \pi(a_0|X) \right\} da_0 \right\} \right] \end{aligned}$$

Note that the $\psi_h(a; t)$ terms in $\mathbb{IF}(\psi_h^{\text{num}}(a; t))$ and $\mathbb{IF}(\psi_h^{\text{den}}(a; t))$ end up cancelling after

distributing the outer $\frac{1}{\psi_h^{\text{den}}(a;t)}$. We can then combine some terms to obtain:

$$\begin{aligned} \mathbb{I}\mathbb{F}(\psi_h(a;t)) &= \frac{1}{\psi_h^{\text{den}}(a;t)} \left[K_h(A-a) \frac{(Y - \mu(X, A))S(\pi(A|X), t)}{\pi(A|X)} \right. \\ &\quad + K_h(A-a) \frac{\partial S(\pi(A|X), t)}{\partial \pi} \{ \mu(X, A) - \psi_h(a;t) \} \\ &\quad \left. + \int K_h(a_0 - a) \{ S(\pi(a_0|X), t) - \frac{\partial S(\pi(a_0|X), t)}{\partial \pi} \pi(a_0|X) \} \{ \mu(X, a_0) - \psi_h(a;t) \} da_0 \right] \end{aligned}$$

This completes the proof. \square

F.1 Analyzing the von Mises Remainder Term of Corollary 2

Note that in the proof of Corollary 2, we found that the EIF $\varphi_h(a;t)$ is:

$$\varphi_h(a;t) = \frac{\varphi_h^{\text{num}}(a;t)}{\psi_h^{\text{den}}(a;t)} - \psi_h(a;t) \frac{\varphi_h^{\text{den}}(a;t)}{\psi_h^{\text{den}}(a;t)}$$

where $\varphi_h^{\text{num}}(a;t)$ and $\varphi_h^{\text{den}}(a;t)$ are the EIFs provided in Theorem 1.

In order for the von Mises expansion (30) to be valid, we must have that $\mathbb{E}_P[\varphi_{t,h,\epsilon}(a;P)] = 0$. In the proof of Theorem 1, we already found that $\mathbb{E}_P[\varphi_{t,h,\epsilon}^{\text{num}}(a;P)] = 0$ and $\mathbb{E}_P[\varphi_{t,h,\epsilon}^{\text{den}}(a;P)] = 0$, and so it immediately follows that $\mathbb{E}_P[\varphi_{t,h,\epsilon}(a;P)] = 0$.

Now we can study the above von Mises expansion for the proposed EIF $\varphi_h(a;t)$. First, note that the von Mises expansions for $\varphi_h^{\text{num}}(a;t)$ and $\varphi_h^{\text{den}}(a;t)$ are

$$\begin{aligned} \mathbb{E}_P[\varphi_{t,h,\epsilon}^{\text{num}}(a;\bar{P})] &= R_2^{\text{num}}(\bar{P}, P) + \psi_h^{\text{num}}(a;P) - \psi_h^{\text{num}}(a;\bar{P}), \text{ and} \\ \mathbb{E}_P[\varphi_{t,h,\epsilon}^{\text{den}}(a;\bar{P})] &= R_2^{\text{den}}(\bar{P}, P) + \psi_h^{\text{den}}(a;P) - \psi_h^{\text{den}}(a;\bar{P}) \end{aligned}$$

Therefore, we have:

$$\begin{aligned}
\mathbb{E}_P[\varphi_{t,h,\epsilon}(a; \bar{P})] &= \mathbb{E}_P \left[\frac{\xi_h^{\text{num}}(a; t; \bar{P})}{\psi_h^{\text{den}}(a; \bar{P})} - \psi_{t,h,\epsilon}(a; \bar{P}) \frac{\xi_h^{\text{den}}(a; t; \bar{P})}{\psi_h^{\text{den}}(a; \bar{P})} \right] \\
&= \frac{\mathbb{E}_P[\xi_h^{\text{num}}(a; t; \bar{P})]}{\psi_h^{\text{den}}(a; \bar{P})} - \frac{\psi_{t,h,\epsilon}(a; \bar{P})}{\psi_h^{\text{den}}(a; \bar{P})} \mathbb{E}_P[\xi_h^{\text{den}}(a; t; \bar{P})] \\
&= \frac{R_2^{\text{num}}(\bar{P}, P) + \psi_h^{\text{num}}(a; P) - \psi_h^{\text{num}}(a; \bar{P})}{\psi_h^{\text{den}}(a; \bar{P})} \\
&\quad - \frac{\psi_{t,h,\epsilon}(a; \bar{P})}{\psi_h^{\text{den}}(a; \bar{P})} \{R_2^{\text{den}}(\bar{P}, P) + \psi_h^{\text{den}}(a; P) - \psi_h^{\text{den}}(a; \bar{P})\} \\
&= \frac{R_2^{\text{num}}(\bar{P}, P) + \psi_h^{\text{num}}(a; P)}{\psi_h^{\text{den}}(a; \bar{P})} - \frac{\psi_{t,h,\epsilon}(a; \bar{P})}{\psi_h^{\text{den}}(a; \bar{P})} \{R_2^{\text{den}}(\bar{P}, P) + \psi_h^{\text{den}}(a; P)\} \\
&= \frac{R_2^{\text{num}}(\bar{P}, P)}{\psi_h^{\text{den}}(a; \bar{P})} + \frac{\psi_{t,h,\epsilon}(a; P)\psi_h^{\text{den}}(a; P)}{\psi_h^{\text{den}}(a; \bar{P})} - \frac{\psi_{t,h,\epsilon}(a; \bar{P})R_2^{\text{den}}(\bar{P}, P)}{\psi_h^{\text{den}}(a; \bar{P})} - \frac{\psi_{t,h,\epsilon}(a; \bar{P})\psi_h^{\text{den}}(a; P)}{\psi_h^{\text{den}}(a; \bar{P})} \\
&= \frac{\psi_h^{\text{den}}(a; P)}{\psi_h^{\text{den}}(a; \bar{P})} \{\psi_{t,h,\epsilon}(a; P) - \psi_{t,h,\epsilon}(a; \bar{P})\} + \frac{R_2^{\text{num}}(\bar{P}, P)}{\psi_h^{\text{den}}(a; \bar{P})} - \frac{\psi_{t,h,\epsilon}(a; \bar{P})R_2^{\text{den}}(\bar{P}, P)}{\psi_h^{\text{den}}(a; \bar{P})}
\end{aligned}$$

Now plugging this into the von Mises expansion, we have:

$$\begin{aligned}
R_2(\bar{P}, P) &= \psi_{t,h,\epsilon}(a; \bar{P}) - \psi_{t,h,\epsilon}(a; P) + \mathbb{E}_P[\varphi_{t,h,\epsilon}(a; \bar{P})] \\
&= \psi_{t,h,\epsilon}(a; \bar{P}) - \psi_{t,h,\epsilon}(a; P) + \frac{\psi_h^{\text{den}}(a; P)}{\psi_h^{\text{den}}(a; \bar{P})} \{\psi_{t,h,\epsilon}(a; P) - \psi_{t,h,\epsilon}(a; \bar{P})\} \\
&\quad + \frac{R_2^{\text{num}}(\bar{P}, P)}{\psi_h^{\text{den}}(a; \bar{P})} - \frac{\psi_{t,h,\epsilon}(a; \bar{P})R_2^{\text{den}}(\bar{P}, P)}{\psi_h^{\text{den}}(a; \bar{P})} \\
&= \{\psi_{t,h,\epsilon}(a; \bar{P}) - \psi_{t,h,\epsilon}(a; P)\} \left(1 - \frac{\psi_h^{\text{den}}(a; P)}{\psi_h^{\text{den}}(a; \bar{P})}\right) + \frac{R_2^{\text{num}}(\bar{P}, P)}{\psi_h^{\text{den}}(a; \bar{P})} - \frac{\psi_{t,h,\epsilon}(a; \bar{P})R_2^{\text{den}}(\bar{P}, P)}{\psi_h^{\text{den}}(a; \bar{P})} \\
&= \frac{1}{\psi_h^{\text{den}}(a; \bar{P})} \left[\{\psi_{t,h,\epsilon}(a; \bar{P}) - \psi_{t,h,\epsilon}(a; P)\} \{\psi_h^{\text{den}}(a; \bar{P}) - \psi_h^{\text{den}}(a; P)\} \right. \\
&\quad \left. + R_2^{\text{num}}(\bar{P}, P) - \psi_{t,h,\epsilon}(a; \bar{P})R_2^{\text{den}}(\bar{P}, P) \right]
\end{aligned}$$

We already confirmed in our proof of Theorem 1 that $R_2^{\text{num}}(\bar{P}, P)$ and $R_2^{\text{den}}(\bar{P}, P)$ are second-order. Thus, at this point we have shown that $R_2(\bar{P}, P)$ is also second-order, since the first term above involves the product of errors in estimating $\psi_h(a; t)$ and $\psi_h^{\text{den}}(a; t)$.

G Details of Simulation Study

In the simulation study in Section 5, we generated datasets where $A|X \sim N(m(X), 0.2^2)$ and $Y|X, A \sim N(\mu(X), 0.5^2)$. The functions $m(X)$ and $\mu(X)$ are visualized in Figure 1 and

are defined as:

$$m(X) = \begin{cases} 0.05 & \text{if } X < 0.25 \\ 0.15 - 24(0.25 - X)(0.5 - X) & \text{if } 0.25 \leq X < 0.5 \\ X & \text{if } X \geq 0.5 \end{cases}$$

$$\mu(X) = \begin{cases} 0.5 - 4(X - 0.2)^2 & \text{if } X \leq 0.25 \\ 0.25 + 2(X - 0.2)^2 & \text{if } 0.25 < X \leq 0.75 \\ 1.25 - X & \text{if } X > 0.75 \end{cases}$$

These were chosen as arbitrary functions that were somewhat complex, thereby motivating nonparametric models, and that were constrained between 0 and 1 for ease of interpretation.

Meanwhile, in the simulation study we considered the estimands $\psi_h(a)$, $\psi(a; t)$, and $\psi_h(a; t)$, shown in Table 1, for treatment values $a \in \{0, 0.05, \dots, 0.95, 1\}$. In the simulation study, we set the bandwidth $h = 0.1$ and the smoothing parameter $\epsilon = 0.01$. In Section 5.1 we set the trimming threshold to $t = 0.1$. The resulting estimands are visualized in Figure 8. The non-trimmed estimand $\psi_h(a)$ is flat, because $\mathbb{E}[Y|X, A] = \mu(X)$ is not a function of A . However, the trimmed estimands $\psi(a; t)$ and $\psi_h(a; t)$ are not flat; as discussed in Section 5.3, this is because the non-trimmed population changes across a . That said, the discrepancy between these estimands is somewhat small, given the small y -axis scale in Figure 8, although this discrepancy could have been made larger by changing the data-generating process. This would not invalidate our simulation results, but nonetheless researchers may find these trimmed estimands difficult to interpret, given that the non-trimmed population changes across a . Thus, in practice, we recommend assessing how the non-trimmed population changes across a , as we illustrated in our application (Section 6).

Meanwhile, in Section 5.2 we considered simulation results when the trimming threshold is estimated. Specifically, we used the trimming estimator \hat{t} in (17) for our estimator and the plug-in estimator \hat{t}^{pi} in (28) for the plug-in estimators, where the proportion of trimmed subjects was set at $\gamma = 0.2$. These estimators correspond to true thresholds t_0 and t_0^{pi} , respectively. In other words, t_0 is defined as the t such that $\psi_h^{\text{den}}(a; t) = 1 - \gamma$, and t_0^{pi} is defined as the t such that $\mathbb{E}[\mathbb{I}(\pi(a|X) > t)] = 1 - \gamma$. Figure 9a displays t_0 and t_0^{pi} for this simulation setup, which makes clear that the threshold changes across a in this case. We see that t_0^{pi} is smaller on the edges of the dose-response curve but higher in the middle of the curve; this is because t_0 corresponds to a quantile that is kernel-smoothed across a , and this smoothing moderates the magnitude of the threshold. Furthermore, these thresholds are smaller than $t = 0.1$ for extreme treatment values but larger for moderate values. Meanwhile,

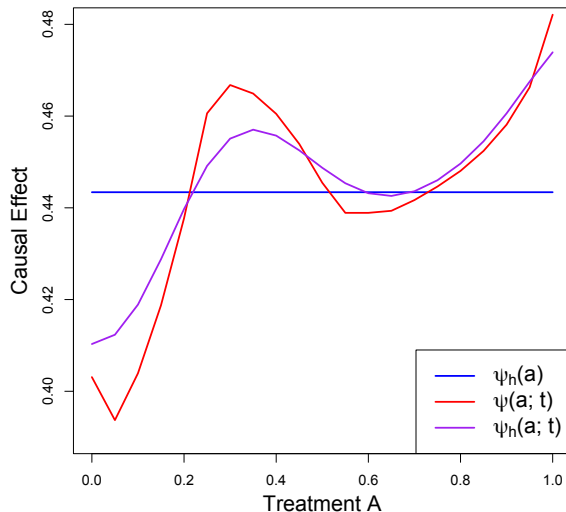


Figure 8: The SATE, TATE, and STATE for $a \in \{0, 0.05, \dots, 0.95, 1\}$ when $t = 0.1$, $h = 0.1$, and $\epsilon = 0.01$. To compute these estimands, we simulated $X \sim \text{Unif}(0, 1)$ $n = 10^5$ times, computed the true $\pi(a|X)$ and $\mu(X, a)$, and empirically computed the SATE, TATE, and STATE. To evaluate the inner integrals in the SATE and STATE, we considered values $a_0 \in [-0.5, 1.5]$ in 0.05 increments, such that $\int \int K_h(a_0 - a) da_0 dP(x) \approx 1$ for all $a \in [0, 1]$.

Figure 9b visualizes the corresponding TATE and STATE estimands, $\psi(a; t_0^{\text{pi}})$ and $\psi_h(a; t_0)$.

H Results for Discrete Treatments

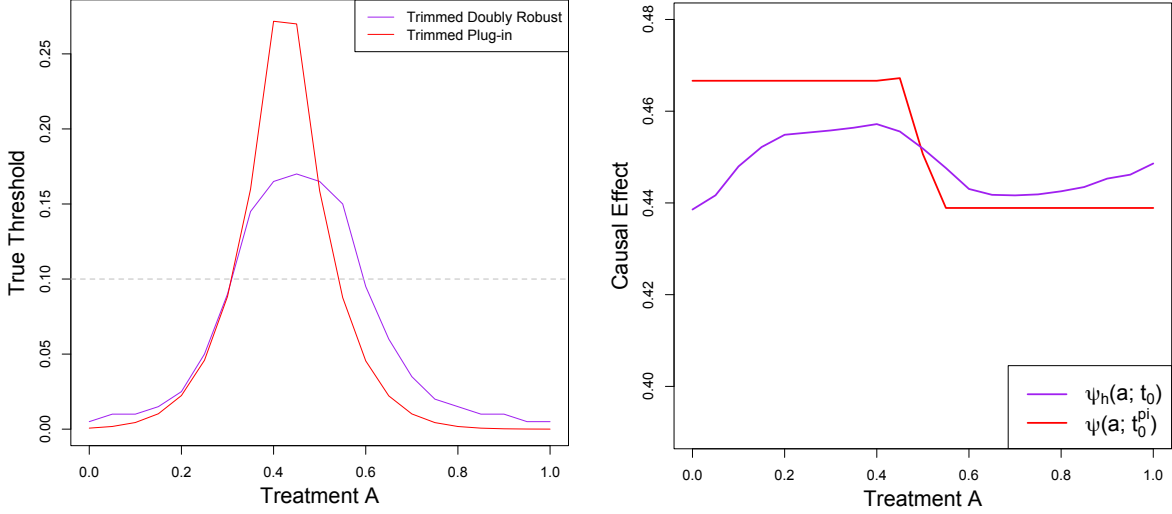
H.1 Estimands and Efficient Influence Functions

In the main text, we considered the estimands $\psi_h^{\text{num}}(a; t)$ and $\psi_h^{\text{den}}(a; t)$, which incorporate kernel smoothing and a smoothed trimming indicator $S(\pi(a|x), t)$. Kernel smoothing is required to define an EIF in the case of a continuous treatment. In this section we instead consider the case where the treatment A is discrete, such that A only takes on a finite number of values. In this case, kernel smoothing is not needed to define estimands that have EIFs, although the smoothed trimming indicator $S(\pi(a|x), t)$ is still required.

Consider the following estimands, for a given treatment value a :

$$\psi_\epsilon^{\text{num}}(a; t) = \int S(\pi(a|x), t) \mu(x, a) dP(x), \quad \text{and} \quad \psi_\epsilon^{\text{den}}(a; t) = \int S(\pi(a|x), t) dP(x),$$

where ϵ is the smoothing parameter for $S(\pi(a|x), t)$. Following the same proof mechanics as that of Theorem 1, we have the following uncentered EIFs when t is fixed.



(a) The true trimming thresholds t_0^{pi} (red) and t_0 (purple). (b) The TATE (red) and STATE (purple) estimands for thresholds t_0^{pi} and t_0 .

Figure 9: The true trimming thresholds (left) and their corresponding dose-response curves (right) when $\gamma = 0.2$.

Proposition 2. *When the trimming threshold t is fixed, the uncentered EIFs for $\psi_\epsilon^{\text{num}}(a; t)$ and $\psi_\epsilon^{\text{den}}(a; t)$ are*

$$\begin{aligned} \varphi_\epsilon^{\text{num}}(a; t) &= \mathbb{I}(A = a) \frac{\{Y - \mu(X, A)\} S(\pi(A|X), t)}{\pi(A|X)} + S(\pi(a|X), t) \mu(X, a) \\ &\quad + \mathbb{I}(A = a) \mu(X, A) \frac{\partial S(\pi(A|X), t)}{\partial \pi} - \mu(X, a) \frac{\partial S(\pi(a|X), t)}{\partial \pi} \pi(a|X), \end{aligned}$$

and

$$\varphi_\epsilon^{\text{den}}(a; t) = S(\pi(a|X), t) + \mathbb{I}(A = a) \frac{\partial S(\pi(A|X), t)}{\partial \pi} - \frac{\partial S(\pi(a|X), t)}{\partial \pi} \pi(a|X).$$

The corresponding one-step estimators based on the above proposition are:

$$\widehat{\psi}_\epsilon^{\text{num}}(a; t) = \mathbb{P}_n \{ \widehat{\varphi}_\epsilon^{\text{num}}(a; t) \}, \quad \widehat{\psi}_\epsilon^{\text{den}}(a; t) = \mathbb{P}_n \{ \widehat{\varphi}_\epsilon^{\text{den}}(a; t) \},$$

where $\widehat{\varphi}_\epsilon^{\text{num}}(a; t)$ and $\widehat{\varphi}_\epsilon^{\text{den}}(a; t)$ are equal to $\varphi_\epsilon^{\text{num}}(a; t)$ and $\varphi_\epsilon^{\text{den}}(a; t)$, but with $\pi(a|x)$ and $\mu(x, a)$ replaced with estimators $\widehat{\pi}(a|x)$ and $\widehat{\mu}(x, a)$. Then, one can compute the ratio $\widehat{\psi}_\epsilon^{\text{num}}(a; t) / \widehat{\psi}_\epsilon^{\text{den}}(a; t)$ to estimate the trimmed causal effect $\psi_\epsilon^{\text{num}}(a; t) / \psi_\epsilon^{\text{den}}(a; t)$.

In the specific case of a binary treatment, researchers are typically interested in the

contrast $a = 1$ versus $a = 0$. Using the above results in this case, the estimand would be:

$$\frac{\psi_\epsilon^{\text{num}}(1; t)}{\psi_\epsilon^{\text{den}}(1; t)} - \frac{\psi_\epsilon^{\text{num}}(0; t)}{\psi_\epsilon^{\text{den}}(0; t)} = \frac{\int S(\pi(1|x), t)\mu(x, 1)dP(x)}{\int S(\pi(1|x), t)dP(x)} - \frac{\int S(\pi(0|x), t)\mu(x, 0)dP(x)}{\int S(\pi(0|x), t)dP(x)}.$$

The above estimand trims treatment and control separately, such that the non-trimmed populations for treatment and control may differ. Instead, researchers may wish to construct a single non-trimmed population. One can consider the following trimmed estimand:

$$\psi_\epsilon(t) = \frac{\psi_\epsilon^{\text{num}}(t)}{\psi_\epsilon^{\text{den}}(t)} = \frac{\int S(\pi(1|x), t)\{\mu(x, 1) - \mu(x, 0)\}dP(x)}{\int S(\pi(1|x), t)dP(x)}. \quad (42)$$

Here, $S(\pi(1|x), t)$ corresponds to a smoothed analog of the trimming indicator $\mathbb{I}(t < \pi(1|x) < 1 - t)$. For example, Yang and Ding (2018) defined $S(\pi(1|x), t)$ as:

$$S(\pi(1|x), t) = \Phi_\epsilon\{\pi(1|x) - t\}\Phi_\epsilon\{t - \pi(1|x)\}.$$

The following proposition establishes the EIFs for $\psi_\epsilon^{\text{num}}(t)$ and $\psi_\epsilon^{\text{den}}(t)$ in (42).

Proposition 3. *When the trimming threshold t is fixed, the uncentered EIFs of $\psi_\epsilon^{\text{num}}(t)$ and $\psi_\epsilon^{\text{den}}(t)$ are*

$$\begin{aligned} \varphi_\epsilon^{\text{num}}(t) &= S(\pi(1|X), t)\{\mu(X, 1) - \mu(X, 0)\} + \frac{\partial S(\pi(1|X), t)}{\partial \pi}(A - \pi(1|X))\{\mu(X, 1) - \mu(X, 0)\} \\ &\quad + S(\pi(1|X), t)\left\{\frac{A(Y - \mu(X, 1))}{\pi(1|X)} - \frac{(1 - A)(Y - \mu(X, 0))}{(1 - \pi(1|X))}\right\}, \end{aligned}$$

and

$$\varphi_\epsilon^{\text{den}}(t) = S(\pi(1|X), t) + \frac{\partial S(\pi(1|X), t)}{\partial \pi}(A - \pi(1|X)).$$

Proof. First, recall that we have the following influence functions when X is discrete:

$$\begin{aligned} \mathbb{IF}\{\mu(x, 1) - \mu(x, 0)\} &= \frac{A\mathbb{I}(X = x)}{\pi(1|x)p(x)}(Y - \mu(x, 1)) - \frac{(1 - A)\mathbb{I}(X = x)}{(1 - \pi(1|x))p(x)}(Y - \mu(x, 0)) \\ \mathbb{IF}\{S(\pi(1|x), t)\} &= \frac{\partial S(\pi(1|x), t)}{\partial \pi} \frac{\mathbb{I}(X = x)}{P(X = x)}(A - \pi(1|x)) \\ \mathbb{IF}\{p(x)\} &= \mathbb{I}(X = x) - p(x) \end{aligned}$$

Thus, we have, by the discretization trick and product rule:

$$\begin{aligned}\mathbb{IF}\{\psi_\epsilon^{\text{den}}(t)\} &= \sum_x \mathbb{IF}\{S(\pi(1|x), t)\}p(x) + S(\pi(1|x), t)\mathbb{IF}\{p(x)\} \\ &= \frac{\partial S(\pi(1|X), t)}{\partial \pi}(A - \pi(1|X)) + S(\pi(1|X), t) - \psi_\epsilon^{\text{den}}(t)\end{aligned}$$

Similarly, we have:

$$\begin{aligned}\mathbb{IF}\{\psi_\epsilon^{\text{num}}(t)\} &= \sum_x \mathbb{IF}\{S(\pi(1|x), t)\}\{\mu(x, 1) - \mu(x, 0)\}p(x) \\ &\quad + S(\pi(1|x), t)\mathbb{IF}\{\mu(x, 1) - \mu(x, 0)\}p(x) \\ &\quad + S(\pi(1|x), t)\{\mu(x, 1) - \mu(x, 0)\}\mathbb{IF}\{p(x)\} \\ &= \frac{\partial S(\pi(1|X), t)}{\partial \pi}(A - \pi(1|X))\{\mu(X, 1) - \mu(X, 0)\} \\ &\quad + S(\pi(1|X), t) \left\{ \frac{A(Y - \mu(X, 1))}{\pi(1|X)} - \frac{(1 - A)(Y - \mu(X, 0))}{(1 - \pi(1|X))} \right\} \\ &\quad + S(\pi(1|X), t)\{\mu(X, 1) - \mu(X, 0)\} - \psi_\epsilon^{\text{num}}(t)\end{aligned}$$

This completes the proof. □

The corresponding estimator for $\psi_\epsilon(t)$ in (42) is $\hat{\psi}_\epsilon(t) = \hat{\psi}_\epsilon^{\text{num}}(t)/\hat{\psi}_\epsilon^{\text{den}}(t)$, where

$$\hat{\psi}_\epsilon^{\text{num}}(t) = \mathbb{P}_n\{\hat{\varphi}_\epsilon^{\text{num}}(t)\}, \quad \hat{\psi}_\epsilon^{\text{den}}(t) = \mathbb{P}_n\{\hat{\varphi}_\epsilon^{\text{den}}(t)\},$$

where $\hat{\varphi}_\epsilon^{\text{num}}(t)$ and $\hat{\varphi}_\epsilon^{\text{den}}(t)$ are equal to $\varphi_\epsilon^{\text{num}}(t)$ and $\varphi_\epsilon^{\text{den}}(t)$, but with $\pi(1|x)$, $\mu(x, 1)$, and $\mu(x, 0)$ replaced with estimators $\hat{\pi}(1|x)$, $\hat{\mu}(x, 1)$, and $\hat{\mu}(x, 0)$.

H.2 Simulation Results for Binary Treatments

Similar to the simulation study in the main text, we consider an illustrative example with a single covariate X that ranges from 0 to 1 and a continuous outcome Y . However, in this example, the treatment A is binary. For simplicity, we focus on estimating the average treatment potential outcome $\psi(1) = \mathbb{E}[Y(1)]$, which is identified as $\psi(1) = \mathbb{E}[\mu(X, 1)]$ when consistency, unconfoundedness, and positivity hold.

The propensity score $\pi(1|X) = P(A = 1|X)$ and outcome regression $\mu(X, 1) = \mathbb{E}[Y|X, A = 1]$ were specified as $m(X)$ and $\mu(X)$, respectively, both visualized in Figure 1 (see Section G for the exact specifications for these functions). The propensity score is small for $X < 0.25$,

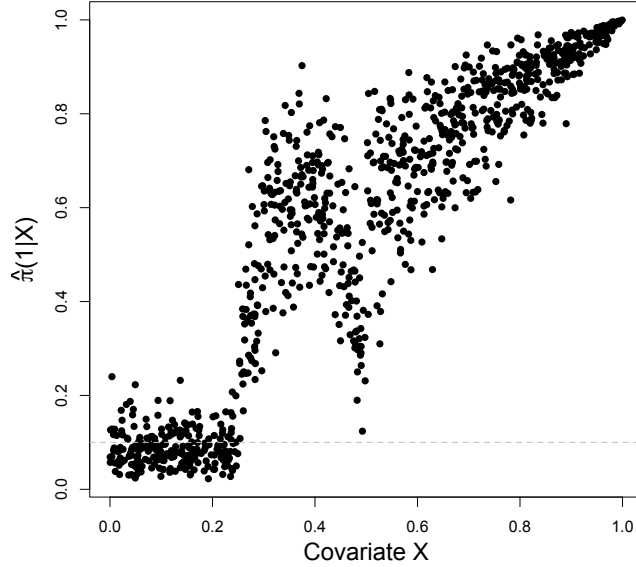


Figure 10: Example of $\hat{\pi}(1|X)$ for the first simulated dataset when convergence rate $\alpha = 0.1$. Horizontal dashed line denotes $t = 0.1$.

such that $\psi(1)$ is difficult to estimate. The trimmed estimands are defined as:

$$\psi(1; t) = \frac{\mathbb{E}[\mu(X, 1)\mathbb{I}\{\pi(1|X) \geq t\}]}{\mathbb{E}[\mathbb{I}\{\pi(1|X) \geq t\}]}, \quad \text{and} \quad \psi_\epsilon(1; t) = \frac{\mathbb{E}[\mu(X, 1)S(\pi(1|X), t)]}{\mathbb{E}[S(\pi(1|X), t)]},$$

where $S(\pi(1|X), t) = \Phi_\epsilon\{\pi(1|X) - t\}$ is a smoothed version of the trimming indicator $\mathbb{I}\{\pi(1|X) \geq t\}$. In this section, we call $\psi(1; t)$ the trimmed average treatment effect (TATE) and $\psi_\epsilon(1; t)$ the smoothed TATE (STATE). The TATE and STATE will be close when ϵ is small; for simplicity we fix $\epsilon = 0.01$.

Similar to the simulation study in the main text, we generated 1000 datasets containing (X, A, Y) , where $X \sim \text{Unif}(0, 1)$, $A \sim \text{Bern}(\pi(1|X))$, and $Y \sim N(\mu(X, 1), 0.5^2)$. Each dataset contained $n = 1000$ subjects. For each dataset we simulated estimators as

$$\begin{aligned} \hat{\pi}(1|X) &\sim \pi(1|X) + \text{expit}[\text{logit}\{\pi(1|X)\} + N(n^{-\alpha}, n^{-2\alpha})] \\ \hat{\mu}(X, 1) &\sim \mu(X, 1) + N(n^{-\alpha}, n^{-2\alpha}), \end{aligned}$$

such that the root mean squared error (RMSE) of $\hat{\pi}(1|X)$ and $\hat{\mu}(X, 1)$ are $O_P(n^{-\alpha})$, and thus we can control the estimators' convergence rate via the rate parameter α . We considered convergence rates $\alpha \in \{0.1, 0.2, \dots, 0.5\}$. As an example, Figure 10 displays $\hat{\pi}(1|X)$ for the first simulated dataset when $\alpha = 0.1$.

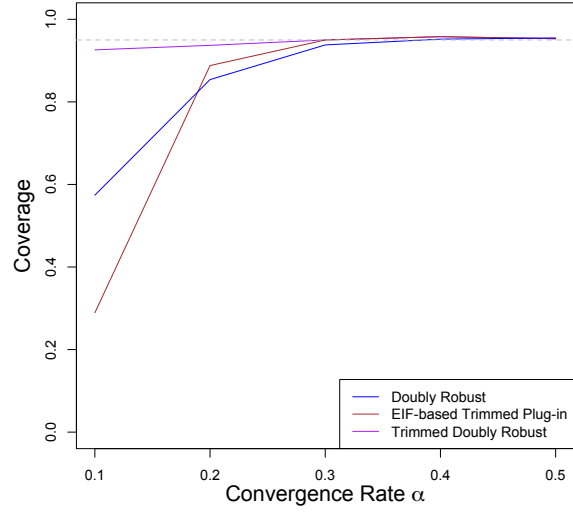
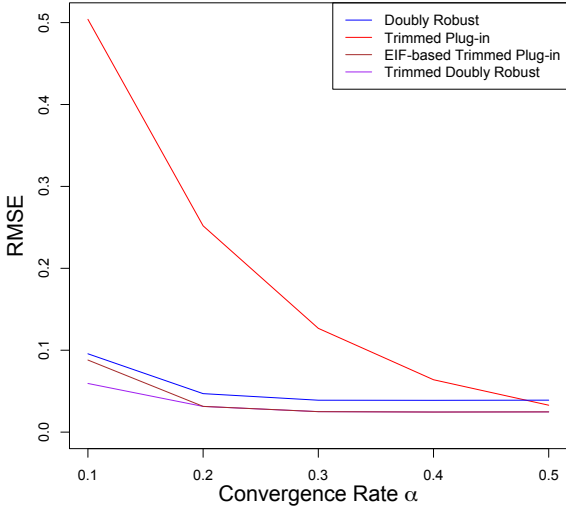
Once $\hat{\pi}(1|X)$ and $\hat{\mu}(X, 1)$ are generated, we computed the following four estimators:

1. **Doubly Robust:** $\hat{\psi}(1) = \mathbb{P}_n\{\hat{\varphi}(1)\}$, where $\hat{\varphi}(1) = \hat{\mu}(X, 1) + \frac{A\{Y - \hat{\mu}(X, 1)\}}{\hat{\pi}(1|X)}$ are the estimated influence function values for the typical doubly robust estimator. This targets the ATE $\psi(1)$.
2. **Trimmed Plug-in:** $\hat{\psi}(1; t) = \frac{\mathbb{P}_n[\hat{\mu}(X, 1)\mathbb{I}\{\hat{\pi}(1|X) \geq t\}]}{\mathbb{P}_n[\mathbb{I}\{\hat{\pi}(1|X) \geq t\}]}$. This targets the TATE and is based on the identification result for $\psi(1; t)$.
3. **EIF-based Trimmed Plug-in:** $\hat{\psi}^{\text{alt}}(1; t) = \frac{\mathbb{P}_n[\hat{\varphi}(1)\mathbb{I}\{\hat{\pi}(1|X) \geq t\}]}{\mathbb{P}_n[\mathbb{I}\{\hat{\pi}(1|X) \geq t\}]}$. This also targets the TATE and averages the typical doubly robust estimator on the trimmed sample.
4. **Trimmed Doubly Robust:** $\hat{\psi}_\epsilon(1; t) = \frac{\hat{\psi}_\epsilon^{\text{num}}(1; t)}{\hat{\psi}_\epsilon^{\text{den}}(1; t)} = \frac{\mathbb{P}_n\{\hat{\varphi}_\epsilon^{\text{num}}(1; t)\}}{\mathbb{P}_n\{\hat{\varphi}_\epsilon^{\text{den}}(1; t)\}}$, where $\varphi_\epsilon^{\text{num}}(1; t)$ and $\varphi_\epsilon^{\text{den}}(1; t)$ are defined in Proposition 2 and represent the EIFs for the numerator and denominator of $\psi_\epsilon(1; t)$. This targets the STATE.

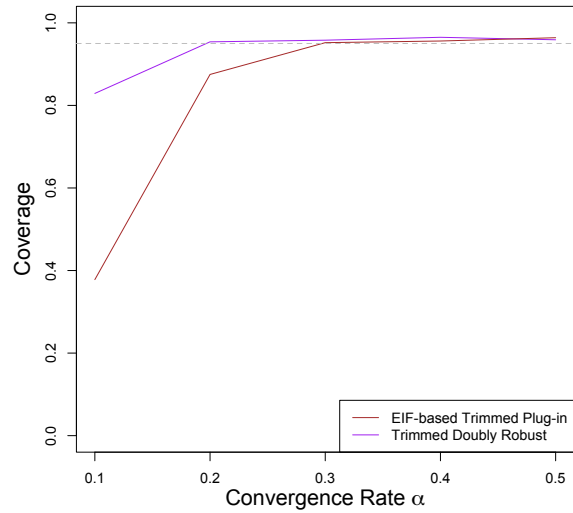
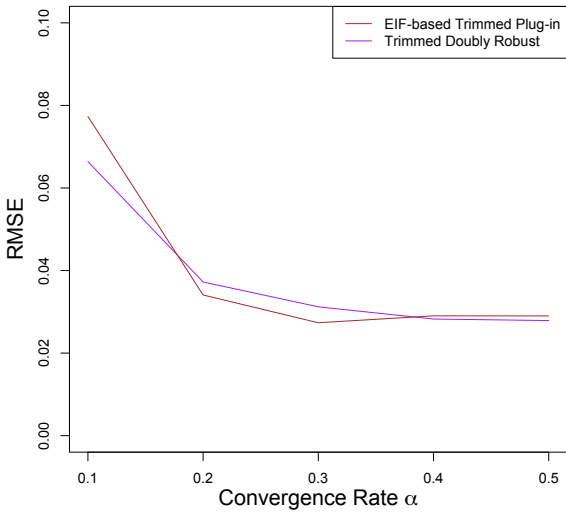
Figure 11 displays the estimators' performance in terms of RMSE and 95% confidence interval coverage when $t = 0.1$ or when it is estimated as the $\gamma = 0.2$ quantile of the propensity score, similar to what was studied in the main text. Note that RMSE and coverage were computed according to each estimator's respective estimand. For example, our estimator targets $\psi_\epsilon(1; t)$ when $t = 0.1$ and $\psi_\epsilon(1; t^0)$ when t is estimated, where t_0 is the threshold such that $\psi_\epsilon^{\text{den}}(1; t_0) = 1 - \gamma = 0.8$. The results are very similar to the results in the main text simulation study. In terms of RMSE, the trimmed plug-in estimator $\hat{\psi}(1; t)$ performs poorly when the convergence rate is slow, whereas our trimmed doubly robust estimator $\hat{\psi}_\epsilon(1; t)$ and the EIF-based trimmed plug-in estimator $\hat{\psi}^{\text{alt}}(1; t)$ outperform the typical doubly robust estimator $\hat{\psi}(1)$. Meanwhile, in terms of coverage, our estimator performs slightly better than the EIF-based trimmed plug-in estimator, although both approach the nominal level as the convergence rate increases.

The fact that $\hat{\psi}^{\text{alt}}(1; t)$ performs similarly to our estimator may at first seem surprising, because this estimator uses a plug-in estimator for the denominator of the TATE, $\mathbb{E}[\mathbb{I}\{\pi(1|X) \geq t\}]$, and thus we may expect this estimator to inherit the convergence rate of $\hat{\pi}(1|X)$. However, even when $\pi(1|X)$ is estimated poorly, the trimming indicator $\mathbb{I}\{\pi(1|X) \geq t\}$ may nonetheless be estimated well. Reconsider Figure 10, which displays an example of $\hat{\pi}(1|X)$ when $\alpha = 0.1$. We see that $\hat{\pi}(1|X)$ is closer to $\pi(1|X)$ when $\pi(1|X)$ is small or large; this is a by-product of constraining $\hat{\pi}(1|X)$ to be between 0 and 1 to be a proper propensity score estimator. As a result, even though $\hat{\pi}(1|X)$ is estimated poorly, the set of trimmed subjects is close to correct; in other words, $\mathbb{I}\{\pi(1|X) \geq t\}$ is still well-estimated.

Lastly, we can note that, in this simulation setup, the typical doubly robust estimator does not degrade as severely as in the simulation setup in the main text. This is likely



(a) RMSE of the four estimators when $t = 0.1$. (b) Coverage of the four estimators when $t = 0.1$.



(c) RMSE of $\hat{\psi}^{\text{alt}}(1; t)$ and $\hat{\psi}_\epsilon(1; t)$ when t is estimated as the 10% quantile of $\pi(1|X)$. (d) Coverage of $\hat{\psi}^{\text{alt}}(1; t)$ and $\hat{\psi}_\epsilon(1; t)$ when t is estimated as the 10% quantile of $\pi(1|X)$.

Figure 11: RMSE (left) and coverage (right) of the estimators when the threshold is fixed at $t = 0.1$ (top) or estimated as the $\gamma = 0.2$ quantile of $\pi(1|X)$ (bottom). Results displayed across different convergence rates α for $\hat{\pi}(1|X)$ and $\hat{\mu}(1, X)$.

because the propensity scores are less severe, compared to the simulation study in the main text. As shown in Figure 10, only some subjects' propensity scores were close to zero in this simulation setup, whereas when the treatment was continuous, subjects' propensity scores were close to zero for many treatment values. In other words, positivity violations at $A = 1$ in this simulation study are less severe than positivity violations across treatment values in the simulation study in the main text. This is also likely why the EIF-based trimmed plug-in estimator performed similarly to our estimator regardless of whether the trimming threshold was fixed or estimated in this simulation study, whereas it could perform worse than our estimator in the continuous case. This illustrates that positivity violations can be a greater concern when the treatment is continuous.